

Supracrustal belts in Godthåbsfjord region, southern West Greenland

Progress report on 2005 field work: geological mapping,
regional hydrothermal alteration and tectonic sections

Julie A. Hollis, Susanne Schmid, Henrik Stendal,
Jeroen A. M. van Gool & Willy Lehmann Weng

(1 DVD included)



Supracrustal belts in Godthåbsfjord region, southern West Greenland

Progress report on 2005 field work: geological mapping,
regional hydrothermal alteration and tectonic sections

Julie A. Hollis, Susanne Schmid, Henrik Stendal,
Jeroen A. M. van Gool & Willy Lehmann Weng

(1 DVD included)

Contents

Executive summary	7
Introduction	9
Background	11
Previous work.....	11
Logistics	12
Tectonothermal evolution of supracrustal belts in the inner Godthåbsfjord region	13
Introduction	13
Background.....	13
Map data	14
Ujarassuit Nunaat to Kangerssuaq.....	14
Isukasia terrane.....	15
Kapisilik terrane.....	16
Map area 4 – Færingehavn terrane?	19
Tre Brødre terrane (map area 5)	20
Akia terrane – Taseressuaq pluton.....	22
Metadolerite dykes	22
Ataneq fault system.....	22
Structural evolution of the Ujarassuit Nunaat area	23
Ivisaartoq belt.....	26
Regional tectonic sections	26
Progress of analytical work	27
Geochemistry	27
Geochronology	27
Concluding remarks	28
Potential for precious metals in hydrothermal systems within the wider Godthåbsfjord region	29
Introduction	29
Analytical methods.....	30
Fiskefjord	30
Geology.....	31
Analytical results	32
Qussuk peninsula.....	35
Geology.....	35
Analytical results	37
Qooqqut Lake.....	38
Geology.....	38
Analytical results	41
Ameralik	41

Kangerdluarssenguup taserssua	42
Analytical results	43
Concluding remarks	48
Acknowledgements	49
References	50
Appendix 1: Explanatory notes to the DVD (Willy Lehmann Weng)	52
Directory structure	52
Use of the DVD	53
Acrobat Reader© 6	53
ArcView© project	53
View 0.1 Frontispiece	54
View 1.1 Index map – Location of the Godthåbsfjord region	54
View 1.2 Topographic map	54
View 1.3 Ujarassuit Nunaat geological map	54
View 1.4 Digital geological map 1:100 000	54
View 1.5 Digital geological maps 1:100 000 (old version)	55
View 1.6 Scanned geological maps 1:100 000 (old version)	55
View 2.1 Visited outcrop localities	55
View 2.2 Geological observations	55
View 2.3 Samples collected	56
View 2.4 Structures	56
View 2.5 Geochronology	56
View 2.6 Photographs	56
Views 3.1: Rock geochemistry and 3.3: Stream sediment chemistry	56
View 3.2 Geochemistry	56
Field Maps	57
Spreadsheets	57
Photographs	57
Appendix 2: Field report 2005 – Ujarassuit Nunaat Region – North (Jeroen van Gool & Ole Stecher)	58
Areas 1 and 9	60
Lithology	60
Amphibolites	60
Metagabbro	61
Ultramafic rocks	61
Quartz-diorite	61
Felsic gneisses	62
Eoarchaeon orthogneisses	62
Pegmatites	63
Metadolerite dykes	63
Structure	63
Area 8	65
Lithology	65

Supracrustal belt	65
Ultramafic rocks.....	67
Pegmatites	67
Orthogneisses	67
Ameralik dykes	67
Structure.....	68
Areas 6 and 7.....	68
Lithology – Kapisilik terrane, east of the Ataneq fault.....	69
Amphibolite belts	69
Leucogranite.....	70
Orthogneisses	70
Lithology – Akia terrane, west of the Ataneq fault	71
Orthogneisses	71
Amphibolites.....	71
Taserssuaq pluton	71
Aplitic dykes	71
Lithology – rock types common to both sides of the Ataneq fault.....	72
Ultramafic dyke.....	72
Metadolerite dykes	72
Structure – east of the Ataneq fault.....	72
Structure – west of the Ataneq fault	73
Structures common to both sides of the Ataneq fault.....	74
Ataneq fault.....	75
Discussion.....	75
Amphibolite belts.....	75
Orthogneisses	76
Structural history	76
Ataneq fault	76

Appendix 3: Field report 2005 - Ujarassuit Nunaat Region – South (Nigel M. Kelly & Susanne Schmid) 78

Introduction and background.....	78
Areas 1 to 3.....	78
Lithologies	79
Felsic Orthogneisses	79
Amphibolite.....	80
Garnet-Biotite Schist.....	81
Ultramafic rocks.....	81
Pegmatite	82
Structure-Metamorphism & Lithological relationships.....	82
Ductile structures, Fold-foliation relationships	82
Contact relationship between supracrustals and felsic orthogneiss	85
Alteration	88
Mineralisation	89
Preliminary Interpretations	89
Protoliths to supracrustal rocks	89
Contact between heterogeneous and migmatitic felsic orthogneiss	90
Correlation of the ‘Undifferentiated’ orthogneiss.....	90

Outcrop pattern of amphibolite in area 3 – a fold axis?	90
Area 4	91
Lithologies	91
Felsic Orthogneiss	91
Amphibolite	91
Biotite (+/- garnet) schist	92
Ultramafic rocks	93
Pegmatite	93
Structure & Lithological relationships	94
Ductile structures, Fold-foliation relationships	94
Late brittle (+ semi-ductile) faulting	97
Metamorphism	97
Alteration	99
Mineralisation	99
Protoliths to supracrustal rocks	99
Area 5	99
Lithologies	100
Felsic Orthogneiss	100
Amphibolite	100
Garnet-biotite schist	101
Ultramafic rocks	102
Pegmatite	102
Structural-lithological relationships	102
Dn	103
Dn+1	104
Dn+2	104
Metamorphism	105
Mineralisation/Alteration	105
Preliminary Interpretations & Discussion	105
Protoliths to supracrustal rocks	105
Tre Brødre – Færingehavn Terrane boundary	106
Regional Structural Correlations	106

Appendix 4: Field report 2005 - Ujarassuit Nunaat Region – East, and Ivisaartoq (Ali Polat) 108

Appendix 5: Field report 2005 - Ujarassuit Nunaat Region – East, and Ivisaartoq (Juan Carlos Ordóñez-Calderón) 112

Introduction	112
Lithological Units	112
Amphibolites and metagabbros	112
Areas 1, 9, and E2	112
Ivisaartoq supracrustal belt	114
Metasedimentary rocks	114
Areas 1, 9, and E2	114
Ivisaartoq supracrustal belt	115
Ultramafic rocks	115
Areas 1, 9, and E2	115

Ivisaartoq supracrustal belt.....	115
Late intrusives	116
Areas 1, 9, and E2.....	116
Hydrothermal alterations	116
Areas 1, 9, and E2.....	116
Ivisaartoq supracrustal belt.....	116
Structures.....	117
Areas 1, 9, and E2.....	117
Ivisaartoq supracrustal belt.....	117
Preliminary conclusions	117

Appendix 6: Structural Geology of the supracrustal belts in the central Godthåbsfjord region, data collection for constraining tectonic cross-sections (Dave and Vincent Coller) 119

Introduction	119
Field Results	121
Alteration within the supracrustal packages	123
Tectonic Cross-Sections	123
Central Storø Sections	123
Regional Sections	124

Appendix 7: Ore mineralogical examination of the Qussuk area (Britt Andreassen) 127

Introduction	127
Previous work and geological setting	127
Methods	129
Main objectives	138
Results	140
Further work.....	140

Appendix 8: Magnetic and geological profiling across the Ataneq fault (Pelle Gulbrandsen) 141

Geological setting.....	142
Method	143
Results	144
Observations and conclusion	147

Appendix 9: A geological and geochemical interpretation of mafic and ultramafic rocks and their economic mineral potential, Fiskefjord region, southern West Greenland (Tine Kristensen) 153

Fiskefjord 1 area	156
Fiskefjord 2 area	158
Sulphide mineralisation	159

Appendix 10: Ataneq fault – hydrothermal alterations (Gorm J.-P. Thøgersen) 161

Introduction	161
The geological setting	161
Regional geology.....	161

Local geology.....	162
Methods and results	162
Ataneq 1	162
Description of the structural features at Ataneq 1	162
Lithological description of the Ataneq 1 area	163
Ataneq 2	167
Ataneq 3	169
Conclusion	171

Executive summary

This report outlines the preliminary results of two related GEUS field-based projects in the Godthåbsfjord region. These projects are:

- Tectonothermal evolution of supracrustal belts in the inner Godthåbsfjord region, and
- Potential for precious metals in hydrothermal systems within the wider Godthåbsfjord region

Field work was carried out by GEUS geologists and partners in the 2005 summer. New map data, field observations and interpretations, preliminary geochemical data, and progress on the collection of additional analytical data are presented.

Tectonothermal evolution of supracrustal belts

In the Ujarassuit area, detailed 2005 field mapping has identified several previously unrecognised amphibolite belts. All amphibolite belts in that area have experienced amphibolite facies metamorphic conditions with associated strong tectonism and recrystallisation, some with later reactivation of structures at greenschist facies. These belts are interpreted as supracrustal in origin on the basis of rare primary features and the lithological association of mafic to intermediate amphibolites, ultramafic, and aluminous and quartzofeldspathic metasedimentary rocks. They differ from the interpreted island-arc belts on the Qussuk peninsula in the lack or low abundance of andesitic amphibolite.

The amphibolite belts occur in Eo- to Neoarchaeal terranes, and in all terranes visited the belts are intruded by the regional orthogneisses. The largest amphibolite belt on Ujarassuit Nunaat is thought to correlate with the Mesoarchaeal Ivisaartoq belt.

Variable pre-metamorphic alteration of the belts has occurred, commonly involving calc-silicate alteration of amphibolites. In some cases mica- and quartz-rich rocks that appear similar to metasedimentary rocks are thought to have been formed via alteration of amphibolite or ultramafic precursors. This interpretation is supported by their elevated Cr and Ni concentrations.

The structure of the Ujarassuit area is dominated by Neoarchaeal west-vergent folds, including the Kangerssuaq antiform and the Ujarassuit Nunaat dome. These overprint several older isoclinal deformations. The Proterozoic Ataneq fault is shown to have a complex history of multiple reactivations of its shear zone system under greenschist facies conditions. These shear zones show widespread evidence for extensional deformation. One shear zone in that area was found to be molybdenite-bearing, though the timing of the shearing and mineralisation is not clear.

The structural evolution of the wider Godthåbsfjord region is being investigated via construction of a series of ten-kilometre-scale tectonic sections that incorporate field and analytical data collected in 2004 and 2005, and which will be reported in mid 2006. Preparation for further geochemical and U-Pb zircon geochronology analyses are also underway. These will provide further constraints on the environments, the age of formation and tectonothermal evolution of the amphibolite belts.

Potential for precious metals in hydrothermal systems within the wider Godthåbsfjord region

Preliminary geochemical results confirm and add evidence for a strata-bound nature for a gold mineralisation discovered in 2004 on the Qussuk peninsula. Up to 8 ppm gold was recorded in samples of a garnet-bearing supracrustal rock (possibly metamorphosed exhalite) within a volcano-sedimentary sequence.

A magmatic complex at Fiskefjord comprises ultramafic rocks, noritic and layered amphibolites. Magnetite and chromite were identified in the ultramafic units and iron-sulphides in norites and amphibolites. Significant platinum (51 ppb), palladium (27 ppb) and gold (326 ppb) were detected in the norites.

The hydrothermal system associated with the Ataneq fault was found to be barren with respect to gold, whereas copper and barium were moderately enriched. Along the fault zone ultramafic rocks are hydrothermally altered to soapstone for a length of at least one km.

Owing to favourable settings for gold mineralisation predicted by statistical modelling by Nielsen *et al.* (2004), the Qooqut Lake area was investigated. Gold mineralisation was not found, but signs of copper and zinc mineralisation were recorded. The first observation in this area of a pillowed mafic sequence, similar to that described at Ivisaartoq, was made.

Two sites in the Ameralik area, which lies between the Mesoarchaeoan Tasiusarsuaq and Neoarchaeoan Tre Brødre terranes, have been investigated (in 2004 and 2005). This area shows evidence for significant hydrothermal alteration, particularly along fault zones. However, neither gold nor the source of an albitised Cu-Au bearing rock found in 2004, has been found.

Anomalous gold and arsenic were identified in mafic sequences and exhalites in the Tasiuarsuaq terrane southeast of Kangerdluarssenguup taseressua. Aside from Storø, this is the only locality identified by GEUS in 2004–2005 in the Godthåbsfjord region where an arsenic-gold association is found.

Introduction

This report presents the preliminary results of two related Geological Survey of Denmark and Greenland (GEUS) field programs in the Godthåbsfjord region in 2005, financially supported by the Greenland Bureau of Minerals and Petroleum. The two programs are:

- 1) Tectonothermal evolution of supracrustal belts in the inner Godthåbsfjord region, and
- 2) Potential for precious metals in hydrothermal systems within the wider Godthåbsfjord region

Figure 1 shows the areas visited by geologists working on these projects during 2005 field work. In the sections discussing the two projects we present the aims, field data, currently available analytical data, and preliminary conclusions for each of the projects. Additional analytical work on samples collected in 2005 will be carried out in the spring of 2006 and reported in mid 2006. The planned work is outlined in the relevant sections below.

Enclosed in this report is a DVD containing:

- 1) the full report in PDF format.
- 2) an ArcView© project file containing geo-referenced compiled field data including localities, sample locations and descriptions, structural data, and maps, along with currently available rock and stream sediment geochemical data, and geochronology data. This also includes data from previous GEUS projects in the region for comparison.
- 3) Digital photographs in JPEG format.
- 4) PDF files of the previous related GEUS reports GEUS2004R110 and GEUS2005R42.
- 5) Relevant existing maps from the GEUS archive (Chadwick 1981; Crewe 1981, 1982; Park 1986a).

Instructions for accessing the information on the DVD are given in Appendix 1. Some photographic figures are printed in the body of this report. These and other photographs in this report are referenced in the following format: xxx2005-*nnn*, where *xxx* gives the official initials of the photographer, and *nnn* gives the identifying number of the photograph. Locality numbers are also used throughout the text, also given in the form: xxx2005-*nnn*, where *xxx* gives the official initials of the relevant geologist and *nnn* gives the identifying number of the locality. Localities (and all field data relating to these) may be viewed in the accompanying ArcView© project.

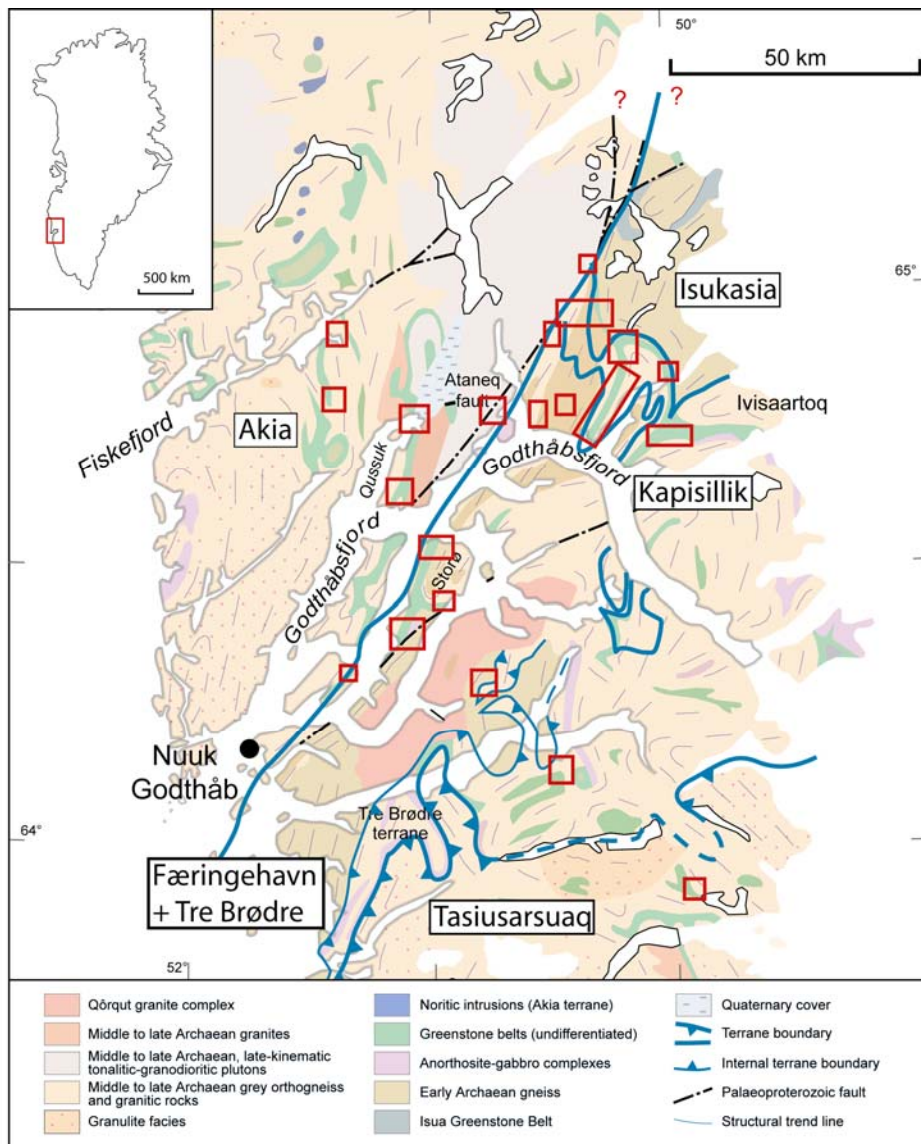


Figure 1. Simplified geological map of the Godthåbsfjord region, after Garde (2003). Names of Archaean terranes are shown in boxes. Red rectangles outline the areas visited by GEUS geologists during 2005 field work.

Background

Previous work

GEUS/GGU (the former Geological Survey of Greenland) has published several regional maps of the Godthåbsfjord region. These include the 1:500 000 scale Frederikshåb Isblink - Søndre Strømfjord geological map sheet (Allaart 1982) and four 1:100 000 scale map sheets: Fiskefjord 64 V.1 Nord (Garde 1989); Ivisârtoq 64 V.2 Nord (Chadwick & Coe 1988); Qôrqt 64 V.1 Syd (McGregor 1984, 1993); and Buksefjorden 63 V.1 Nord (Chadwick & Coe 1983). Further descriptions and references to recent GEUS work in the region of interest to this study can be found in Appel *et al.* (2003, 2005), Garde (1997), Hollis *et al.* (2004), Hollis (2005) and McGregor (1993).

The regional geology of the Godthåbsfjord region has been recently reviewed in Garde (2003) and Hollis *et al.* (2004) and so is outlined only briefly here (Fig. 1). The Godthåbsfjord region forms part of the Archaean North Atlantic craton (correlated with the Nain craton in Canada). The geology is dominated by amphibolite facies tonalitic orthogneiss with lesser basic magmatic rocks (anorthosite-gabbro complexes) and supracrustal belts comprising basic metavolcanic and volcanoclastic, ultramafic, and minor metasedimentary rocks.

The geology of the region has been subdivided into several chronologically distinct crustal blocks, known as terranes, which are thought to represent the remnants of small Archaean continents. These terranes probably formed via magmatic emplacement of tonalitic to granodioritic magmas in subduction-related tectonic environments. Major crust-forming events of this kind occurred at c. 3.87–3.65, 3.2–2.96, 2.94–2.86, and 2.83–2.75 Ga. During the Archaean, the different terranes experienced complex high-grade tectonothermal histories, with thermal events and associated deformation in some cases thought to be the product of amalgamation of different terranes via continental collision. Complete amalgamation of all the different crustal components that comprise the region was complete by c. 2.7 Ga. Resolving the distinct and shared tectonothermal evolutions of the different terranes is a complex puzzle that is the subject of continuing investigations by various research groups.

Supracrustal belts in the Godthåbsfjord region are known to have formed at c. 3.87, 3.71, 3.07, and 2.8 Ga. These belts occur both within and, more commonly, between distinct terranes. The timing of their formation in all cases corresponds with important episodes of magmatic crustal-growth. The generation of tonalitic magmas, in most cases at a similar time to volcanism and sedimentation, may be underpinned by a common tectonic environment, eg. subduction. However the relationship between supracrustal belts and the tonalitic orthogneisses is not well understood on the whole and is the subject of continued research.

Logistics

Logistics for the 2005 GEUS field work were the combined effort and responsibility of GEUS personnel, Greenland Resources A/S (GRAS), and Air Greenland. Three GEUS personnel – Tove Nielsen, Jakob Lautrup and Henrik Stendal – organised the transport of field equipment from Nuuk to the NunaMinerals A/S basecamp on Storø, from which GEUS also operated. GRAS was responsible for supply of food. Transport of equipment to Storø on July 12 was followed by the arrival of field geologists on and after July 15.

Four large GEUS projects operated in the Nuuk region from July 15 to August 26: 1) the Kapisillit 1:100 000 scale geological map sheet project; 2) ore geology work on Storø, Ivisaartoq and Isukasia; and the two projects reported here, ie. 3) investigation of supra-crustal rocks at Ujarassuit nunaat and regional follow-up work; and 4) regional investigations of hydrothermal systems. The field campaign comprised 40 participants representing scientists from GEUS, universities and Surveys (Danish and foreign). All field work was co-ordinated from the NunaMinerals A/S basecamp on Storø. GEUS and NunaMinerals A/S shared a full-time charter of an AS350 helicopter that was based on Storø for the period July 13 to August 26, . Thomas V. Rasmussen and Jakob Lautrup (GEUS) managed GEUS logistical operations, with support from Anders Lie (NunaMinerals A/S logistical co-ordinator) and GRAS.

Tectonothermal evolution of supracrustal belts in the inner Godthåbsfjord region

Introduction

Field mapping work in 2005 was concentrated in the Ujarassuit region (Figure 2), with sampling and follow-up work in the Ivisaartoq belt and the central Godthåbsfjord region. The main goals of the field work were to extend the investigation of supracrustal belts in the Nuuk region to the northeast, where map data is sparse in some areas, and where important Archaean and Proterozoic structures are not well understood.

The main field tasks included (1) detailed mapping and sampling of the supracrustal belts on Ujarassuit nunaat, and west to the Ataneq fault/Kangerssuaq, (2) mapping and sampling – mainly for geochemical studies – in the Ivisaartoq supracrustal belt, (3) mapping and characterisation of important structures in the vicinity of the Ataneq fault, and (4) follow-up work in the central Godthåbsfjord region based on key areas identified for understanding regionally important structures.

This summary outlines the current status of investigations, the main preliminary findings, and initial interpretations of the 2005 field work. Complete reports by the field geologists are given in Appendixes 2 to 6. Some whole rock trace and major element geochemical work has been carried out at ActLabs, Canada, and is available both in an ArcView© project and an Excel spreadsheet on the accompanying DVD. The results of that work are referred to in the relevant sections below. A further program of geochronological work is underway and will be presented in a report in 2006. Details of the work in progress are given below.

Background

Supracrustal rocks in the Ujarassuit region are thought to be associated with the Mesoproterozoic Ivisaartoq supracrustal belt, based on extrapolation of regional structural trends, but little field-based study of these rocks has been carried out. The supracrustal belt at Ujarassuit lies in a region between the Eo- to Palaeoproterozoic Isukasia and Færingehavn terranes, and possibly has genetic links to the Mesoproterozoic Akia terrane to the west (Friend and Nutman, 2005). The Akia terrane in this area is thought to be bound to the east by the extension of the Neoproterozoic Ivinnguit fault, which is also sub-parallel with the Proterozoic Ataneq fault here. However, no detailed mapping work has been undertaken in this particular area to test that interpretation or to investigate in detail the timing and degree of reworking of some of these important structures.

Map data

Field mapping was carried out by Ali Polat and Carlos Ordonez (University of Windsor), Ole Stecher, Jeroen van Gool, and Susanne Schmid (GEUS), and Nigel Kelly (University of Edinburgh). Eleven areas were selected as mapping targets of which ten have been mapped in detail during the field season. In this report area numbers refer to the map in Figure 2. Field reports by the mapping geologists are given in Appendixes 2–6. Compiled 2005 map data are available in ArcView© format on the accompanying DVD. The compiled map takes into account data from older GEUS field maps including Chadwick (1981), Crewe (1981, 1982), and Park (1986a). The DVD also includes data from related work in the Godthåbsfjord region carried out in 2004 and 2005 (GEUS reports 2004/110 and 2005/42). Explanatory notes to the DVD are given in Appendix 1.

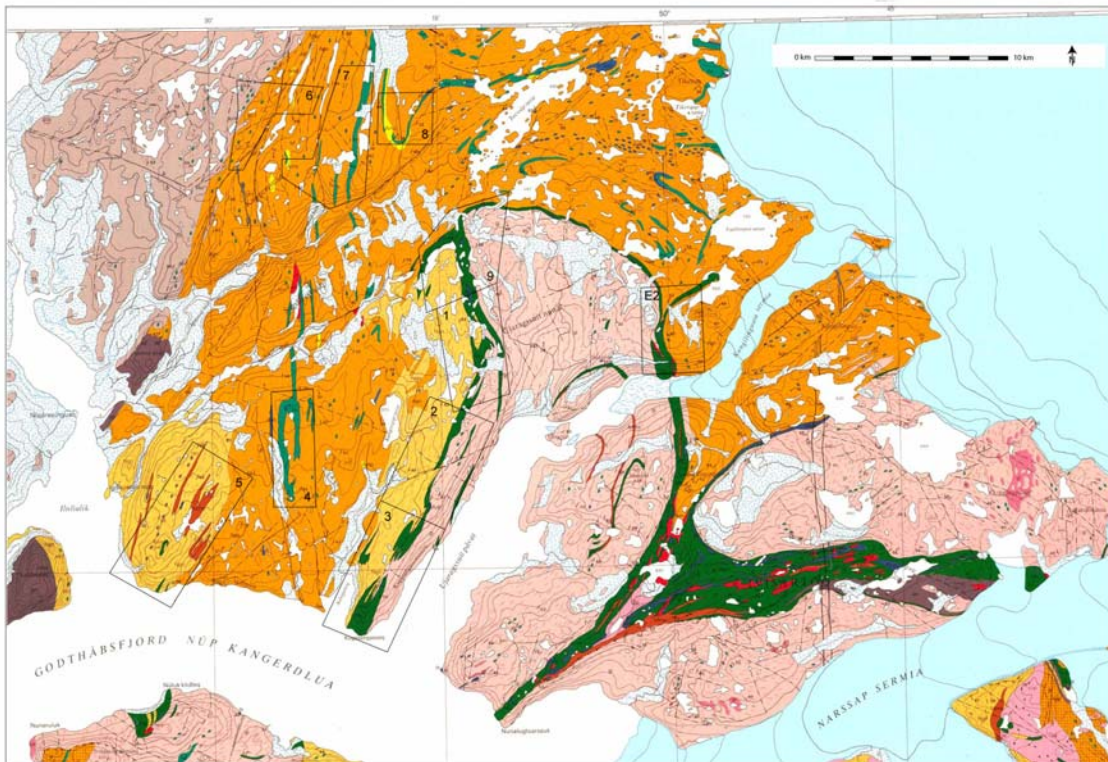


Figure 2. Areas 1–9 and E2, visited by field teams and referred to in the main text and Appendixes. The map is from a scan of the Ivisârtoq 1:100 000 scale geological map sheet (Chadwick & Coe 1988).

Ujarassuit Nunaat to Kangerssuaq

The mapping area between the Ujarassuit Nunaat dome (surrounding Ujarassuit Pavaat fjord) and the Ataneq fault consists of orthogneisses and supracrustal rocks that form part of four different terranes (Fig. 1). From northeast to southwest these are: the Isukasia terrane, Kapisilik terrane, Færingehavn terrane and the Tre-Brødre terrane in the extreme southwest. West of all these is the Akia terrane, occupied by the rocks of the Taserssuaq complex, and to a large extent separated from the others by the Ataneq fault. Since these belts are unnamed, they are referred to by the name of the terrane they occur in, and by the numbered mapping areas (Fig. 2).

All areas have in common that the rocks are highly deformed at amphibolite facies metamorphic grade and were intensely recrystallised. This hampers the recognition of protoliths, and primary textures in the rocks, and so interpretations of the primary nature of these rocks should be made with care. However, several lines of evidence support the interpretation that the amphibolite belts are supracrustal in origin. Banded amphibolites (subordinate to the homogeneous variety) display compositional banding on centimetre to decimetre scales, which is likely a primary feature based on the relatively low grade metamorphic grade (i.e. it is not likely to represent metamorphic differentiation). The protoliths to these rocks are thought to be volcanic and/or volcanoclastic rocks. Also, garnet-mica-bearing schist layers are intimately interleaved with the amphibolites, possibly reflecting a volcanogenic and reworked sedimentary component.

Hydrothermal alteration has affected the area, mainly visible in the alteration of amphibolites to biotite-bearing and more felsic lithologies.

Isukasia terrane

The supracrustal belt in the northeast of the mapping area is up to 500 m wide and consists predominantly of homogeneous amphibolite, which contains ultramafic lenses, and a quartz-rich garnet-biotite gneiss. Locally, the quartz-rich gneiss contains thin magnetite seams. Up to 50m wide sheets of homogeneous diorite to quartz-diorite are less deformed and appear intrusive into the belt. Leucogranite forms massive intrusive sheets up to 50 m wide in the supracrustal belt. Furthermore, the belt is heavily intruded by sheets of the surrounding orthogneiss complex, which is especially obvious near the main fold hinge. The orthogneisses in this area contain abundant amphibolite inclusions, some of which are obviously discordant dykes (Ameralik dykes), and are of Eoarchaean age (previously Amîtsoq gneisses). The supracrustal rocks are also of Eoarchaean age (previously the Akilia association). Geochronological analysis on a sample collected in 2005 by P. Appel confirmed the Eoarchaean provenance age, and gave a metamorphic age of c. 2.65 Ga (P. Appel and J. Hollis, pers. comm., December 2005).

The supracrustal belt defines the kilometre-scale Kangerssuaq antiform (Chadwick *et al.* 1983), of which the axial trace can be traced southwards through most of the mapping area. The antiform is overturned to the west and plunges gently to the south. The youngest fold structures on outcrop scale throughout the mapping area have orientations and asymmetries that are consistent with this antiform. They deform the regional dominant foliation and at least one generation of isoclinal folds.

Disseminated sulphides, predominantly pyrite, occur within amphibolite at the eastern contact of the quartz diorite, and west of the main leucogranite body in the western flank of the antiform. Analysed samples gave no economically significant results. Red staining of feldspars and epidote alteration occur commonly along some of the brittle faults, while Malachite staining was observed within amphibolite in two faults. Minor magnetite occurs in quartz-rich metasedimentary rocks.

Kapisilik terrane

The main supracrustal belt of Kapisilik terrane lies on the flanks of the Ujarassuit Nunaat dome, surrounding Ujarassuit Pavaat fjord, and is thought to be continuous with the Ivisaartoq belt to the east (Friend and Nutman, 2005). In the central and northern part of the mapping area, several other smaller supracrustal/amphibolite belts occur, which have a slightly different character.

The main supracrustal belt west of Ujarassuit Pavaat and along the eastern margin of the Kapisilik terrane in the north is dominated by amphibolite. Ultramafic inclusions are common and felsic gneisses ± garnet, garnet-biotite schists and anthophyllite schists occur commonly near the contact between amphibolite and ultramafic rocks. Amphibolites are highly variable in composition, and can be 1) finely banded, commonly of intermediate composition and fine-grained (Fig 3 photo jvg2005-039), 2) irregularly heterogeneous with abundant felsic veins and pods, as well as minor diopside, but also 3) homogeneous, medium-grained, more mafic parts occur (Fig. 4 photo nmk2005-032). None of these lithologies formed mappable entities on the scale of the map. Felsic veins occur in all lithologies. Medium-grained, homogeneous, foliated gabbro occurs locally in small bodies, up to 20 m wide, but highly deformed equivalents may be wide-spread. A 20-50 m wide band of homogeneous, massive diorite/quartz-diorite occurs at the western margin of the main belt in map areas 1 and 9. Also this supracrustal belt is intruded by sheets of orthogneiss and therefore older than one of the components of the surrounding orthogneisses. Friend *et al.* (2005) report a U-Pb zircon age of 3075 ± 15 Ma for metavolcanic rocks of the Ivisaartoq supracrustal belt.



Figure 3. *Banded amphibolite with abundant diopside.*

Several smaller satellite amphibolite belts of similar composition occur on either side of the main belt. A large, irregularly shaped amphibolite belt in the north is highly agmatized. Leuco-amphibolite and garnet biotite schist is uncommon here. These amphibolites were

not previously mapped as coherent belts but indicated as trains of inclusions, but they form fairly coherent bodies with well defined boundaries to the adjoining orthogneisses. These amphibolites are intruded by the regional orthogneiss, as well as by up to c. 50 m wide sheets of leucogranite and large volumes of pegmatite.



Figure 4. *Homogeneous mafic amphibolite with folded leucosome.*

The surrounding orthogneisses, dated by Friend and Nutman (2005) at c. 3070 Ma, consists of two components, a heterogeneous, locally banded tonalitic gneiss with abundant amphibolite inclusions, and a homogeneous, more massive granitic rock with a simple fabric. Near the amphibolite belt, the orthogneisses contain abundant amphibolite inclusions, which have a fabric that predates the main fabric in the orthogneiss. The contacts between the orthogneisses and amphibolites are irregular, as a combined result of the original intrusive nature of the contact, and subsequent isoclinal folding.

A preliminary inspection of the first geochemistry data suggest that at least some of the more felsic schists and gneisses are alteration products, based on their high Ni and Cr content. Thin rusty layers of biotite- and garnet-biotite schist or garnetiferous amphibolite occur commonly within the amphibolites (Fig. 5 photo jvg2005-287), and also these are assumed to be alteration products. Calc-silicate (diopside) alteration occurs along felsic veins on a centimetre to metre scale, often together with abundant garnet (Fig. 6 photo jvg2005-031). Locally, these felsic veins contain dispersed sulphides. None of the analysed samples from such alteration zones contained significant concentrations of economically interesting elements. A train of ultramafic rocks in the southern part of the agmatized amphibolite belt is intensely altered to talc and serpentine and may form a source for soapstone.



Figure 5. *Rusty, garnet rich layers within amphibolite.*



Figure 6. *Felsic veins in this banded amphibolite contain garnet, and are surrounded by calc-silicate-rich rock.*

Map area 4 – Færingehavn terrane?

Map area 4 lies within the area that was defined by Friend and Nutman (2005) as part of the Færingehavn terrane. However, new unpublished U-Pb geochronology data (C. Friend and A. Nutman, pers. com. 2005) suggest that orthogneisses in this area have a Mesoproterozoic age that is similar to the age of the orthogneisses in the Kapisilik terrane, which would reduce the size of the Færingehavn terrane in the map area considerably. This hypothesis will be tested by further geochronological analyses.

The supracrustal belt in area 4 outlines a kilometre-scale fold interference structure (see Fig. A3_4 in Appendix 3). The rocks in this belt are dominated by a variety of amphibolites with large ultramafic lenses, and are interleaved with bands of a garnet-quartz-rich gneiss (Fig 7. photo nmk2005-119), which is commonly biotite- and magnetite-bearing. Orthogneisses in the area have a strong gneissic fabric of alternating felsic and biotite-rich domains, and contain abundant leucosome, in veins parallel to the gneissosity. A more massive, homogeneous grey orthogneiss is subordinate. Orthogneisses intruded into the amphibolites of the supracrustal belt.



Figure 7. *Less than 1cm sized garnet porphyroblasts in garnet-biotite-quartz-rich rock.*

Amphibolites occur both in a homogeneous variety, which is dominant, and as banded amphibolites of intermediate compositions, which form discontinuous layers. The homogeneous amphibolites may be sub-divided into a massive, mafic variety and a weakly banded grey amphibolite, which is slightly finer-grained, compared to the mafic one. Garnet-quartz-

rich gneiss forms thin discontinuous layers within amphibolite and contains quartz, biotite, plagioclase magnetite and commonly abundant garnet. Ultramafic rocks include 1) green-brown rocks composed mainly of large, pale amphibole porphyroblasts in a matrix of amphibole, serpentine and olivine, ± phlogopite; and 2) black dunitic rocks composed of coarse-grained hornblende with disseminated olivine and minor phlogopite.

The occurrence of quartz-rich garnet- and magnetite-bearing rocks is most reminiscent of metasedimentary rocks in the Isukasia terrane (area 8) and has not been recognised in amphibolite belts in the Kapisilik terrane. This correlation would be in contrast with new (yet unpublished) interpretation that the supracrustal rocks of area 4 lies within the Kapisilik terrane.

Observed alteration is limited to retrogression in brittle faults to epidote and chlorite, and minor hydration of ultramafic rocks to serpentine-talc.

Tre Brødre terrane (map area 5)

This area consists of several isoclinally folded narrow belts of supracrustal rocks within orthogneiss. These supracrustal rocks are portrayed on the 1:100 000 scale map as Malene metasediments. Although garnet-biotite schists are dominant in these belts, significant volumes of amphibolite were found as well, of which a few had been indicated on the pre-existing field map of Crewe (1982, see file on DVD). Rocks of the Tre Brødre terrane are of Neoproterozoic age (Friend & Nutman 2005).

The dominant garnet-biotite schist has variable abundance of biotite, and is commonly rather felsic in composition (Fig. 8 photo nmk2005-296). Garnets are common and occur as single grains or large clusters; sillimanite ± staurolite or orthoamphibolite are less common. Amphibolites in the area comprise: 1) banded amphibolite, with a compositional layering on centimetre- to metre-scale, locally garnet-bearing and contains interlayered garnet-biotite schist; 2) homogeneous grey amphibolite, which is typically medium-grained and mafic to intermediate in composition, locally with disseminated garnet (Fig. 9 photo nmk2005-276); and 3) massive mafic amphibolite, mainly coarse-grained and commonly garnet-rich. The banded version is the most abundant, with the other two types commonly forming layers within it. A large mappable unit of the garnetiferous, mafic amphibolite occurs in the south-west of area 5. Ultramafic rocks occur as lenses or layers associated with the amphibolites.

Orthogneisses in the area, presumably Ikkattoq gneisses, are typically homogeneous to weakly banded with minor volumes of spaced leucosome, and rare layers and inclusions of amphibolite. The orthogneiss is commonly garnet-bearing where it occurs interlayered with garnet-biotite schist or amphibolite. In the southeast, these gneisses are in contact with a complex, migmatitic orthogneiss, which is assumed to be part of the Færingehavn terrane.

Mineralisation and alteration of rocks is insignificant. Few rust zones developed in biotite-rich rocks, but no sulphide or oxide mineralisation was observed.



Figure 8. *Garnet-biotite-bearing felsic schist; moderately migmatitic and deformed.*



Figure 9. *Homogeneous garnet-bearing mafic to intermediate amphibolite.*

Akia terrane – Taserssuaq pluton

The north-western part of the map area is underlain by rocks of the Taserssuaq pluton, which are part of the Akia terrane. They form mainly medium- to coarse-grained foliated tonalites to granodiorites and are locally porphyritic. In the mapping area these rocks are weakly deformed, but they are cut by a few narrow shear zones. The rocks of the pluton have an intrusive contact with orthogneisses and amphibolites to the east, which appear in outcrop more like those of the Kapisilik terrane occurring mainly east of the Ataneq fault, than like Nuuk gneisses. This needs to be tested by geochronology.

Metadolerite dykes

Mafic dykes in the area occur predominantly in two orientations, striking east-west and north-south. They consist predominantly of fine-grained clinopyroxene and plagioclase, and have been affected by minimal recrystallisation, although locally remnant igneous textures occur. Five to ten centimetres wide dykes are common, and few are between 2 and 6 metres wide. A single, north-south trending dyke is up to 100 m wide, locally ultramafic in composition and medium to coarse-grained. It can be traced for more than 100 km. All these dykes are assumed part of the Proterozoic dyke systems in West Greenland.

Ataneq fault system

The Ataneq fault occurs in a 4 km wide zone containing one or more systems of faults and shear zones. The Ataneq fault ss. is a brittle fault system to the west of the centre of this zone with at least 4 km dextral displacement of Proterozoic metadolerite dykes. At least three distinct types of deformation seem to be associated with the fault and show extended or repeated activity with reworking of older shear structures in different kinematic regimes.

A few ductile shear zones were observed, consisting of straight gneisses containing porphyroclasts. These show oblique, top-to-the-west dextral displacement. Retrograde, fine-grained shear zones are common in the 4 km wide zone around the Ataneq fault. Lineations are commonly weak, and kinematic indicators show a reasonably consistent top-down-to the east, extensional displacement (Fig. 10 photo jpg2005-455). Some of these zones show cataclastic fabrics, indicating a late brittle reworking. Some of the retrograde zones and all the cataclastic ones form rusty zones with minor sulphide mineralisation. Molybdenite was found in one of the cataclastic zones.

Although along parts, the Ataneq fault separates different terranes, it is not a terrane boundary in the strict definition. It displaces (possibly reworks) the pre-existing Ivinnuit fault terrane boundary along parts of its exposed length, but since the Taserssuaq pluton occurs on both sides of the Ataneq fault it is not a terrane boundary in itself. In map area 6, the Ataneq fault is located within orthogneisses and does not form the boundary to the Taserssuaq pluton.



Figure 10. *Shear zone with top down to the east kinematic indicators (looking north).*

Structural evolution of the Ujarassuit Nunaat area

In the whole region, we can commonly recognise the following succession of events:

1. deformation of supracrustal belts
2. intrusion of regional orthogneisses
3. development of main foliation, presumably in several stages
4. isoclinal folding
5. overturned folding over shallowly south plunging axes
6. retrograde shearing
7. brittle faulting

The latest structural features, brittle faults (7), retrograde shear zones (6) and upright folds (5) are common to all terranes, but the earlier features (2 and 4) must be diachronous in the different terranes in rocks of significantly different ages. However, no discordant foliations have been observed at terrane boundaries, suggesting that the latest deformation that transposed earlier structures into a common foliation, was synchronous with, or post-dated the juxtaposition of the terranes.

The main foliation (3) consists of a gneissic fabric with differentiation of leucosome in the orthogneisses and a foliation defined mainly by amphiboles in the amphibolites. A weakly developed lineation commonly plunges shallowly to the south. In areas of low strain in the Kapisilik terrane and in area 4, amphibolite inclusions contain a foliation that is truncated by the orthogneisses and predates the regional main foliation (Fig. 11 photo jpg2005-047). However, the older foliation in the amphibolites has been transposed to the main foliation orientation in most of the mapping area. Throughout the area, indications were found that the main foliation is a composite fabric, resulting from several deformation phases. Evi-

dence for this includes rootless folds (Fig. 12 photo nmk2005-240) and variably deformed pegmatites and leucosomes that truncate and are deformed by the main foliation. A ductile shear fabric occurs locally in orientations that cannot be distinguished from the main foliation, and this composite fabric includes locally a phase of ductile shearing. In the northwest of the map area (areas 6 and 7) reverse, top to the west kinematic indicators are observed within these shear zones.



Figure 11. *Inclusions of amphibolite within migmatitic orthogneiss, the former containing an early foliation.*

Isoclinal folds that deform the main foliation (4) are common on outcrop scale (Fig. 13 photo jpg2005-444), and occur also on map scale, commonly seen in map areas 4 and 5 (Fig. A3_4 in Appendix 3). In few locations, overprinting isoclinal folds indicate that at least 2 generations exist locally.

The dominant folding phase (5; F_{n+3} in Appendix 3; F_3 in Appendix 2) affects all terranes and their contacts similarly. These folds are overturned to the west and fold axes plunge shallowly to the south. The large-scale folds in the map, including the Ujarassuit Nunaat dome and Kangerssuaq antiform, are all of this generation. Outcrop scale parasitic folds are common and are commonly asymmetric, predominantly west-vergent to the west of the trace to the Kangerssuaq antiform. No axial planar fabric is associated with these folds. The orientation of the fold axes is sub-parallel to that of the dominant lineations in the region, which may indicate a common origin, but no evidence for this was observed.

All structures described above are typically associated with amphibolite facies mineral grain shapes. Retrograde shear zones (6) that occur predominantly in a 4 km wide zone surrounding the Ataneq fault are of greenschist facies. Amphibolites are altered to biotite and/or chlorite-rich schists in these shear zones. Locally, the zones are overprinted by a phase of cataclastic deformation. They are slightly anastomosing, but overall parallel with, or at a small angle to the main foliation. Mineral lineations are weakly developed and variable in orientation, but predominantly east to southeast plunging, and kinematic indicators

give a top down to the east, extensional movement pattern, which is in contrast with earlier reports on shearing in the area (Park 1986b), but consistent with late extensional deformation near the Ataneq fault reported from the Isua area further north (Hanmer & Green 2002). The retrograde shear zones appear not to displace the metadolerite dykes. Many of these zones are rusty and include locally disseminated sulphides (pyrite and chalcopyrite), and molybdenite was observed in one location. Beside the molybdenite sample, geochemical analyses revealed no significantly elevated concentrations of economic elements.

Vertical brittle faults (7) occur mainly in three orientations trending north-south, northeast-southwest and east-west. These faults have not been studied systematically, but dextral offsets appear to be dominant. Proterozoic dolerite dykes are seen offset by the northeast trending faults, which means that at least some of these faults are Proterozoic. But the occurrence of different fabric types in the Ataneq fault suggests that the fault systems were reactivated at different times.



Figure 12. *Folded layering and leucosome in deformed felsic orthogneiss.*



Figure 13. *Refolded isoclinal folds of foliation in amphibolite.*

Ivisaartoq belt

Field work in the Ivisaartoq supracrustal belt was aimed at further investigating the geological environment of the belt via a geochemical study. Field work involved description of the main lithologies, primary structures, and alteration zones, with field work based on existing detailed geological maps of this belt (Chadwick 1981; Crewe 1981, 1982; Park 1986). Previous related geochemical studies in the Ivisaartoq region are reported in Polat (2005). 2005 investigations were particularly focussed on the geochemistry of mafic to ultramafic volcanic rocks and gabbros, to constrain their likely environment/s of formation, and on locally pervasive calc-silicate alteration, to constrain the nature and timing of sea-floor hydrothermal alteration as well as post-magmatic metamorphic alteration. A summary of the field work is reported in Appendixes 4 and 5. Geochemical data for the samples collected are not yet available and will be reported in 2006.

Regional tectonic sections

Regional tectonic sections are useful for understanding the important regional structures and structural evolution of the distinct crustal terranes. Seven ten-kilometre-scale traverses in key selected areas of the central Godthåbsfjord are currently being constructed based on existing and GEUS map data collected in 2004 and 2005. Progress on the construction of these sections is reported in Appendix 6. The sections take into account field mapping and structural data, geochronology, and geophysical data.

The detailed tectonic sections across Storø are designed to illustrate the three-dimensional structure of the gold-mineralised supracrustal belt and the Storø shear zone. The regional sections are designed to illustrate and interpret the significance of some of the large-scale

structures including the Ivinnguit fault and the Storø shear zone. Reactivation and tectonic overprinting of major structures from the Mesoproterozoic to the Late Neoproterozoic is found to be important in both the Storø shear zone and the Ivinnguit fault. The completed tectonic sections will be reported in 2006.

Progress of analytical work

Geochemistry

During the field work over 130 samples were collected for geochemical analysis. The main purpose was to geochemically characterise the supracrustal belts and to investigate their original intrusive/depositional environment/s. In addition, all samples are or will be also analysed for precious metals.

To date, the results of two sets of samples, which have been analysed for whole rock major and trace element geochemistry have been completed. A selection of the most important elements is shown in the ArcView© project, and the full dataset are given in an Excel spreadsheet on the accompanying DVD. The remaining analyses will be carried out and the results presented in mid 2006, and will include major, trace and rare earth element analyses.

The composition of sulphide-bearing quartzo-feldspathic gneisses and aluminous gneisses within the amphibolite belts are interpreted as alteration products, based on their trace element compositions. Samples 498410 and 498411 were collected in map area 1 in a felsic gneiss outcrop adjacent to an ultramafic rock within the main amphibolite belt. High Ni, Zn and Cr values suggest that these rocks are likely altered from an original ultramafic composition. Elevated molybdenum was found in a cataclastic to low temperature shear zone in the northwest of the map area (sample 498473). An additional c. 100 samples were collected by Polat and Ordonez, to be analysed for major and trace element geochemistry in the laboratories of the University of Windsor. The results of these analyses will also be reported in mid 2006.

Geochronology

Of 73 samples that were collected for potential geochronology, 23 samples were selected for analysis. The samples are selected with the purpose of establishing the ages of the supracrustal belts, to investigate the detrital zircon populations of metasedimentary rocks, and to establish the ages of the surrounding orthogneisses and the felsic igneous rocks that intrude the supracrustal belts. Furthermore, the ages of metamorphism will be investigated in the different terranes.

Mineral separates of the selected samples are currently being prepared. U-Pb analyses will be carried out on zircons at the laser ablation-sector field-inductively coupled plasma-mass spectrometer laboratory at GEUS. Results will be reported in mid 2006.

Concluding remarks

- Existing geological maps of the Ujarassuit area have been revised to include several previously unrecognised amphibolite belts, and including revision of some lithologies in parts of the area.
- The amphibolite belts are interpreted as supracrustal in origin on the basis of the lithological association of basic volcanic or volcanoclastic, ultramafic, and metasedimentary rocks.
- The amphibolite belts are intruded by the regional orthogneisses in each of the terranes investigated.
- Variable alteration in the amphibolite belts that in a few cases has produced mica-rich and quartz-rich rocks that appear similar to metasedimentary rocks, but are thought to be derived from amphibolite and ultramafic precursors. This is supported by their unusual trace element geochemistry, enriched in Cr and Ni. However, in other cases true metasedimentary rocks are present (as mentioned above).
- The amphibolite belts have all experienced amphibolite facies metamorphism and are strongly tectonised and recrystallised.
- The structure of the Ujarassuit area is dominated by a number of large late Archaean west-vergent folds that include the Kangerssuaq antiform and the Ujarassuit Nunaat dome, which overprints several older isoclinal map-scale structures.
- The Proterozoic Ataneq fault has a complex history that involves multiple reactivation of shear zones under greenschist facies conditions.
- Widespread extensional deformation has occurred in these shear zones.
- A molybdenite-mineralised shear zone was identified in the vicinity of the Ataneq fault.
- The construction of seven regional tectonic sections through the Godthåbsfjord region is underway. These are designed to aid in interpretation of the regional structural evolution.
- Geochemical analyses, in addition to those reported here and particularly from the Ivisaartoq supracrustal belt, are underway.
- Twenty-three key samples have been selected for U-Pb zircon geochronology, with sample preparation for LA-SF-ICP-MS analyses underway.

Potential for precious metals in hydrothermal systems within the wider Godthåbsfjord region

Introduction

The aim of the fieldwork was to investigate the geological setting and evolution of important supracrustal rocks (greenstone belts) with respect to their mineral potential especially for precious metals. The study was focussed on hydrothermal systems in the Fiskefjord region (F1 & F2; Fig. 14), two areas on Qussuk peninsula (Qu; Fig. 14), three areas along the Ataneq fault (At; Fig. 14), south of Ameralik (Am; Fig. 14), Qooqqut (Qo; Fig. 14), and southeast of Kangerdluarssenguup taserssua (Kang; Fig. 14). The investigations comprised hydrothermal alterations along the Proterozoic Ataneq fault zone; investigation of the border zone between the Tre Brødre and Tasiuarsuaq terranes including studies of the terranes themselves for possible gold-bearing rocks (e.g. Ameralik); detailed investigations in the Fiskefjord region, where mafic- to ultramafic rocks were studied with the purpose of evaluating the Cu-Ni and PGE potential of ultramafic and mafic rocks of a magmatic complex; and, finally, studies of the mafic volcanic sequence in the Tasiuarsuaq terrane south-east of Kangerdluarssenguup taserssua.

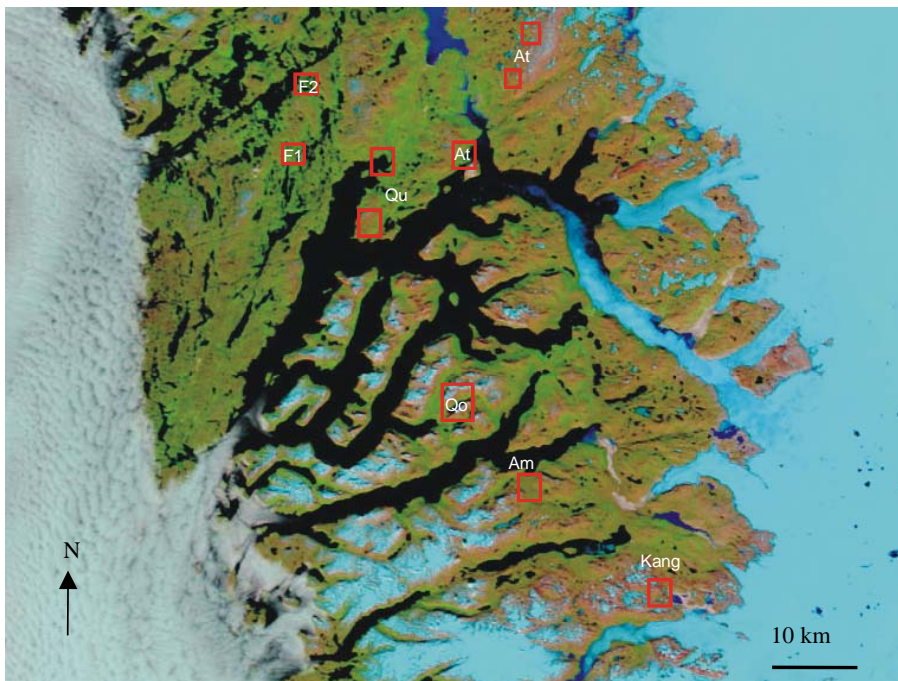


Figure 14. *Satellite photo of the Nuuk region. Red squares outline the investigated areas by the hydrothermal systems project in 2005. Am: Ameralik S area; At: Ataneq fault areas; F1 & F2: Fiskefjord areas; Kang: area southeast of Kangerdluarssenguup taserssua; Qo: Qooqqut area; and Qu: Qussuk peninsula.*

Analytical methods

Geochemical data were obtained at Activation Laboratories, Ancaster, Canada. Analyses were made by various methods, referred to by their abbreviations in the tables, including nickel sulphide fire assay – inductively coupled plasma mass spectrometry (FA-MS), total digestion-inductively coupled plasma emission or mass spectrometry (TD-ICP), fusion-X-ray fluorescence spectrometry (FUS-XRF), and instrumental neutron activation analysis (INAA).

Fiskefjord

The southern Fiskefjord location was at the position N 64°49.054' and W 051°28.356' at 310 m elevation (Figs. 14 & 15). The location is the same as visited during the field season 2004 (HST camp 1; Appel et al. 2005). The studied area covers ~8 km². The northern Fiskefjord 2 area (Fig. 15) is located at N 64°55.688' and W 051°25.657' at ~125 m elevation. The size of the area is about 0.5 km². The mafic- to ultramafic rocks of a magmatic complex were studied with the purpose of assessing their Cu-Ni and PGE potential. The two areas were investigated by Tine Kristensen (TK), University of Aarhus and Henrik Stendal (HST), GEUS. TK did fieldwork for her M.Sc. thesis and was assisted by Lizette Apel Jensen.

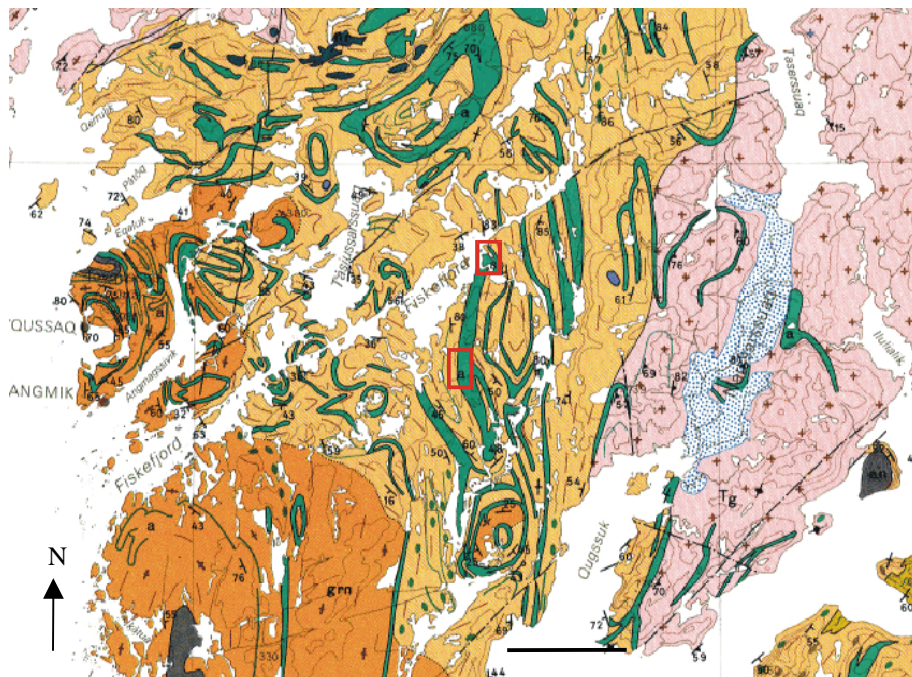


Figure 15. Fiskefjord area – part of the 1:500,000 scale Greenland map sheet 2 (Allaart 1982). The target for the investigations was the green N-S striking band, which in the map legend is designated as undifferentiated amphibolite.

Geology

The Fiskefjord area is located in the c. 3.2-2.97 Ga Akia terrane, covered by the geological map sheet Fiskefjord (scale 1:100 000; Garde 1989; 1997). The detailed investigations included geological mapping and sampling of specimens (see Appendix 9 for further detailed description and maps of the areas). The main focus was on a mafic- to ultramafic sequence including dunite, peridotite, pyroxenite, norite and amphibolites hosted by tonalitic and trondhjemitic gneisses. The ultramafic bodies in the Fiskefjord area are dominated by peridotites, some very olivine-rich sections weather easily to form deposits of olivine sand. Pyroxenites commonly border the peridotites. The ultramafic rocks commonly have a characteristic brown alteration colour (Fig. 16). The bodies are up to 50 m wide and can be followed for over 2 km along strike and the general structural strike is N-S. Light grey, middle- to coarse-grained norite overlies the ultramafic suite (Fig. 16). The norite have cm-dm thick strata-bound rusty layers (Fig. 17) with low-grade disseminated sulphides (pyrrhotite, chalcopyrite). The amphibolites are uniform, fine- to middle-grained and often layered (cm–dm layers) that have intercalated weakly sulphide-bearing layers. The amphibolites are mostly characterised by lack of alterations. Besides sulphides, occasionally magnetite occurs in both ultramafic and mafic rocks.



Figure 16. *Brown weathered peridotite and olivine-rich sand. Blocks of light grey norite are seen in the foreground*



Figure 17. *Strata-bound rusty layers in norite, Fiskefjord area F1.*

Analytical results

Analytical data for selected rock samples from the Fiskefjord area show enhanced values of precious metals such as gold (Au), platinum (Pt) and palladium (Pd; Table 1). The highest values are (FA-MS method) 326 ppb Au, 51 ppb Pt and 27 ppb Pd from a rusty band with disseminated sulphides. It seems that the weakly sulphide-bearing norite and amphibolite sequences have the highest concentrations of precious metals. The precious metal values clearly demonstrate that the magmatic mafic-ultramafic complex is a promising target for PGE exploration.

Chromite is present in rocks with high magnetite content, e.g. 497825 with 1.4% Cr (Tables 1 & 2). The magnetite is often an alteration product from chromite, but primary magnetite also occurs. The content of both Cu and Ni vary with values up to 0.17% for. There is no correlation between Cu and Ni, because Ni occurs in both sulphides and olivine, and Cu mainly in sulphides. The SiO₂ content varies from 37 – 63% (Table 2), and elevated silica together with elevated sodium and potassium in the mafic to ultramafic rocks is ascribed to hydrothermal alteration. The alteration processes are serpentinisation, silicification and albitisation. The ultramafic rocks are characterised by high MgO content up to 40%.

Table 1. Selected trace element concentrations in the Fiskefjord samples.

Element:	Au	Pt	Pd	Au	Cu	Ni	Zn	As	Co	Cr	Sr	V	Mass Description
Units:	ppb	ppb	ppb	ppb	ppm	ppm	ppm	ppm	ppm	ppm	ppm	ppm	g
Detection Limit:	1	0.5	0.5	2	1	1	1	0.5	1	2	1	2	
Reference Method:	FA-MS	FA-MS	FA-MS	INAA	TD-ICP	INAA / TD-ICP	INAA / TD-ICP	INAA	INAA	INAA	TD-ICP	TD-ICP	INAA
497801	9	12,2	16,4	21	569	200	87	< 0.5	70	3700	85	289	22,5 Rusty amphibolite
497802	< 1	2,7	1,7	< 2	8	682	25	1,3	115	5510	7	87	17,7 Peridotite with chrom-diopside and magnetite banding
497809	32	5,8	6,2	46	1360	168	231	2,2	94	601	272	248	22,5 Rust band with disseminated sulphides in banded amphibolite
497810	< 1	0,7	< 0.5	< 2	30	116	97	< 0.5	52	276	476	328	27,5 Banded amphibolite
497811	< 1	4,9	5,1	< 2	32	244	127	< 0.5	44	967	190	236	19,4 High-strain gneiss with quartz pegmatites
497812	< 1	2,2	2,2	< 2	120	1130	28	6,8	151	2000	18	103	26,3 Dark peridotite with disseminated sulphides
497813	< 1	11,2	9,1	< 2	6	240	80	< 0.5	58	888	330	206	22,2 Massive banded amphibolite
497816	326	51	27,2	502	788	154	81	6,9	107	791	73	243	24,8 Rust band in norite with disseminated sulphides and chromite
497817	< 1	1,8	< 0.5	< 2	7	1610	34	1,9	178	2510	< 1	45	25,6 Peridotite with magnetite/chromite and fuchsite
497820	< 1	2	< 0.5	7	3	1300	30	6,5	161	4590	5	66	29 Peridotite with magnetite/chromite
497823	< 1	< 0.5	5,7	6	52	83	28	2,8	82	20	52	13	21,5 Dark norite/pyroxenite
497824	3	20,5	< 0.5	< 2	234	107	75	4,8	34	28	415	568	18,4 High-strain norite with bands of magnetite
497825	< 1	2,3	2	< 2	4	1670	58	1,8	156	14000	14	129	23,9 Norite with bands of magnetite
497826	84	6	26,3	111	953	396	124	4,7	89	42	8	1280	19,4 Norite with bands of magnetite
497827	1	4,8	4,6	< 2	128	154	95	2,8	66	413	184	339	20,9 Dark, homogeneous amphibolite with bands of rust
497829	2	3,3	13,2	< 2	1740	76	30	3,3	81	1820	5	218	21,6 Rust band with disseminated sulphides in norite
497830	< 1	6,4	2,2	< 2	70	114	99	< 0.5	59	411	252	251	20,8 Rust band with disseminated sulphides in high-strain norite
497831	4	1,3	< 0.5	< 2	525	211	69	1,8	97	468	175	253	23,6 Rust band with disseminated sulphides in dark, banded norite
497832	< 1	6,7	3,7	< 2	7	325	66	5,6	80	1120	129	199	21,4 Dark norite
497833	< 1	23,4	4,4	< 2	3	1410	75	3,3	194	8470	4	87	24,5 Peridotite/dunite with magnetite/chromite
497835	< 1	12,8	10,6	< 2	70	116	98	1,5	64	832	343	390	24,8 Rusty metasediment with garnet
497836	60	1,9	< 0.5	51	1530	86	173	1,8	76	399	332	168	20 Rust band with disseminated sulphides in dark, banded norite/amphibolite
497838	< 1	7,1	8,1	< 2	2	738	23	< 0.5	111	4040	6	174	23,9 Fine-grained peridotite with magnetite/chromite
497839	< 1	3,9	13,2	3	3	1570	64	2,4	186	6250	1	65	28,4 Fine-grained peridotite with magnetite/chromite and chrom-diopside
497840	3	0,8	< 0.5	< 2	422	212	66	8,8	92	395	118	277	20,4 Rust band with disseminated sulphides in dark, banded norite
497843	19	< 0.5	< 0.5	27	510	17	147	1,5	98	16	144	537	23,9 Rust band with disseminated sulphides in dark, banded norite
497844	4	4,6	3,2	< 2	153	18	116	2,2	48	11	166	588	21,6 Rust band with magnetite in dark, banded norite
497845	3	1	1	< 2	206	245	82	< 0.5	99	429	278	361	21,7 Rust band with disseminated sulphides in banded norite
497846	3	< 0.5	< 0.5	15	91	38	118	1,1	51	15	337	425	22,1 Banded amphibolite with garnet and magnetite
497847	248	0,9	0,5	393	217	69	152	2,7	49	178	234	320	20,9 Rust band in dark amphibolite with magnetite
497848	< 1	3,8	2	7	70	161	70	3,1	60	454	195	265	22,9 Banded amphibolite
497849	< 1	1	1,4	< 2	3	241	18	2,2	59	992	85	113	21,7 Light norite

Table 2. Major element oxide concentrations in selected Fiskefjord samples.

	SiO2	Al2O3	Fe2O3	MnO	MgO	CaO	Na2O	K2O	TiO2	P2O5	Cr2O3	LOI	Total	Description
	%	%	%	%	%	%	%	%	%	%	%	%	%	%
	0.01	0.01	0.01	0.001	0.01	0.01	0.01	0.01	0.01	0.01	0.01	0.01	0.01	0.01
	FUS-XRF	FUS-XRF	FUS-XRF	FUS-XRF	FUS-XRF	FUS-XRF	FUS-XRF	FUS-XRF	FUS-XRF	FUS-XRF	FUS-XRF	FUS-XRF	FUS-XRF	FUS-XRF
497801	47,59	12,1	13,63	0,198	10,72	11,01	1,06	0,07	0,6	0,03	0,44	1,83	99,28	Rusty amphibolite
497802	48,62	3,11	7,91	0,082	32,48	4,14	0,07	0,03	0,09	0,01	0,6	1,85	99	Peridotite with chrom-diopside and magnetite banding
497809	37,15	18,65	17,21	0,209	8,26	11,11	1,11	1,09	1,14	0,05	0,08	3,44	99,5	Rust band with disseminated sulphides in banded amphibolite
497810	46,8	14,85	14,91	0,198	7,48	10,17	2,95	0,37	1,73	0,15	0,04	0,07	99,71	Banded amphibolite
497811	59,04	23,42	6,44	0,04	4,79	0,97	0,89	1,19	0,93	0,02	0,11	1,17	99,01	High-strain gneiss with quartz pegmatites
497812	41,85	6,45	15,27	0,177	27,18	5,05	0,17	0,06	0,3	0,03	0,25	2,01	98,8	Dark peridotite with disseminated sulphides
497813	50,11	12,12	11,07	0,196	9,95	12	1,84	0,31	0,52	0,04	0,11	1,33	99,6	Massive banded amphibolite
497816	48,02	13,82	14,58	0,231	14,58	6,99	0,77	0,08	0,22	0,01	0,09	0,83	100,2	Rust band in norite with disseminated sulphides and chromite
497817	40,08	2,12	16,16	0,218	40,23	0,99	< 0.01	0,02	0,06	0,01	0,31	< 0.01	99,93	Peridotite with magnetite/chromite and fuchsite
497820	42,42	3,43	16,09	0,213	36,86	0,82	0,05	0,04	0,08	0,02	0,59	< 0.01	100,4	Peridotite with magnetite/chromite
497823	62,02	10,76	16,59	0,148	1,91	5,37	1,74	0,27	0,94	0,17	< 0.01	< 0.01	99,65	Dark norite/pyroxenite
497824	62,81	14,73	7,56	0,069	3,85	4,14	3,32	1,57	0,78	0,02	0,01	0,56	99,4	High-strain norite with bands of magnetite
497825	40,49	3,46	15,69	0,185	35,63	1,63	0,12	0,04	0,2	0,02	1,7	0,28	99,45	Norite with bands of magnetite
497826	37,99	3,04	43,5	0,582	12,01	0,69	0,32	0,11	1,53	0,02	0,01	< 0.01	99,17	Norite with bands of magnetite
497827	48,42	15,31	13,69	0,206	7,24	11,83	2,28	0,21	1,07	0,08	0,05	0,08	100,5	Dark, homogeneous amphibolite with bands of rust
497829	47,75	5,53	15,23	0,166	24,53	4,36	0,78	0,16	0,18	0,02	0,2	0,95	99,85	Rust band with disseminated sulphides in norite
497830	--	--	--	--	--	--	--	--	--	--	--	--	--	-- Rust band with disseminated sulphides in high-strain norite
497831	44,91	20,01	12,26	0,122	5,09	11,8	2,04	0,09	0,56	0,04	0,06	3,04	100	Rust band with disseminated sulphides in dark, banded norite
497832	47,76	11,87	12,58	0,209	12,84	11,25	1,33	0,22	0,5	0,03	0,13	0,35	99,07	Dark norite
497833	38,46	1,44	15,95	0,36	39,13	2,06	0,07	0,04	0,06	0,01	1,04	1,33	99,95	Peridotite/dunite with magnetite/chromite
497835	50,81	17,75	13,63	0,237	8,18	4,3	2,39	0,54	1,22	0,05	0,1	< 0.01	98,93	Rusty metasediment with garnet
497836	50,67	12,89	16,26	0,24	10,01	5,88	2,19	0,11	0,47	0,07	0,05	0,93	99,77	Rust band with disseminated sulphides in dark, banded norite/amphibolite
497838	47,28	3,9	9,26	0,173	31,01	5,84	0,37	0,05	0,1	0,01	0,5	0,89	99,38	Fine-grained peridotite with magnetite/chromite
497839	39,33	1,05	16,48	0,285	39,75	1,23	0,02	0,02	0,04	0,01	0,82	0,19	99,22	Fine-grained peridotite with magnetite/chromite and chrom-diopside
497840	54,96	17,95	8,15	0,09	3,31	11,3	1,74	0,08	0,68	0,05	0,05	1,34	99,7	Rust band with disseminated sulphides in dark, banded norite
497843	--	--	--	--	--	--	--	--	--	--	--	--	--	-- Rust band with disseminated sulphides in dark, banded norite
497844	--	--	--	--	--	--	--	--	--	--	--	--	--	-- Rust band with magnetite in dark, banded norite
497845	--	--	--	--	--	--	--	--	--	--	--	--	--	-- Rust band with disseminated sulphides in banded norite
497846	46,7	12,33	17,77	0,285	4,81	13,12	2,02	0,19	2,49	0,2	< 0.01	0,15	100,1	Banded amphibolite with garnet and magnetite
497847	43,21	12,38	21,92	0,42	6,72	11,17	1,3	0,26	0,84	0,07	0,02	0,47	98,78	Rust band in dark amphibolite with magnetite
497848	47,91	14,74	11,26	0,237	6,21	15,64	1,77	0,1	0,75	0,05	0,06	0,47	99,2	Banded amphibolite
497849	48,05	18,22	6,05	0,088	15,92	9,53	0,72	0,06	0,11	0,01	0,11	0,12	98,99	Light norite

Qussuk peninsula

Two sites were studied in Qussuk peninsula (Fig. 14) with the objective of locating areas of hydrothermal alteration and determining the types of mineral occurrences within them. The position of the southern field area was N 64°39.321 and W 051°08.472 at 610 m elevation. The focus areas were the southern part of Qussuk peninsula with supracrustal sequences, the eastern part with the Ataneq fault and the western part (one day reconnaissance at the coast of Qussuk). Britt Andreassen (BAN), University of Copenhagen, HST and Adam Garde (AAG), GEUS made geological investigations (Appendix 7) and suggested some modifications of the map by Adam Garde (Hollis *et al.* 2004). Gorm Thøgersen (GOT), University of Aarhus and HST, GEUS carried out geological sampling and mapping in the hydrothermally altered rocks in the surroundings of the Ataneq fault zone (Appendix 10). Pelle Gulbrandsen (PEG), University of Copenhagen carried out ground magnetic surveys across the Ataneq fault zone (Appendix 8). BAN, GOT and PEG all collected samples and made observations for their M.Sc. theses at the universities of Copenhagen and Aarhus.

Geology

The Qussuk area is located in the south-eastern part of the c. 3.2–2.97 Ga Akia terrane, and is covered by the geological map sheet Fiskefjord (scale 1:100 000; Garde 1989, 1997). This area has escaped the 2975 Ma granulite facies event recorded elsewhere in the Akia terrane, and is hence considered to have a larger gold potential (Hollis *et al.* 2004, Hollis 2005). Newly discovered remnants of a 3070 Ma, strongly deformed island arc with andesitic volcanoclastic rocks host low-grade (0.1–2 ppm) gold mineralisation at Qussuk peninsula and Bjørneøen (Garde *et al.* 2006). The volcanic rocks hosts two different types of pre-metamorphic alteration at Qussuk peninsula: (1) spatially constrained lenses of meta-epidosite up to 200 x 400 m, which can be interpreted as relicts of a hydrothermal feeder system, and (2) a garnet-rich alteration system of presumed volcanic-exhalative origin with gold mineralisation. The latter association has the highest potential for gold. It comprises tectonically disrupted lenses of massive garnetite (Fig. 18) and garnet-quartz-biotite rocks (\pm sillimanite-plagioclase-tourmaline; Fig. 19) and irregular compositional layering, located along amphibolite horizons with finely disseminated Fe-sulphides, and with pockets of less altered volcanic and sedimentary rocks within them. The gold occurs both in the altered lithologies and in closely adjacent hosts (Garde *et al.* 2006).



Figure 18. Garnitite – garnet alteration in a volcano-sedimentary sequence, Qussuk.



Figure 19. Rust bands of amphibolite (mafic volcanic rocks) – a combination of intercalated exhalites and alteration processes, Qussuk Bay.

Detailed descriptions of the lithologies and the geological setting can be found in Hollis *et al.* (2004), and these subjects will only be briefly mentioned in this report. Large parts of the supracrustal belts in the southern and western part of the Qussuk area consist of leucocratic andesitic amphibolite, which generally contains biotite in addition to hornblende and plagioclase. The andesitic amphibolites contain primary fragmental textures and are proba-

bly of volcanoclastic origin (Hollis *et al.* 2004; Garde *et al.* 2006). Large and very prominent, rusty weathering exposures of sillimanite-garnet-biotite-rich metasedimentary rocks occur on the south-facing hills north of the head of Qussuk. The rust staining is in part derived from local iron sulphides. Similar lithologies are found in the coastal areas of Qussuk .

Massive silica precipitation and impregnation occur along the Proterozoic Ataneq fault in the eastern part of the Qussuk peninsula. Similar silicification has been described from the adjacent western part of the Ivisaartoq map sheet area (Park 1986b).

Ultramafic rocks are hydrothermally altered to soapstone (talc) in a tectonic lineament parallel to and situated between the Ataneq fault and the Ivinnguit fault . The soapstone formation is exposed at 600–700 m of elevation, it strikes 55° and can be followed for at least one kilometre with varying thickness from 0.5 – 4 metres It is estimated to continue both towards NE and SW (Thøgersen *et al.* 2006).

Measured magnetic profiles (Appendix 8) showed, in general, that the magnetic intensity of the rocks increases away from the Ataneq fault zone. This can be seen in all the profiles, but is most obvious in the southernmost Ataneq profile (Fig. 14). The point of lowest magnetic intensity is located a small distance away from the fault zone, which reflects that the Ataneq fault dips 60°NW and strikes 58°, see Appendix 8 for details. At a first glance there seems to be a good correlation between geological features and magnetic properties. Areas with tonalites have higher magnetic intensity than the thoroughly silicified areas. Pegmatites in this area have very high magnetic response.

Analytical results

The samples collected in 2004 on the Qussuk peninsula showed that the supracrustal rocks amphibolite and quartz-mica-garnet gneiss carry a little bit of gold, i.e. up to 233 ppb Au. The highest values were often derived from garnet-bearing mica schists. In Hollis *et al.* (2004) several gold anomalous samples were reported, two of which exceeded 1 ppm Au (2.26 and 1.43 ppm). Special attention was focussed on the areas during the fieldwork in 2005. In the southern part of Qussuk peninsula, a mafic volcanic sequence (80 m wide), intercalated with rusty metasediments (exhalites), contains disseminated iron sulphides associated with garnet alteration. Within this sequence, a two metres rusty altered amphibolite (metasediment?; samples 497608–011) yielded gold values from 819 to 8160 ppb and copper values from 0.13 – 0.39% (Table 3). Within the 80 m profile, another rusty layer (1.5 m wide) yielded up to 500 ppb Au (497612–013; Table 3). At the head of the Qussuk, similar volcano-sedimentary sequences are found resembling the rocks on southern Qussuk peninsula. Quartz-bearing rusty layers (10–100 cm wide; exhalites?) with disseminated iron sulphides and surrounding calc-silicate alteration have gold up to 5.1 ppm (497686; Table 3; Fig. 19).

The black magnetic amphibolites are in general low in gold, except for one sample with 338 ppb Au (497627; Table 3). These black mafic sections of the amphibolites have high Cr contents (up to nearly 0.2%), elevated Ni (often 500–1000 ppm), elevated Cu and rather high Fe, Mg and Ca contents (e.g. 497627–631; Table 3).

The hydrothermally altered Ataneq fault zone has a completely different geochemical signature than the supracrustal rocks. The hydrothermal zone is not gold-bearing. The only anomalously high element concentrations in the zone are Ba and Cu, which had also been observed previously (Appel *et al.* 2005).

Qooqut Lake

The Qooqut Lake area (Fig. 14) was investigated due to its predicted gold potential (Nielsen *et al.* 2004).

Geology

The quartzo-feldspathic gneisses of the area have been strongly deformed, migmatized and intruded by Ikkattoq gneisses and granite veins of the Qôrquq granite complex. Younger supracrustal rocks are intercalated with the Amitsoq gneisses and intruded by the Ikkattoq gneisses. The mafic supracrustal sequence is up to 100 m wide and comprises abundant amphibolites and minor exhalites (quartz-garnet rocks), metasediments (rusty garnet-bearing layers) intercalated with layered mafic, and ultramafic rocks. Both the ultramafic rocks and the amphibolites have magnetite-bearing markers, which occur as dm–m wide layers within the rock units. The rock associations also carry minor bodies of textured metagabbros and metadolerites. A pillowed mafic volcanic sequence was recorded (Fig. 20) at the southern end of the Lake Qooqut, in a place where mafic rocks do not appear on the 1:100,000 scale geological map (McGregor 1993). The amphibolites and exhalite layers have varying amounts of sulphides, most commonly pyrrhotite with minor chalcopyrite. The amphibolites are bleached and calc-silicate altered, commonly in the vicinity of the rusty metasediments (exhalites).



Figure 20. *Mafic pillowed metavolcanic sequence, southwest of Qooqut Lake.*

Analytical results

One exhalite within the amphibolites is Cu, Ni and Zn-bearing (499013–016) with maximum values 0.13%, 0.17% and 0.4%, respectively (Tables 4 & 5). The highest Ni values are found in ultramafic rocks (up to 0.3%), which also have high Cr (up to 0.58% and high Mg (up to 23%). Other exhalite bands are mainly Cu-bearing (Table 3) with up to 0.61% (e.g. 499002–003 and 499031–034). The precious metal values are low except for one sample (499014) with elevated Pt (26 ppb). Gold is not detected in the analysed samples.

Ameralik

In 2004, one locality was investigated in the area south of Ameralik (Appel *et al.* 2005), where one big loose block (one cubic metre in size) was albitised and contained disseminated sulphides (pyrite and chalcopyrite). The analyses gave nearly 2% copper and 200 ppb gold. Another area was chosen this time (Fig. 14), in the border zone between the Tasiusarsuaq and Tre Brødre terranes, where an up to 50 m wide sequence of amphibolites is intercalated by tonalitic orthogneisses. The area is transected by N-S and E-W fault zones, which are easily recognised in the field by deep valleys/gorges filled with rivers. Along the fault zones extensive hydrothermal alteration occur including silicification, albitisation, and epidotisation. The iron-sulphide contents in the rocks are generally low. The area revealed no gold but up to 0.2% Cu and up to 0.35% Zn (Tables 4 & 5).

Kangerdluarssenguup taseressua

The Tasiarsuaq terrane southeast of Kangerdluarssenguup taseressua (Kang) is dominated by mafic rocks (amphibolite) and tonalitic gneiss. The mafic rocks comprise pillowed amphibolite (calc-silicate alteration), massive amphibolite (meta-gabbro), and ultramafic pods associated with magnetite-bearing, black amphibolite. The thickness of the amphibolitic sequences varies from 50 to 200 m. The study area is crosscut by brown-weathering dykes (up to 30 m wide), which generally strikes roughly E-W (Fig. 21). The calc-silicate-altered amphibolite (\pm garnet) has intercalations of 1–2 m wide rusty, sulphide-bearing layers (exhalites; Fig. 22). The sulphides are pyrite, pyrrhotite, chalcopyrite and arsenopyrite. It is worth noting that this area is the only place in the greater Godthåbsfjord region outside Storø, which carries arsenic in considerable amounts.



Figure 21. *Brown weathered dykes, narrow dykes in the foreground and wider dykes in the background, Kang area.*



Figure 22. *Rusty exhalite in amphibolite. The sulphides of the exhalite are pyrite, pyrrhotite, and arsenopyrite, Kang area.*

Analytical results

In general, the gold content is low except for one sample (499087, Tables 4 & 5), which yielded 456 ppb Au and 1.48% As. The same sequence has enhanced gold values (~20 ppb; 499082–084, Tables 4 & 5). The mafic rocks have some Cu concentrations up to 0.16% and average contents of Ni and Cr, which are much lower than the contents of the mafic sequence in the Qooqut Lake area (Tables 4 & 5).

Table 5. *Record of samples collected and used in Table 4.*

Sample #	Waypt	Lat	Long	UTM Easting	UTM Northing	Sample description
507697	507697	64,264480	-50,836825	507905E	7126496N	Stream sediment
507698	507698	64,275700	-50,814090	509003E	7127749N	Stream sediment
507699	507699	64,291750	-50,794516	509945E	7129540N	Stream sediment
507702	3	64,775640	-50,820404	508540E	7183462N	Stream sediment
507703	4	64,767260	-50,813570	508867E	7182529N	Stream sediment
507704	5	64,760380	-50,801795	509430E	7181764N	Stream sediment
507705	507705	64,089360	-50,509729	523903E	7107064N	Stream sediment
507706	507706	64,080010	-50,493277	524713E	7106028N	Stream sediment
507707	507707	64,091670	-50,506827	524042E	7107322N	Stream sediment
507708	507708	64,090780	-50,560938	521405E	7107203N	Stream sediment
507709	507709	64,078050	-50,515577	523627E	7105801N	Stream sediment
507710	507710	64,073320	-50,524187	523211E	7105270N	Stream sediment
507711	507711	64,046630	-50,052064	546287E	7102555N	Stream sediment
499001	499001	64,282040	-50,801811	509596E	7128458N	Dark hornblende rich gabbro
499002		64,281960	-50,800669	509651E	7128449N	Fine-grained amphibolite with disseminated Fe-sulfides
499003		64,281960	-50,800669	509651E	7128449N	Granite in contact to amphibolite with Fe-sulfides
499004	HST189	64,280490	-50,801683	509602E	7128285N	Magnetite-bearing gabbro/hornblende
499005	HST190	64,280560	-50,803147	509531E	7128293N	Black amphibolite with magnetite
499006	HST191	64,279700	-50,804885	509447E	7128196N	Pyroxenite with mica
499007	HST192	64,273750	-50,826176	508418E	7127531N	Rusty amphibolite with garnet
499008		65,273750	-49,826176	508418E	7127531N	Dark amphibolite
499009	HST194	64,286980	-50,787456	510289E	7129010N	Serpentinised ultramafic (UM) rock
499010		65,286980	-49,787456	510289E	7129010N	Magnetite-bearing, fine-grained, pyroxene rich UM rock
499011	HST195	64,826350	-51,485919	476937E	7189190N	Black amphibolite with magnetite
499012		64,297800	-50,734053	512869E	7130226N	Black pyroxenite(?)
499013	HST196	64,303680	-50,740882	512536E	7130879N	Bleached amphibolite with disseminated Fe-sulfides
499014	HST197	64,304790	-50,743538	512407E	7131003N	Fine-grained UM rock
499015	HST198	64,304560	-50,742824	512441E	7130977N	Altered amphibolite with disseminated Fe-sulfides
499016	HST199	64,301400	-50,741456	512509E	7130625N	Altered and bleached amphibolite with disseminated Fe-sulfides
499017	HST201	64,299050	-50,754878	511861E	7130361N	Altered magnetite-bearing amphibolite (UM rock)
499018		64,299050	-50,754878	511861E	7130361N	Altered magnetite-bearing UM rock
499019	HST202	64,266030	-50,837474	507873E	7126669N	Dark greenish, magnetite-bearing, fine-grained amphibolite
499020	HST203	64,262950	-50,843010	507606E	7126325N	Dark amphibolite from banded amphibolite
499021	HST204	64,812930	-51,467332	477808E	7187688N	Dolerite dike
499022	HST205	64,263660	-50,836160	507938E	7126404N	Pillowed amphibolite
499023		64,263660	-50,836160	507938E	7126404N	Pillowed amphibolite, calc-silicate alteration
499024	HST206	64,262490	-50,837131	507891E	7126274N	Bleached amphibolite with disseminated Fe-sulfides
499025	HST207	64,263770	-50,836712	507911E	7126417N	Magnetite-bearing dark-green amphibolite/UM rock
499026	HST208	64,284350	-50,796747	509840E	7128716N	Magnetite-bearing amphibolite (cm-banding)
499027	HST209	64,285530	-50,797713	509793E	7128847N	Garnet amphibolite with disseminated Fe-sulfides
499028	HST210	64,292090	-50,796146	509866E	7129579N	Dolerite dike
499029	HST212	64,292120	-50,797370	509807E	7129582N	Quartz-garnet, rusty layer (chert) with disseminated Fe-sulfides
499030		64,292120	-50,797370	509807E	7129582N	Quartz-garnet-calc-silicate amphibolite with diss. Fe-sulfides
499031	HST213	64,291140	-50,799328	509713E	7129473N	Quartzite (chert) with disseminated Fe-sulfides
499032		64,291140	-50,799328	509713E	7129473N	Quartz-garnet banded gneiss (exhalite) with cpy. and pyrrhotite
499033		64,291140	-50,799328	509713E	7129473N	Coarse-grained hbl-rich amphibolite with 10 cm thick diss. Fe-S
499034		64,291140	-50,799328	509713E	7129473N	Banded calc-silicate amphibolite with disseminated Fe-sulfides
499035	HST220	64,768960	-50,816413	508732E	7182718N	Dolerite dike
499036	HST221	64,776240	-50,828081	508174E	7183528N	Fine-grained, dark and dense amphibolite
499037	HST222	64,776230	-50,829036	508129E	7183526N	Dark and rusty amphibolite in contact to granite
499038	HST232	64,088310	-50,504660	524151E	7106948N	Epidotite with pyrite
499039	HST234	64,082570	-50,498588	524452E	7106311N	Silicified and bleached amphibolite with diss. Fe-sulfides
499040	HST235	64,078550	-50,501409	524318E	7105862N	Silicified gneiss

Table 5 continued. Record of samples collected and used in Table 4.

Sample #	Waypt	Lat	Long	UTM Easting	UTM Northing	Sample description
499041	HST236	64,091630	-50,509086	523932E	7107316N	Rusty amphibolite with disseminated Fe-sulfides
499042		64,091630	-50,509086	523932E	7107316N	Epidote dike in amphibolite
499043	HST237	64,094430	-50,529422	522939E	7107621N	Dark amphibolite+garnet
499044		64,095090	-50,529701	522924E	7107694N	Green UM rock - mica and serpentinite
499045		64,095090	-50,529701	522924E	7107694N	Greenish amphibolite with disseminated Fe-sulfides (cubes)
499046		64,095090	-50,529701	522924E	7107694N	Garnet-biotite gneiss (metasediment)
499047	HST238	64,095960	-50,542978	522277E	7107787N	Rusty quartz-rich gneiss (metasediment), + mica
499048	HST239	64,096460	-50,560193	521437E	7107836N	Green pyroxene rich Um rock
499049	HST240	64,087290	-50,562692	521322E	7106813N	Silicified amphibolite with disseminated Fe-sulfides
499050	HST241	64,089530	-50,560611	521422E	7107064N	Rusty quartz-rich gneiss (metasediment) with pyrite
499051	HST246	64,073420	-50,528205	523015E	7105280N	Altered, green, silicified amphibolite with diss. pyrite
499052	HST247	63,880630	-50,104625	543980E	7084021N	Fine-grained, dense amphibolite (dyke?), pyrrhotite
499053		63,880630	-50,104625	543980E	7084021N	Carbonate altered, silicified rock, Mn-coating on joints
499054		63,880630	-50,104625	543980E	7084021N	Light, greenish amphibolite
499055		63,880630	-50,104625	543980E	7084021N	Black garnet-amphibolite with pyrite
499056	HST248	63,940340	-50,067326	545715E	7090700N	Magnetite-bearing UM, malachite staining
499057		63,940340	-50,067326	545715E	7090700N	Epidotite with cubes of pyrite, chalcopyrite, malchite
499058	HST249	63,938300	-50,039184	547097E	7090493N	Garnet amphibolite with disseminated Fe-sulfides
499059	HST250	63,900700	-49,919874	553016E	7086397N	Rusty, dark amphibolite with disseminated Fe-sulfides
499060	HST251	63,899450	-49,912707	553370E	7086263N	Black amphibolite with disseminated Fe-sulfides
499061		63,899450	-49,912707	553370E	7086263N	Black amphibolite with metallic staining(?)
499062		63,899450	-49,912707	553370E	7086263N	Black amphibolite with metallic staining(?)
499063		63,899450	-49,912707	553370E	7086263N	Olivine and magnetite bearing UM rock
499064	HST252	63,899680	-49,913405	553336E	7086289N	Magnetite-bearing, calc-silicate alterations, amphibolite
499065	HST253	63,898810	-49,911060	553452E	7086194N	Banded grey gneiss (tonalite)
499066	HST255	63,896000	-49,921119	552964E	7085872N	Garnet amphibolite - grey brown
499067	HST256	63,889030	-49,920137	553025E	7085097N	Dolerite dike
499068	HST257	63,885800	-49,918909	553092E	7084738N	Dark amphibolite with disseminated Fe-sulfides
499069		63,885800	-49,918909	553092E	7084738N	Light amphibolite with disseminated Fe-sulfides
499070	HST258	63,885880	-49,920716	553003E	7084745N	Medium-grained gabbro
499071	HST260	63,887580	-49,904468	553798E	7084949N	Black garnet-amphibolite with little pyrite
499072	HST262	63,894380	-49,896705	554166E	7085713N	Dark gabbro
499073	HST263	63,901383	-49,914166			Rusty garnet bearing amphibolite with disseminated Fe-sulfides
499074	HST264	63,901090	-49,912611	553372E	7086447N	White quartz vein
499075	HST265	63,901700	-49,914553	553276E	7086513N	Rusty, albitised amphibolite
499076	HST266	63,902320	-49,913743	553314E	7086582N	Exhalite, quartzite with garnet
499077	HST267	63,901160	-49,921559	552933E	7086447N	Dark amphibolite with disseminated Fe-sulfides
499078	HST268	63,900960	-49,925464	552741E	7086421N	Exhalite from light epidotised amphibolite with pyrite
499079	HST269	63,901370	-49,926800	552675E	7086466N	Dolerite dike
499080	HST271	63,903150	-49,919037	553053E	7086671N	Rusty exhalite in amphibolite
499081	HST273	63,910450	-49,932540	552376E	7087473N	Grey garnet bearing exhalite with tourmaline and with diss. Fe-S
499082		63,913410	-49,933559	552321E	7087803N	Rusty exhalite in garnet amphibolite with diss. Fe-sulfides
499083		63,913410	-49,933559	552321E	7087803N	Light grey amphibolite
499084		63,913410	-49,933559	552321E	7087803N	Rusty exhalite in garnet amphibolite with diss. Fe-sulfides
499085		63,913410	-49,933559	552321E	7087803N	Rusty garnet bearing amphibolite (exhalite) with diss. Fe-sulfides
499086		63,913410	-49,933559	552321E	7087803N	Dark grey amphibolite
499087	HST275	63,913960	-49,935898	552205E	7087862N	Exhalite with disseminated Fe-sulfides and arsenopyrite
499088	HST276	63,915440	-49,938204	552089E	7088025N	Garnet amphibolite
499089	HST277	64,040400	-50,047022	546543E	7101864N	Dolerite dike
499090	HST278	64,753750	-50,785600	510203E	7181027N	Talc - soapstone
499091	HST280	64,751640	-50,786791	510147E	7180792N	Soapstone with unaltered core
499092	HST281	64,748840	-50,789285	510029E	7180480N	Fine-grained, carbonatised UM rock
499093	G-14-1	64,748990	-50,809520	509066E	7180493N	Silicified tonalite
499094		64,748990	-50,809520	509066E	7180493N	Sheared quartz (hydrothermal)
499095		64,748990	-50,809520	509066E	7180493N	Sheared quartz (hydrothermal)

Concluding remarks

- The preliminary results of the fieldwork in the Nuuk region 2005 confirm that the Qussuk peninsula has an interesting gold potential. New samples of a garnet-bearing supracrustal rock unit, interpreted as an original exhalite, yielded gold values up to 8 ppm, thereby confirming and extending results from 2004 that suggested the presence of a strata-bound gold mineralisation.
- A complex of mafic to ultramafic rocks at Fiskefjord is interpreted as a magmatic layered complex consisting of dunites, peridotites, pyroxenites, norites and layered amphibolites. Magnetite and chromite occur in the ultramafic sequences and iron-sulphides are found in certain rusty layers of the norites and amphibolites. The norites are the most interesting concerning precious metals. Platinum, palladium and gold are detected with values up to 51 ppb Pt, 27 ppb Pd, and 326 ppb Au (fire assay analyses).
- The hydrothermal system of the Ataneq fault (eastern Qussuk) seems barren with respect to gold. Elevated copper and barium is recorded in samples from the fault. Ultramafic rocks along the Ataneq fault are hydrothermally altered to soapstone that can be followed for at least one km.
- The presence of gold-bearing lithologies in the Qooqut Lake area as predicted in the report by Nielsen *et al.* (2004) was not confirmed. The mafic metavolcanic rocks of this area resemble those described from the Ivisaartoq area, and pillow-basalt was observed for the first time in this area. The analytical data show elevated copper and zinc contents.
- The Ameralik area in the border zone between the terranes Tasiusarsuaq and Tre Brødre exhibits much hydrothermal alteration, especially along fault zones. The source of an albitised Cu-Au-bearing boulder found in 2004 was not located in 2005, and analyses of samples collected in 2005 did not reveal any elevated gold concentrations. Mafic metavolcanic rocks southeast of Kangerdluarssenguup taseressua contain metamorphosed exhalites with anomalous gold and arsenic contents. It is the only locality outside Storø where a gold-arsenic association has been identified during GEUS field work in 2004–2005.

Acknowledgements

This project was financially supported by the Greenland Bureau of Minerals and Petroleum (BMP). The topographic base was produced by GEUS in 2004, financed by BMP. The following people are acknowledged for involvement in analytical work and discussion of results: Britt Andreasen, Peter Appel, Juan Carlos Ordóñez-Calderón, Margareta Christoffersen, Dave and Vincent Coller, Clark Friend, Pelle Gulbrandsen, Karen Merete Henriksen, Nigel Kelly, Christian Knudsen, Tine Kristensen, Hanne Lamberts, Louise Josephine Nielsen, Marianne Nørgaard Nielsen, Ali Polat, Ole Stecher, Agnete Steenfelt, Gorm J.-P. Thøgersen, Mikkel Vognsen.

References

- Allaart, J.H. 1982: Geologisk kort over Grønland, 1:500 000, Sheet 2 Frederikshåb Isblink - Søndre Strømfjord. Copenhagen: Grønlands Geologiske Undersøgelse.
- Appel, P.W.U., Garde, A.A., Jørgensen, M.S., Moberg, E.D., Rasmussen, T.M., Schjødt, F. & Steenfelt, A. 2003: Preliminary evaluation of the economic potential of the greenstone belts in the Nuuk region. Danmarks og Grønlands Geologiske Undersøgelse Rapport **2003/94**, 147pp.
- Appel, P.W.U., Coller, D., Coller, V., Heijlen, W., Moberg, E.D., Polat, A., Raith, J., Schjødt, F., Stendal, H. & Thomassen, B. 2005: Is there a gold province in the Nuuk region? Report from field work carried out in 2004. Danmarks og Grønlands Geologiske Undersøgelse Rapport **2005/27**, 79pp.
- Chadwick, B. 1981: Geological field map 64V2-043, eastern Ujarassuit Nunaat at scale 1:20 000. GEUS map archive.
- Chadwick, B. and Coe, K., 1988: Geologisk kort over Grønland, 1:100 000, Ivisârtoq 64 V.2 Nord. Copenhagen: Grønlands Geologiske Undersøgelse.
- Chadwick, B., Crewe, M.A., & Park, J.F.W. 1983: Field work in the north of the Ivisârtoq region, inner Godthåbsfjord, southern West Greenland. Grønlands Geologiske Undersøgelse, rapport **115**, p. 49–56.
- Crewe, M.A., 1981: Geological field map 64V2-044, southern Ujarassuit Nunaat at scale 1:20 000. GEUS map archive.
- Crewe, M.A., 1982: Geological field map 64V2-049a, southern Ujarassuit Nunaat at scale 1:20 000. GEUS map archive.
- Friend, C.R.L. and Nutman, A.P., 2005: New pieces to the Archaean jigsaw puzzle in the Nuuk region, southern West Greenland: steps in transforming a simple insight into a complex regional tectonothermal model. *Journal of the Geological Society, London* **162**, 147-162.
- Garde, A.A. 1989. Geological map of Greenland, 1:100 000, Fiskefjord 64 V.1 Nord. Copenhagen: Geological Survey of Greenland.
- Garde, A.A. 1997. Accretion and evolution of an Archaean high-grade grey gneiss-amphibolite complex: the Fiskefjord area, southern West Greenland. *Geology of Greenland Survey Bulletin* **177**, 114 pp.
- Garde, A.A., Friend, C.R.L., Nutman, A.P. and Marker, M. 2000. Rapid maturation and stabilisation of middle Archaean continental crust: the Akia terrane, southern West Greenland. *Bulletin of the Geological Society of Denmark* **47**, p. 1-27.
- Garde, A.A., Hollis, J.A., Kelly, N., A., S., Stendal, H. & van Gool, J.A.M. 2006: Archaean island arc - hosted gold mineralisation at western Godthåbsfjord, southern West Greenland. In: *The 27th Nordic Geological Winter Meeting, Abstract Volume, Oulu, Special issue I, Bulletin of the Geological Society of Finland*, 39 only.

- Garde, A.A., Larsen, O. and Nutman, A.P., 1986: Dating of late Archaean crustal mobilisation north of Qugssuk, Godthåbsfjord, southern West Greenland. Rapport Grønlands Geologiske Undersøgelse 128, 23-36.
- Hanmer, S. and Greene, D.C., 2002: A modern structural regime in the Paleoproterozoic (~3.64 Ga); Isua Greenstone Belt, southern West Greenland. *Tectonophysics* 346, 201-222.
- Hollis, J.A., van Gool, J.A.M., Steenfelt, A. & Garde, A.A. 2004: Greenstone belts in the central Godthåbsfjord region, southern West Greenland. Danmarks og Grønlands Geologiske Undersøgelse Rapport **2004/110**, 110 pp.
- Hollis, J.A., van Gool, J.A.M., Steenfelt, A. & Garde, A.A. 2005: Greenstone belts in the central Godthåbsfjord region, southern West Greenland. Geological Survey of Denmark and Greenland Bulletin **7**, 65-68.
- Hollis, J.A.(ed.) 2005: Greenstone belts in the central Godthåbsfjord region, southern West Greenland: geochemistry, geochronology and petrography arising from 2004 field work, and digital map data. Danmarks og Grønlands Geologiske Undersøgelse Rapport **2005/42**, 215pp.
- McGregor, V.R. 1993: Geological map of Greenland 1:100 000. Descriptive text. Qôrqt 64 V.1 Syd. The regional geology of part of the Archaean block of southern West Greenland, including a segment of the late Archaean mobile belt through Godthåbsfjord, 40 pp. Copenhagen: Grønlands Geologiske Undersøgelse.
- Nielsen, B.M., Rasmussen, T.M. & Steenfelt, A. 2004: Gold potential of the Nuuk region based on multiparameter spatial modelling of known gold showings. Interim report 2004. Danmarks og Grønlands Geologiske Undersøgelse Rapport **2004/121**, 155pp.
- Park, J.F.W. 1986a: Geological field map 64V2-050a, northwestern Ujarassuit Nunaat at scale 1:20 000. GEUS map archive.
- Park, J.F.W., 1986b: Fault systems in the inner Godthåbsfjord region of the Archaean block, southern West Greenland. Unpublished Ph.D. thesis, University of Exeter. 305 pp.
- Polat, A. 2005: Geochemical and petrographic characteristics of the Ivisaartoq and Storø greenstone belts, southern West Greenland: progress report. In: Hollis, J.A.(ed.) Greenstone belts in the central Godthåbsfjord region, southern West Greenland: geochemistry, geochronology and petrography arising from 2004 field work, and digital map data.. Danmarks og Grønlands Geologiske Undersøgelse Rapport **2005/42**, 215pp.
- Stendal, H., Nielsen, B.M., Secher, K. & Steenfelt, A. 2004: Mineral resources of the Precambrian shield of central West Greenland (66° to 70°15'N). Part 2. Mineral occurrences. Danmarks og Grønlands Geologiske Undersøgelse Rapport 2004/20, 212 pp.
- Thøgersen, G.J.-P., Stendal, H. & Zimmermann, H.D. 2006: Hydrothermal alteration along the Ataneq fault in the Nuuk region, West Greenland. In: The 27th Nordic Geological Winter Meeting, Oulu, Abstract Volume Special issue I, Bulletin of the Geological Society of Finland, 161 only.

Appendix 1: Explanatory notes to the DVD (Willy Lehmann Weng)

This DVD contains digital data accompanying GEUS report 2006/7, 'Supracrustal belts in the Godthåbsfjord region, southern West Greenland: Progress report on 2005 fieldwork: geological mapping, regional hydrothermal alteration and tectonic sections'. The DVD is basically an update of the DVD from GEUS report 2005/42, 'Greenstone belts in the central Godthåbsfjord region, southern West Greenland: Geochemistry, geochronology and petrography arising from 2004 field work, and digital map data'. All data on this DVD are copyright of GEUS (2006). The DVD contains the full report and compiled field maps in PDF format, as well as an ArcView© project file containing geo-referenced compiled field data including localities, geological descriptions, sample localities, structural data, geo-chronology, and references to digital photographs (see below). It also contains reduced resolution digital photographs in JPEG format from the field work. Descriptions of the views in the ArcView© project, maps, geochemistry data, and photographs are given below. An installation kit for Acrobat Reader© version 6.0 is included on this DVD. After installation, PDF-files can be open from within the reader, or just by double-clicking the files.

Directory structure

The DVD contains the following directories and main files:

Directories:

AcrobatReader6

Field_maps

Geochemistry

Spreadsheets

Geology

Photographs

Topography

Files in the root directory:

Explanatory_notes.pdf

Frontispiece.jpg

GEUS2004R110.pdf

GEUS2005R42.pdf

GEUS2006R7.pdf

Godthaabsfjord2005.apr

Terms_of_Delivery.pdf

Note that all files on the DVD use spelling without special letters to avoid problems reading files.

Use of the DVD

1. Place the DVD into DVD reader.
2. Read the Explanatory_notes.pdf file. This provides explanations of the contents of the DVD.
3. Run ArcView© 3.2 on your computer.
4. Open the ArcView© file.
5. The file Godthaabsfjord2005.apr will open on a cover view. When this cover view is closed, a list of available views will become visible. Choose the desired view to begin exploring the data.

Acrobat Reader© 6

This folder contains an installation kit for Acrobat Reader© version 6.0. After installation, PDF-files can be open from within the reader, or by double-clicking the files.

ArcView© project

The ArcView© project (constructed in ArcView© version 3.2) contains the geo-referenced data collected during the 2004 and 2005 fieldwork, as well as new geochemical and geochronology data and pre-existing 1:100 000 geological maps both in the original and new updated and enlarged version. The data are placed in separate views and can be explored and combined within the program. The ArcView© project, Godthaabsfjord2005.apr, is contained within the root directory of the DVD and refers to the Frontispiece.jpg file within the root directory and to files within the folders Geochemistry, Geology, and Topography.

The following is a list of the views within the ArcView© project file (Godthaabsfjord2005.apr), containing different types of digital data sets.

0.1 Frontispiece

1.1 Index map - Location of the Godthåbsfjord region

1.2 Topographic map

1.3 Ujarassuit Nunaat geological map

1.4 Digital geological map 1:100 000

1.5 Digital geological maps 1:100 000 (old version)

1.6 Scanned geological maps 1:100 000 (old version)

2.1 Visited outcrop localities

2.2 Geological observations

2.3 Samples collected

2.4 Structures

2.5 Geochronology

2.6 Photographs

3.1 Rock geochemistry

3.2 Geochemistry

3.3 Stream sediment chemistry

View 0.1 Frontispiece

This displays the title and authors. The photograph shows the Innajuattoq anorthosite in the Ilulialik bay (picture towards SW direction), inner Godthåbsfjord.

View 1.1 Index map – Location of the Godthåbsfjord region

This view shows the location of the Godthåbsfjord region in southern West Greenland.

View 1.2 Topographic map

This topographic map is prepared digitally at scale of 1:100 000 from aerial photographs, at the Photogeological Laboratory at GEUS. Aerial photographs and point control by Kort & Matrikelstyrelsen, Copenhagen, with permission A.200/87. The map is in UTM coordinates. Projection parameters: UTM-zone 22 (i.e. the central meridian is 51° W, false easting 500 000 metres), geodetic reference WGS84. Contour interval: 100 m. The map is included as a georeferenced TIF-file.

The bounding coordinates of the area shown here are:

64° N to 65° N

49°30' W to 51°50' W.

Additional to the topographic map, the view also shows as a separate theme some of the main topographic names used in the text.

Two additional topographic maps are included, the Ujarassuit Nunaat area (see view 1.3) and the central Godthåbsfjord region (see view 1.5). Both are georeferenced TIF-files, as for the main map.

View 1.3 Ujarassuit Nunaat geological map

This view contains the 2005 field map of the Ujarassuit Nunaat area (64°07' N to 65° N, 50° 07' W to 50° 37' W).

View 1.4 Digital geological map 1:100 000

This view contains the updated versions of the three old geological maps used in view 1.4 (see also the section 'Digital geological maps', pp. 9-11 of GEUS report 2005/42). Most of the data for the view are stored in the catalogue \Geology\Newmaps. The view uses four shape files containing geology for the three maps:

geotri_a.shp	mainly boundary lines between units
geotri_p.shp	mapped units
trentri.sph	trend-, faults, etc.
pointtri.shp	structural data etc.

The files have a large number of attributes. The key attribute in all files is called gm_label. It is a code to the type of point, line or polygon. See also the attribute description.

The catalogue also includes the three new maps (and a corresponding legend) as EPS-files and as georeferenced TIF-files. The TIF-files are used in view 1.3. They can be used with the transparent version of the geology polygons.

View 1.5 Digital geological maps 1:100 000 (old version)

This view contains the digital version of the three published 1:100 000 scale maps that cover the central Godthåbsfjord region (64°05' N to 64°50' N, 49°30' W to 51°50' W. This area is also used in view 1.6). These maps are:

Fiskefjord 64 V.1 Nord (Garde 1989) in the north-west
Ivisârtoq 64 V.2 Nord (Chadwick & Coe 1988) in the north-east
Qôrquut 64 V.1 Syd (McGregor 1984) in the south-west

These maps were based on older versions of the topographic data, and the latter two are based on a Lambert conformal conic projection with standard parallel 60°30'N. These maps do not have a perfect fit with each other, or with the newest topographic data presented in View 1.2. The lithologies are shown as polygons, with legends for each of the three maps presented separately. The maps are cut so they only cover the central Godthåbsfjord region.

View 1.6 Scanned geological maps 1:100 000 (old version)

This view contains scans of the originals of the same three maps as in the previous view.

View 2.1 Visited outcrop localities

In this view the outcrop localities that were visited during the fieldwork are plotted on the topographic map, with a colour code indicating the different geologists that collected the data as presented in the following views. Each locality is coded with the locality number, as referenced in the text of the report, consisting of the collectors initials, year of collection and locality number (e.g. abc2005-023). Also the geographical and UTM coordinates of each locality are given, together with the approximate altitude as determined by GPS. Each of the data in the following views is linked to one of these localities.

View 2.2 Geological observations

This view presents a lithological name and a brief description of the geology of most of the localities.

View 2.3 Samples collected

The location of collected samples is shown in this view. Each of the samples is linked to one of the localities (see View 2.1). Most samples have a brief description and a general purpose is indicated for each. The samples have been separated into different themes, based on their purpose/s.

View 2.4 Structures

This view contains all the structural data from the field work, each linked to one of the localities in View 2.1. Furthermore, the view includes structural data that were digitised from the published 1:100 000 scale maps, for the central area only. The data are plotted with a colour code, separated for foliations, lineations and fold axes. The colours indicate dip direction or plunge direction and are subdivided into 6 orientation segments.

View 2.5 Geochronology

This view contains the geochronology data from samples collected in 2004. See GEUS Report 2005/42 for more details.

View 2.6 Photographs

This view presents the locations at which digital photographs were taken, subdivided per geologist. The data contain a brief description of the subject of each of the photos. The reduced resolution photographs themselves (in JPEG format) can be found in the 'Photographs' folder (see below).

Views 3.1: Rock geochemistry and 3.3: Stream sediment chemistry

Analytical data acquired so far are presented on land surface maps in two views. View 3.1 presents data for rock samples and View 3.2 for stream sediment/soil data. For both views the attribute table associated with the uppermost theme contains all analytical data together with locality, information on the samples, and the identity of the collector. The themes in each view are graduated symbol plots illustrating the distribution of seven selected elements and the Ni-Mg ratio.

View 3.2 Geochemistry

This view shows the locations of samples analysed for geochemistry. See GEUS Report 2005/42 for details of the samples collected in 2004.

Field Maps

The directory with the maps contains PDF files of digitised field maps produced by GEUS in 2004 (see also report 2004/110) and of pre-existing scanned field maps relevant to the Ujarassuit area.

Spreadsheets

The folder contains Microsoft Excel© spreadsheets:

Hydrothermal_Rock_analyses_Godthaabsfjord_2005.xls

Rock_analyses_Godthaabsfjord_2004.xls

StreamSed_analyses_Godthaabsfjord2004.xls

Tectonothermal_fielddata_2005.xls

These contain data used in the ArcView© project (see above). Geochemical data were collected at Activation Laboratories in Ancaster, Canada using the 'Au+48' and 'complete analysis' element suites.

Photographs

Most of the photographs taken during fieldwork are digitally available. Reduced resolution copies of these photographs are placed in this folder on the DVD. A brief description of each of these photographs and the location where they were taken can be found in the ArcView© project (see above, view 2.6).

Appendix 2: Field report 2005 – Ujarassuit Nunaat Region – North (Jeroen van Gool & Ole Stecher)

Five weeks of field work were carried out in the Ujarassuit Nunaat area, in the north-western corner of the Ivisârtoq map sheet area (Chadwick & Coe 1988; Fig. A2_1). The field work concentrated on the investigation and mapping of the amphibolite belts in the area. The belts were characterised with respect to their constituting lithologies, their depositional environment, the relation to the surrounding grey gneisses, and their structural setting. Four main amphibolite belts were investigated in four map areas (Fig. A2_2). Since the amphibolite belts are supposedly located in different tectonic terranes, of which there are four in the area (Fig. A2_2) as defined by Friend & Nutman (2005), the relations between the different terranes were also investigated.



Figure A2_1. *The northern part of the Ivisârtoq geological map sheet, with an outline of the mapping area (Fig. 2) in Ujarassuit Nunaat. From Chadwick and Coe (1988).*

The main amphibolite belt of the Ujarassuit Nunaat area crops out in areas 1 and 9 (camps 1 and 2). It is presumed to continue to the Ivisârtoq supracrustal belt to the east. It covers part of the Kapisilik terrane, and it is bounded to the north by the Isukasia terrane. Area 8 (camp 3) is located within the Isukasia terrane, and contains a supracrustal belt formerly referred to as part of the Malene metasediments, which is of Eo- to Palaeoarchaeon age. Area 7 (camp 4) contains the presumed north-western extension of the amphibolite belt in area 1 and 9 in the Kapisilik terrane, and the boundary with the Isukasia terrane to the east. Area 7 also contains a previously unknown highly agmatized amphibolite belt in the north-

west. Area 6 (camp 5) straddles the Ataneq fault and contains the eastern margin of the Tasersuaq pluton of the Akia terrane, and is characterised by a large number of shear zones that fall into at least two age groups. Areas 6 and 7 are neighbouring and largely underlain by similar rocks or the same terrane, and are discussed together.

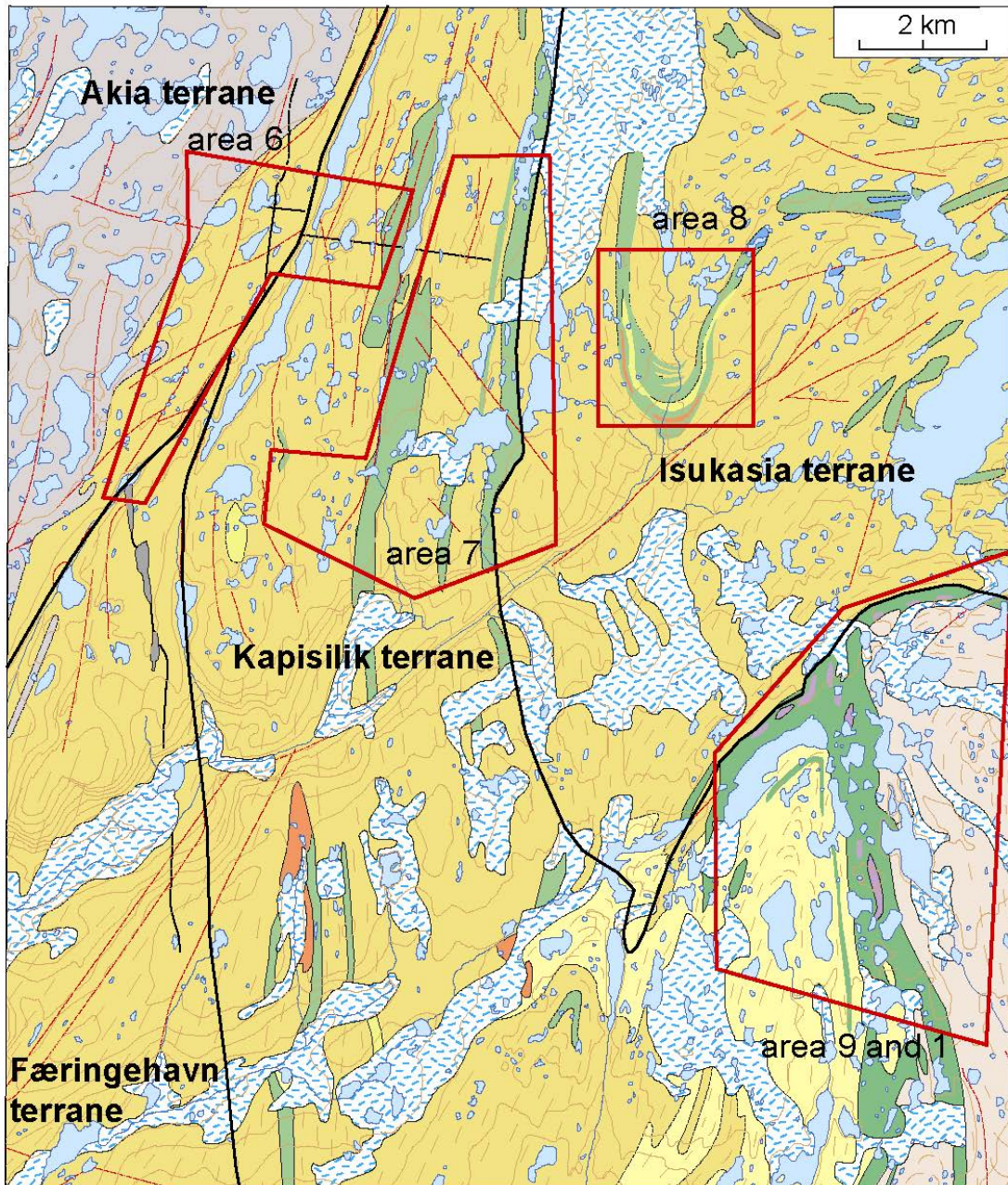


Figure A2_2. Geological map of northern Ujarassuit Nunaat, referred to in the text as the mapping area. The four key mapping areas are outlined. Location shown in Fig. A2_1. Modified from Chadwick and Coe (1988).

The map area lies north of where Nigel Kelly and Susanne Schmid worked (Appendix 3), and especially mapping of the main amphibolite belt in area 1 and 9 forms a continuation of their effort. Ali Polat and Carlos Ordonez joined us in the first two camps, area 1 and 9.

Exposure in the area is reasonable, although extensive boulder fields cover some areas. Especially the more elevated regions, the northern part of area 7 and all of area 6, are well-exposed. Weather was fairly stable, although the work in area 8 was hampered by rain, and was limited to the most essential.

The accompanying geological map shows the newly mapped areas. In the map the geology is interpreted across the smaller areas of Quaternary cover, which commonly contain small scattered outcrops from which the main trends can be constructed. Only the larger covered areas are indicated, in which outcrops are too few for such an interpretation.

Areas 1 and 9

Areas 1 and 9 contain the main amphibolite belt in the region, which shows a T-junction in the north of the area. The amphibolite and the gneisses on either side form part of the Mesoarchaeon Kapisilik terrane. The northern boundary of the NE-SW and E-W-trending parts of the belt is the terrane boundary against the Eoarchaeon Isukasia terrane. The belt is c. 1 km wide and is dominated by amphibolites and includes large lenses of ultramafic rocks. The rocks are intensely deformed at amphibolite facies, and virtually all have a strong, penetrative foliation. Contacts between the amphibolite belt and the surrounding felsic orthogneisses are commonly intrusive transition zones, where multiple sheets of orthogneiss intrude into the amphibolite. The amphibolite belt is commonly cut by a number of alteration zones.

Lithology

Locally a fairly consistent tectono-stratigraphic sequence can be recognised, but this is definitely not the case everywhere. From structurally lowest to highest this sequence is: lenses of ultramafic rocks, commonly with some amphibolite at the lower contact. These ultramafic rocks are surrounded by more felsic material, varying from felsic biotite gneiss, biotite schist and aluminous garnet-sillimanite gneiss, to fine-banded hornblende-bearing felsic gneiss (leuco-amphibolite) which grades into more mafic and commonly more homogeneous amphibolite, which forms the bulk of the belt.

Amphibolites

The amphibolites were generally described in terms of their homogeneity (versus banded appearance) and the content of mafic minerals, as well as the extent and type of alteration. The belt is dominated by a fairly homogeneous to subtly banded mafic amphibolite. This banding may be the result of transposition of original small compositional variations due to the strong deformation. Hornblende and plagioclase are dominant, with minor quartz and biotite. Rocks are usually medium-grained, and have a black colour. Thin quartz veins or quartz-feldspar veins are common (photo jvg2005-092). These homogeneous rocks grade into banded amphibolites, which are more fine-grained, more felsic, and show a clear banding on cm to dm scale. These rocks may contain thin, isolated felsic layers (photo jvg2005-024). Ten to fifty centimetres wide homogeneous, medium-grained mafic amphibolite bands occur within the banded rocks. Thinly-banded felsic hornblende gneisses occur locally as part of the banded amphibolite sequence, and are loosely referred to as light am-

phibolites. These are fine-grained and show clear compositional layering (photo jvg2005-071). These are most commonly found in the vicinity of zones including ultramafic lenses. Anthophyllite schists with dark brown needles up to 8 cm long occur locally as part of these felsic to intermediate parts of the banded amphibolite sequences (photo jvg2005-082). These schists occur commonly near ultramafic rocks and locally connect trains of ultramafic lenses. The mafic to intermediate composition amphibolites can contain garnet, locally forming up to 50% in volume of the rock. Calc-silicates, primarily diopside, occur in the more heterogeneous parts of the rocks, most commonly where felsic veins are abundant. Besides feldspar and quartz these veins may contain also coarse-grained hornblende, garnet and rarely diopside (photo jvg2005-098). Where the felsic veins occur, alteration gives a heterogeneous character to the rocks and calc silicates are common in the matrix, often predominantly in layers that contain the felsic veins (photo jvg2005-031).

Metagabbro

At the T-junction of the amphibolite belt few rather low-strain metagabbro bodies occur, which are medium to coarse-grained and have a weak foliation, but contain remnant igneous textures (photo jvg2005-195). These rocks are very homogeneous and contain hornblende and plagioclase, and possibly minor quartz. Poor exposure and snow cover precluded the mapping of the bodies of metagabbro, but it is likely that part of the foliated, finer-grained homogeneous amphibolite of intermediate composition represents more intensely de-formed metagabbro (photo jvg2005-152, 192). These rocks have a fairly wide distribution in this part of the belt.

Ultramafic rocks

Ultramafic rocks occur as lenses of less than 1 metre to more than 50 metres long: The largest in the centre of the amphibolite belt is about 1 km long. These rocks are homogeneous, commonly coarse-grained and have a metamorphic mineralogy that contains predominantly pale brown amphibole (probably cummingtonite), phlogopite and rarely remnants of olivine. Talc and serpentinite are common. Orthopyroxene cumulates are locally preserved. The ultramafic rocks are commonly well foliated. They are commonly surrounded by banded amphibolite, or by felsic biotite gneiss ± garnet. Garnet sillimanite gneiss (photo jvg2005-076) and felsic garnet biotite gneiss occurs along the western margin of the 1 km long ultramafic body in the centre of the belt. In the garnet-sillimanite gneiss, the garnets occur commonly in augen of sillimanite. The ultramafic rocks occur most commonly along the margins of the belt, and in zone through the centre.

Quartz-diorite

In the outlier of amphibolite, west of the main belt, a c. 30 m wide massive, homogeneous hornblende gneiss (quartz-diorite) occurs. It is medium-grained, dark grey, and with thin felsic veins, and contains isolated lenses and schlieren of amphibolite. The western contact against the felsic orthogneiss is sharp, but towards the east it grades into a regular, banded mafic amphibolite.

A rusty white felsic rock forms a laterally very consistent 1–5 m wide sheet along the western margin of the western outlier of amphibolite (photo jvg2005-115). It is mainly homogeneous, medium grained and appears to consist predominantly of quartz, with rounded

grains, c. 1% biotite, few tiny garnets, which locally can be abundant and minor pyrite. It is predominantly well foliated (photo jvg2005-094) but can also be massive. Locally, the unit is more heterogeneous and appears as a microgranite/aplite, where both feldspar and quartz may occur, but observations were not consistent. The rusty felsic rock occurs together with a banded amphibolite and pegmatites west of the main amphibolite belt.

Felsic gneisses

The amphibolite belt is surrounded by a complex of tonalitic to granodioritic orthogneisses. Friend and Nutman (2005) proposed that the gneisses to the north of the amphibolite belt are Eoarchaean orthogneisses of the Isukasia terrane, and that those to the east and west are Mesoarchaean gneisses which, together with the amphibolite belt, are included in the Kapisilik terrane. The latter are clearly intrusive into the amphibolite belt, whereas the northern contact of the amphibolite belt with the quartzo-feldspathic gneisses is very sharp and shows signs of high strain, in accord with the inferred terrane boundary that occurs here.

The quartzo-feldspathic gneisses of the Kapisilik terrane younger phases are intrusive into the amphibolites. The contacts between amphibolites and orthogneisses can be sharp, but are more commonly formed by transition zones of few metres to c. 100 m.

The most common orthogneiss is medium-grained biotite-bearing quartzo-feldspathic gneiss that is heterogeneous as a result of abundant lenses, layers and schlieren of amphibolite (photo jvg2005-106). Homogeneous parts display a very regular differentiated layering spaced at 2 to 5 mm (photo jvg2005-110). These rocks contain quartz, plagioclase, biotite, \pm K-feldspar, and \pm hornblende.

The contacts between the amphibolites and the orthogneisses of the Kapisilik terrane are intrusive (gneiss intruding into amphibolite), and mainly gradual. A transition zone consisting of interleaved sheets of amphibolite and orthogneiss is common, and can be between 5 and 100 m wide (photo jvg2005-013, 070, 165). Inclusions of a banded amphibolite occur along the eastern margin (location jvg2005-018, photo jvg2005-048) and several locations west of the belt (photo jvg2005-096).

This orthogneiss is intruded by a homogeneous, medium to coarse-grained granite-granodiorite with biotite or hornblende (photo jvg2005-111, 112). This rock is poorly foliated, and has locally an L>S fabric, i.e. it has a much simpler fabric than the heterogeneous orthogneiss, and is light grey to slightly pink in colour. West of the main amphibolite belt, this lithology separates the main belt from the elongate outlier of amphibolite. The rocks here contain hornblende rather than biotite, whereas biotite is more common where it intrudes into the felsic orthogneiss.

Eoarchaean orthogneisses

North of the WSW-ENE part of the belt the orthogneisses are presumably of Eoarchaean age (Friend & Nutman 2005 and references therein), previously referred to as Amitsoq gneisses. They were only visited in a narrow strip along the contact with the amphibolites, where they are fairly homogeneous (on the large scale), have a white to light grey colour, and have a coarse, irregular gneissic fabric, with several generations of leucosome and

locally complex deformation patterns (photo jvg2005-170, 173). Near the contact the rocks are highly strained, but no obvious consistent kinematic pattern was observed. No Ameralik dykes were recognised. In aerial photographs a c. 2 km wide zone closest to the contact is obviously more strongly foliated than the remainder of the orthogneisses, with a rather sharp contact to the more massive orthogneisses to the north. It should be noted that the 1:500 000 scale geological map of the area (Allaart 1982) shows a narrow strip of Mesoproterozoic gneisses along part of the northern margin of the northwestern part of the amphibolite belt, which coincides with part of that highly foliated belt. It may well be possible that a strip of younger, more intensely deformed orthogneisses separates the Mesoproterozoic orthogneisses to the north from the Mesoproterozoic amphibolites to the south. This would imply that the terrane boundary is located c. 2 kilometres north of the amphibolite belt, and not at its northern margin.

Pegmatites

Pegmatites occur throughout the map area, but are most abundant in zones parallel with the amphibolite belt. They are white, virtually undeformed, or cut by thin anastomosing shear bands. They truncate all other fabrics. One marked zone in the centre of the northern part of the belt occurs together with abundant ultramafic lenses. It is not uncommon for amphibolites along the contacts with pegmatites to be altered to mafic/ultramafic biotite schists, consisting almost exclusively of biotite.

Metadolerite dykes

Fine-grained mafic dykes were observed on the scale of few cm to 2 m wide. Locally a remnant igneous texture can be recognised, consisting of plagioclase laths (presumably partially recrystallised) in a dark matrix of fine-grained pyroxene and hornblende. The dykes are discordant, intrude in both amphibolite and orthogneiss and are left stepping. The largest, 2 m wide dyke is north-trending, while the smaller, cm-scale dykes appear not to have a consistent orientation.

Structure

At least four deformation phases could be recognised throughout the area in the orthogneisses, while a foliation parallel to banding in amphibolite inclusions predates the main foliation in the orthogneisses.

The main planar fabric S1 forms a gneissosity in the orthogneisses and a penetrative foliation in the amphibolites and the other rocks of the amphibolite belt. Strain intensity varies considerably, but virtually all rocks have a penetrative foliation. Locally, a mylonitic fabric was observed. Kinematic indicators are rare, and don't give a consistent movement pattern. The S1 is locally axial planar to isoclinal folds in leucosome veins (photo jvg2005-045) but no obvious older fabric is folded. It appears that the fabric in the terrane boundary in the north of map area 1 and 9 is continuous with S1, although S1 may have overprinted an older, now obliterated shear fabric. Lineations are weakly developed, except in zone of high shear strain. They consist of preferred orientation of amphibole, elongate quartz or feldspar (photo jvg2005-152). Lineations are commonly moderately SSE plunging (Fig. A2_3).

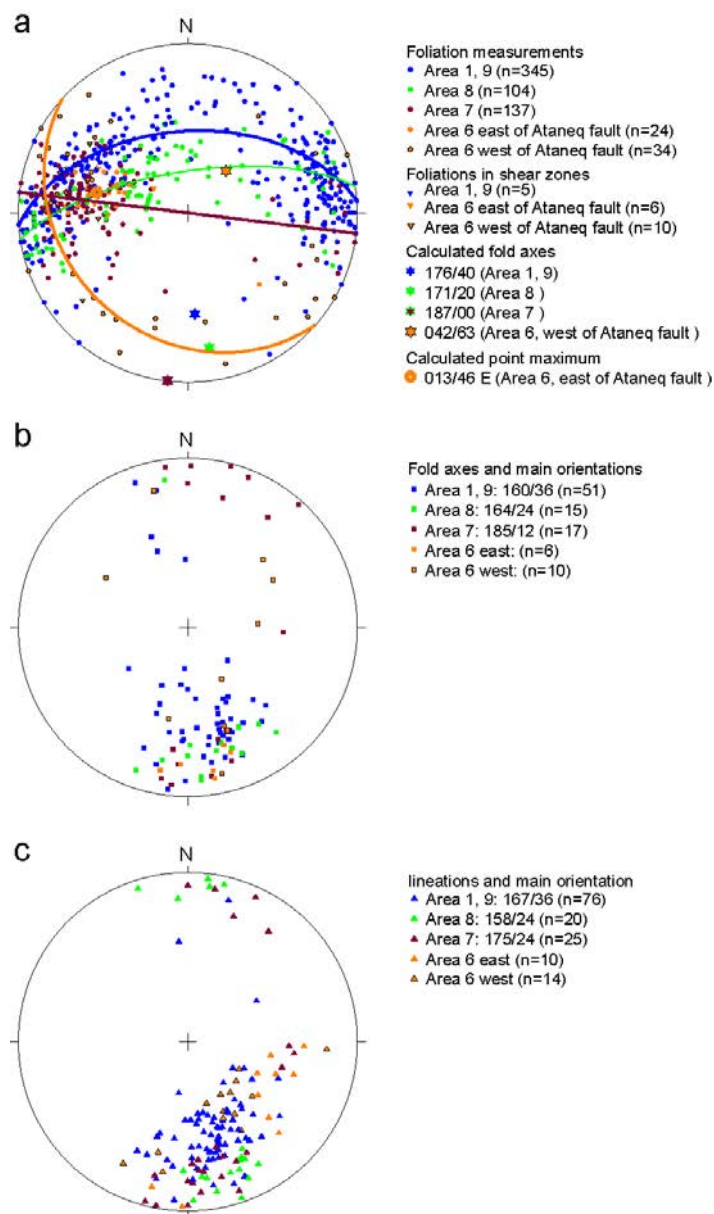


Figure A2_3. Stereo plots of the structural measurements of all four map areas. Data are plotted in lower hemisphere, equal area projection. The data are subdivided by map area, each area represented by its own colour. Statistical analyses were carried out for each map area separately, where a consistent distribution pattern existed. Fold axes were calculated for those foliation data that have a great circle distribution, using eigenvector analysis. The plotted fold axes in b are F3. Main orientations of lineations and fold axes are the orientations of the highest concentration in a contoured plot.

The foliation is deformed in at least two generations of folds, but is predominantly east-dipping.

F2 folds are not commonly observed. They are isoclinal to tight folds, with axial planes sub-parallel with the regional foliation (photo jpg2005-013, 015, 044).

The youngest fold generation (F3) dominates the map pattern and is characterised by upright to overturned folds that plunge shallowly to moderately to the south, with steeply east

dipping axial planes (Fig. A2_3). Inter-limb angles are between c. 50 and 120 degrees (photo jpg2005-114, 165). Overprinting of F2 and F3 folds are commonly observed (photo jpg2005-044, 059). Parasitic and outcrop scale folds are consistently west vergent, up to the kilometre-scale fold hinge west of the amphibolite belt, where the asymmetry of these folds switches, i.e. this is an F3 fold.

Narrow shear zones occur locally. They consist of mm to cm-thin anastomosing retrograde shear bands occurring within zones of about 1 m wide, and appear not to be laterally very consistent, since they could not be connected between outcrops. They are marked by retrogression of amphibolites to biotite schists and intense grain size reduction. No overprinting relationships are observed, but the significant lower metamorphic grade of these shear zones suggest that they post-date the very ductile F3 folds. These shear zones are approximately parallel with the S1 fabric.

The latest features are brittle fractures and faults (photo jpg2005-014). These are not ground-truthed in all cases, but are drawn in from aerial photographs. Predominant orientations are NW-trending with sinistral offset and E-W trending or WSW-trending with dextral offset. Only offset on the scale of centimetres has been observed in map areas 1 and 9.

Area 8

The second map area lies north of map areas 1 and 9, within the Isukasia terrane, and contains Eoarchaean felsic orthogneisses and rocks of the former Akilia supracrustal complex. The supracrustal rocks form a narrow belt that defines an antiformal structure, plunging south.

Poor weather limited the mapping in this area to only three and a half days. Results of the work show a map pattern that is significantly different from the pre-existing published maps.

Lithology

Supracrustal belt

The rocks of the supracrustal belt form a distinct tectono-stratigraphic sequence, which is complete in the southwest of the map area, but the individual units are not all laterally consistent. From bottom to top the units are: lower amphibolite and quartz-diorite, garnet-bearing quartzo-feldspathic gneiss, leucogranite, upper amphibolite. Near the top of the sequence lenses of ultramafic rocks are common. On either side of the supracrustal belt are quartzo-feldspathic biotite gneisses that are characterised by the occurrence of concordant and slightly discordant but deformed metadolerite dykes. Only the upper part of the supracrustal sequence, consisting of the garnet-bearing quartzo-feldspathic gneiss and the upper amphibolite are laterally consistent.

Lower amphibolite and quartz-diorite

The present base of this unit is a mafic, slightly banded amphibolite, medium grained and overall rather mafic and well foliated to platy (photo jpg2005-236). It grades upwards into a

dark grey, homogeneous, quartz-diorite which is medium grained and well foliated. Locally this rock is more dioritic in composition. The quartz diorite is c. 20–40 m wide and is again overlain by another mafic amphibolite, generally more heterogeneous than the one at the base of the sequence. Generally, no sharp boundary exists between the quartz diorite and the surrounding amphibolites. The amphibolites vary in thickness from just a few metres on the limbs of the large antiform, to more than 100 m (including intrusive gneiss sheets) in the core. Rusty bands with minor sulfides (pyrite and chalcopyrite) are common, especially near the contact with the quartz-diorite. Garnet is not common in these rust zones. In contrast with most other rock types the quartz-diorite contains only rare felsic veins. But like all other lithologies, it is intruded by abundant pegmatite dykes.

This unit was mapped from the southern part of the western flank, and continues from there around the hinge into the eastern flank of the antiform. The quartz diorite has only been noted in the western flank.

Garnet-bearing quartzo-feldspathic gneiss

The lower amphibolite is overlain by 20 to 100 metres of garnet-bearing quartzo-feldspathic gneiss. It is grey, medium to coarse-grained (photo jvg2005-245), overall quartz-rich and vaguely layered on dm- to m-scale, although compositions usually vary only slightly (photo jvg2005-247). It consists predominantly of quartz, plagioclase, biotite and garnet. Garnet occurs predominantly in fairly large (2–3 cm diameter) clusters (photo jvg2005-244), less commonly as small grains dispersed through the rocks. Biotite-rich layers, with or without garnet are locally abundant. Magnetite occurs very locally in the eastern limb, either dispersed or as thin seams in quartz-rich rocks. This provides a tentative link to the banded iron formations of Isua. Up to 5 cm wide melt veins are common, but not very abundant, and may contain garnet clusters. The quartz-rich composition suggests that the protolith of this gneiss is indeed clastic sediment. Geochronological analyses of zircons from a sample of this rock type, collected by P. Appel on the eastern flank of the antiform, suggests that the zircons are indeed detrital and they give an age range of 3.79 – 3.6 Ga, while metamorphic zircons in the same sample yield an age of c. 2.65 Ga (P. Appel and J. Hollis, pers com. December 2005). In the basal 5 metres few cm to dm wide amphibolite layers occur (photo jvg2005-238), which locally cross-cut the garnet-bearing quartzo-feldspathic gneiss.

Leucogranite

A 10 to 50 m wide sheet of leucogranite occurs predominantly at or near the contact between the garnet-bearing quartzo-feldspathic gneiss and the upper amphibolite (photo jvg2005-239). It is best developed on the western limb of the antiform, where it forms a fairly consistent sheet. On the eastern limb, near the hinge it forms a more irregular swarm of thin sheets in the upper amphibolite that presumably also intrudes the orthogneisses to the east. The leucogranite is medium to coarse-grained, white and consists of quartz, plagioclase, K-feldspar and minor (but variable) biotite. Garnet is uncommon. It has a variably developed foliation or gneissic fabric (photo jvg2005-205, 206), which commonly is weak and fairly simple and regular, which may suggest that it has a simpler deformation/migmatization history. The leucogranite is cut by E-W-trending undeformed pegmatites, but some older, deformed pegmatite lenses may be associated with the leucogranite, and the two may not always be distinguished.

Upper amphibolite

The leucogranite is overlain with a sharp contact by 50-100 m of heterogeneous, commonly banded amphibolite (photo jvg2005-217, 257). It is medium grey to black, medium grained, and consists predominantly of hornblende, plagioclase and quartz. The compositional variation of the rocks commonly increases towards the top of the unit. Melt veins are common, but never very wide.

Thin rusty horizons occur sporadically, but no sulphides or garnets have been observed in them. In a narrow contact zone along the leucogranite and along pegmatite dykes, the amphibolite can be metasomatically altered to a very mafic to ultramafic biotite schist.

Ultramafic rocks

Large lenses of ultramafic rocks occur in the upper amphibolite, commonly close to the upper contact with the orthogneisses. They are variable in composition, and both green, actinolite-rich (?) foliated ultramafic rocks, and massive, dark hornblendites are observed. Lenses are commonly 5–20 m wide, while the longest in the northwest are up to several hundreds of metres long.

Pegmatites

Several generations of pegmatites cut all lithologies. They are white and coarse-grained. East-west trending pegmatites tend to be undeformed, while more deformed ones are more concordant. In parts of the area they form very dense swarms of irregular dykes of 0.5 to 3 m wide, while some of the younger ones are locally 10 to 20 m wide.

Orthogneisses

Orthogneisses in the area form a heterogeneous complex, in which the main component is a light grey, medium-grained biotite orthogneiss of tonalitic protolith (photo jvg2005-228). These rocks have a well developed gneissic fabric; in the most homogeneous parts a very regularly spaced differentiated layering (photo jvg2005-228). These gneisses contain abundant inclusions, layers and schlieren of amphibolites of variable compositions (photo jvg2005-211, 212), as well as minor biotite-bearing gneisses. Several generations of melt veins in different states of deformation occur (photo jvg2005-211). They contain deformed, but clearly recognisable metadolerite dykes (presumably Ameralik dykes, photo jvg2005-197, 213), which suggests these rocks are Eoarchaeon, formerly named Amitsoq gneisses.

Based on field observations, no distinction could be made between the gneisses above and below the supracrustal belt.

In several locations, c. 10 to 50 m wide sheets of orthogneiss occur within the supracrustal belt near the contacts of the belt. In the antiformal hinge, large (> 100 m), more equidimensional blocks or lenses of the lower amphibolite occur within a network of orthogneiss. The orthogneiss is clearly intrusive into the supracrustal belt.

Ameralik dykes

Deformed and foliated metadolerite dykes occur in the orthogneisses, both concordant and discordant. They vary in width from c. 2 cm to over 1 m. Discordant intrusive relationships

are well preserved (photo jvg2005-198, 224), especially in sections perpendicular to the regional fold axis/extension lineation, in which also remnant igneous textures can be observed, in spite of the intense recrystallisation of the dykes. They are homogeneous, medium-grained and consist of hornblende + plagioclase ± quartz. Locally, < 3 cm large phenocrysts occur, which have an obvious white reaction rim (likely are cumulates dragged in from the magma chamber, but in disequilibrium with the dyke melt composition).

Structure

The structural history of the rocks in area 8 appears to be simpler than that of areas 1 and 9, but this may well be due to sparse observations. The main planar fabric has similar characteristics to areas 1 and 9, and forms a gneissic fabric in the orthogneisses, and a penetrative foliation in the supracrustal rocks. Commonly, the rocks have a weak lineation. The Ameralik dykes contain a foliation (S2) that is at a small angle to the gneissic fabric (S1) that they truncate (photo jvg2005-244). This suggests that two foliation-forming events occurred, and that the gneissosity is a composite fabric. No evidence was found for an older event in the supracrustal rocks. And in contrast to areas 1 and 9, no isoclinal F1 or F2 folds were observed.

The structure of area 8 is dominated by the kilometre-scale hinge (F3) of the Kangersuaq antiform. This is an open antiform that plunges about 20 degrees to the south and has a steep to overturned western limb. The hinge area is rather complex, where irregular blocks of amphibolite occur within a network of orthogneiss in the core of the hinge, and the fold plunges only slightly steeper than the slope of the terrain, resulting in an interference pattern between the folded layering and the irregular topography. F3 parasitic folds on outcrop scale are common throughout the area, and have moderately east-dipping axial planes, and shallow south-plunging fold axes, parallel with that of the main antiform (photo jvg2005-207, 209; Fig. A2_3). The regionally consistent mineral lineation is also here sub-parallel with the F3 fold axes. No axial planar fabric exists in the parasitic F3 folds. The Ameralik dykes and their internal S2 fabric are also folded by the F3 folds (photo jvg2005-213).

Brittle fractures are common, and are associated with the faults that cross the area. Two main faults exist in area 8, one in the bottom of the valley, striking N-S and running through the core of the antiform, the other striking E-W. The latter has shallowly ESE-plunging slickensides and a dextral displacement of c. 100 m, whereas the displacement of the former was not determined, due to the poor exposure in the valley. The E-W trending fault shows extensive red staining and minor epidote alteration. A major lineament is marked by a deeply incised valley south of area 8. It is not obvious whether there is any offset on the fault, since no lithological units have been directly correlated across it. In absence of evidence of displacement, the terrane boundaries in the map have been drawn to continue unaffected by the fault.

Areas 6 and 7

This part of Ujarassuit Nunaat is called Kangersuaq. It contains several amphibolite belts which alternate with orthogneisses with tonalitic protoliths. The eastern-most amphibolite belt presumably can be correlated with the belt in areas 1 and 9 (Fig. A2_2). This eastern

belt has the same tectonic position at the base of the Kapisilik terrane, against the underlying Isukasia terrane to the east. On the existing 1:100 000 scale map (Chadwick and Coe 1988) other thin and discontinuous amphibolite belts are indicated, but mapping in areas 6 and 7 revealed that other extensive amphibolite belts are present. These are all agmatized by pegmatites and leucogranites which intrude the region. Photo jvg2005-330 shows an overview of a km-wide agmatized amphibolite belt in the northwest of map area 7, which did not occur on previous maps. Area 6 straddles the NNE-SSW trending Ataneq fault, and in the west it is underlain by tonalites of the Mesoarchaeon Taserssuaq pluton. The easternmost intrusions of the Taserssuaq pluton are separated from the Ataneq fault by a 500 m wide zone of orthogneiss and amphibolites. The majority of the gneisses on either side of the fault are not obviously different in lithological aspects, but the orientation of the structures is quite distinct. The Ataneq fault separates the Akia terrane in the west from the Kapisilik terrane to the east, but based on field observations, there is no obvious distinction between the main rock types on either side. The fault is presumably a structure with an extended structural history with a significant dextral offset. Three phases of shear zones were recognised. Rocks of the Isukasia terrane exposed in the eastern margin of area 7 are not described separately here.

Lithology – Kapisilik terrane, east of the Ataneq fault

Amphibolite belts

Lithologically the amphibolite belts in this area are very similar to the one in areas 1 and 9, and only some of the differences are highlighted here. The amphibolites are variable from mafic homogeneous rocks to thin layers with intermediate compositions (photo jvg2005-277, 312, 368). Coarse-grained felsic veins with amphibole ± garnet (photo jvg2005-333) are less common than in area 1, and contain rarely diopside. Calc-silicate alteration is overall rare and garnet-bearing amphibolites occur in only few locations (photo jvg2005-313). Ultramafic lenses are common (photos jvg2005-340, 366) and seem to be more evenly distributed through the belts. Foliated gabbro was recognised in one location in the western amphibolite belt (photo jvg2005-329), but highly foliated quartz-poor, intermediate composition amphibolites recognised in several other locations may represent their deformed equivalents. Garnet-biotite gneiss panels between 0.5 and 2 metres wide are common in the amphibolites. They have a rusty weathering colour (photo jvg2005-361 shows an extreme case) and have a diffuse transition zone to the adjoining amphibolite, which commonly is garnet-bearing (photo jvg2005-287). Disseminated iron sulphides occur sporadically. Aluminous, garnet-sillimanite schist was not observed.

The eastern amphibolite band contains 10 to 50 m wide quartz-dioritic gneiss. It is a medium-grained, homogeneous, foliated plagioclase, hornblende-quartz-bearing igneous rock of intermediate composition (photo jvg2005-289, 290), which has a much simpler fabric than the surrounding amphibolites, and is therefore interpreted to be intrusive into the amphibolite belt.

The amphibolite belts in the western part of map area 7 and in area 6 are all heavily agmatized, with the volume of intruding felsic melt increasing towards the west (photo jvg2005-288, 360). The intruding phases here are leucogranite and pegmatite, which are not always

strictly distinguishable. The main belt is over 500 m wide, but has not previously been shown on any map. The amphibolites in these belts tend to be more mafic than in the belt to the east, but also the banded, more intermediate composition types occur. In a zone c. 1 km east of the Ataneq fault, several narrower agmatized amphibolite belts occur, which are all less than 50 m wide.

Leucogranite

White, massive discordant sheets of leucogranite (photo jvg2005-440) occur throughout areas 6 and 7, but are most abundant in the west, agmatizing the amphibolite belts that occurs there (photo jvg2005-284, 317, 357). They are discordant and generally irregularly shaped and form sheets, lenses and veins on the scale of cm to c. 50 m. The leucogranite consists of quartz, K-feldspar, plagioclase and minor biotite and are medium- to coarse-grained, with a weak foliation.

Orthogneisses

The most widespread background orthogneiss west of the easternmost amphibolite belt is similar to that in area 1 and 9, a homogeneous, light grey biotite-bearing orthogneiss with a differentiated layering and abundant melt veins (photo jvg2005-280, 387). Friend et al. have designated these orthogneisses as being of Mesoarchaeon age. Locally also amphibolite inclusions are abundant (photo jvg2005-378), giving the rock a heterogeneous aspect. In the extreme southwest of area 7 few small lenses of anorthosite occur within the orthogneiss (photo os2005-205, 207). In area 6 hornblende-bearing orthogneisses with a banded aspect are more common (photo jvg2005-445, 447). In a zone c. 500 to 1000 m east of the Ataneq fault, more homogeneous, bluish grey tonalitic orthogneisses occur, consisting of a complex of slightly different phases with similar composition (photo jvg2005-488). They contain quartz, plagioclase and minor biotite. These rocks are massive and have a simple foliation, defined by alignment of biotite and elongate quartz grains. They contain inclusions of the banded gneiss and amphibolite (photo jvg2005-463). These homogeneous, massive gneisses include a slightly coarser-grained foliated plagioclase-porphyritic tonalite (photo jvg2005-460, 461).

The heterogeneous orthogneisses show the same intrusive relationships with the amphibolite belt as in areas 1 and 9, including enclaves of amphibolite in the gneisses, and gneiss sheets in the margins of the amphibolite belts.

Both leucogranites and pegmatites intrude the orthogneisses, the same way they intrude the amphibolites. Several phases of white, coarse-grained pegmatites are common, and they vary from concordant veins and sheets, foliated and folded, to virtually undeformed and discordant dykes. Locally, the older phases are difficult to distinguish from the leucogranite. Where the younger, less deformed pegmatites intrude into amphibolites, they commonly have cm- to dm- wide rims of biotite schist, consisting of c. 90 percent of biotite. These rims are likely formed by alteration during intrusion of the pegmatites, under influence of a potassium-rich fluid. At location jvg2005-237 such a biotite schist rim contained abundant disseminated pyrite.

Lithology – Akia terrane, west of the Ataneq fault

Orthogneisses

West of the Ataneq fault are predominantly heterogeneous, banded orthogneisses are intruded by the Taserssuaq pluton to the west. The orthogneisses include both biotite- and hornblende-bearing, medium-grained quartzo-feldspathic rocks, which contain layers and lenses of amphibolite (photo jvg2005-433). A differentiated layering occurs locally in the background gneiss, but the regularly-spaced layering typical for the background orthogneiss in area 1 and 9 is not common. These gneisses are intruded by cm- to dm- wide veins and thin sheets of leucogranite (photo jvg2005-418), which become more abundant towards the contact with the Taserssuaq tonalite.

Amphibolites

The gneisses include also wider zones (< 50 m) that are dominated by amphibolite, with abundant sheets of orthogneiss. These zones appear discontinuous, but since they are truncated by shear zones, it is not certain whether the discontinuity of these belts is original, or a result of the structural truncations. The amphibolites are fine to medium-grained, intermediate to mafic in composition and commonly well banded (photo jvg2005-422). Calc-silicate alteration is common.

Taserssuaq pluton

To the west the orthogneisses are intruded by a leucocratic, massive, homogeneous tonalite, with a felsic vein network (photo os2005-225, 226). This tonalite is the eastern margin of the large Taserssuaq pluton which occupies an area of about 30 by 100 km. A sample collected near the eastern shore of Taserssuaq Lake, c. 15 km west of area 6, gave a zircon U-Pb age of 2982 ± 7 Ma (Garde et al. 1986). The tonalitic rocks have a variable, commonly weakly developed foliation. The rocks are medium-grained, light grey to white, and contain quartz, plagioclase and minor biotite. The porphyroclastic augen type, which is common for the core of the pluton, was not observed here in the margin. The contact with the orthogneisses west of the Ataneq fault is clearly intrusive and little disturbed by later deformation. The contact forms a c. 500 m wide transitional zone, in which inclusions of both amphibolite and a felsic orthogneiss occur within tonalite (photo jvg2005-400, 409), while in the eastern part sheets of tonalite intrude in the gneisses and amphibolites. In the external (eastern) part of the contact zone, a hornblende-rich dioritic phase is seen both as intruding phase, and as inclusions of a more felsic phase of the Taserssuaq pluton (photo jvg2005-393, 394). The tonalite truncates a mylonitic fabric in the orthogneisses (photo jvg2005-403, 410), and the intrusion of the tonalite must postdate the orthogneisses west of the Ataneq fault by the period of time covered by deformation phase D1 plus a phase of shearing.

Aplitic dykes

The latest intrusive phase in the contact zone is formed by 10 cm to 1 m wide leucocratic aplitic dykes, which are bluish grey, fine-medium grained (photo jvg2005-412, 421). These dykes post-date any deformation in the area, including the latest retrograde mylonitic shear zones.

Lithology – rock types common to both sides of the Ataneq fault

Ultramafic dyke

An ultramafic dyke of variable width runs N-S through the map area, and is offset by the Ataneq fault by c. 4 km. The dyke is sub-vertical and can with few gaps be traced through the whole Ivisârtoq map sheet (see also Appendix 3). Along most of its exposed length the width of the dyke is in the order of 50 m, but locally it is up to 150 m wide. It is homogeneous, massive, medium grained and consists of hornblende, olivine, a light brown amphibole and phlogopite. At the margins, the dyke contains plagioclase.

Metadolerite dykes

Two large discordant metadolerite dykes are 3–5 m wide and run in a ESE-WNW through the northern part of area 7, extending into area 6 where they join into one (photo jvg2005-439). The dykes are massive, fine-grained with locally remnant igneous textures, but overall recrystallised. They form an array of left-stepping, segments, and thin branches occur on the northern side of the dyke in area 6 (photo jvg2005-451). Few smaller dykes between few cm and 30 cm wide (photo jvg2005-291) occur in the area. These dykes are assumed to be part of the Palaeoproterozoic metadolerite dyke swarm of western Greenland.

Structure – east of the Ataneq fault

The structural style of map areas 6 and 7 is similar to that of area 8 and is consistent with the structural position on the western overturned flank of an antiform in area 8. Orientations of the structures are similar to those in area 8, although the data reflect that area 7 is slightly tilted to the north with respect to area 8. The western part of map area 7 contains a set of north-south trending shear zones, which are common to (and continuous into) map area 6, and are described there.

The main foliation S1 is consistently east-dipping and no older fabric has been recognised. In the agmatized amphibolite belts, smaller veins of agmatizing melt are tightly folded, with the main foliation forming an axial planar fabric (photo jvg2005-285, clearly visible 10 cm to the right of the hammer handle in the centre of the photo). On the other hand, the fabric in the intruding leucogranitic sheets is not nearly as intense as in the surrounding amphibolites, or as in the orthogneisses outside the amphibolite belt. Both the small and the larger leucogranite veins and sheets are fairly irregular, and have not undergone the same transposition as the orthogneiss sheets, which now are concordant with the main fabric. It is therefore assumed that, as in areas 1 and 9, the S1 foliation is a composite fabric, formed during several deformation phases both predating and postdating the intrusion of the leucogranite. A mineral lineation is commonly poorly developed, and is strongest in the more highly strained parts of the amphibolite belt. The lineations are sub-horizontal, plunging north or south (Fig. A2_3c). Isoclinal F2 folds that fold the main fabric are rare but occur throughout the area (photo jvg2005-444, 471). Upright and overturned F3 folds (photo jvg2005-276, 360) overprint isoclinal folds (photo jvg2005-444) and have an east-vergent asymmetry. F3 folds are not very common and are most abundant in the western part of map area 7. They are commonly very open structures (photo jvg2005-360). A set of small

fractures, with quartz and epidote fill, were observed along the axial plane of F3 folds in one location (photo jvg2005-276). Fold axes, both small scale and large scale plunge shallowly south or north (Fig. A2_3a and b).

The terrane boundary in the east of the area is marked by a zone of anastomosing narrow ductile shear zones with a mylonitic fabric (photo jvg2005-307, 308). The shearing deforms both amphibolite and the leucogranitic veins. No lineations were noted, but it should be noted that observation of these was hampered by the rounded character of the outcrops where the shear zone was best exposed. Porphyroclasts suggest a top-to-the north sense of shear. It is not clear whether this shear zone is associated with terrane juxtaposition or merely the result of strain localisation at the lithological contact between the amphibolite and the orthogneiss to the east during general deformation. In that respect it should be noted that similar narrow ductile shear zones occur in the orthogneisses further west (photo jvg2005-316), but other amphibolite-orthogneiss contacts lack such zones of high strain. Intense folding occurred in one of the ductile shear zones in amphibolite with abundant leucogranite veins (photo jvg2005-317).

High-grade ductile shear zones are parallel with the main foliation, have straight to slightly anastomosing foliations and contain abundant tailed porphyroclasts which are derived from strongly deformed pegmatitic veins (photo jvg2005-316, 373, 375, 477, 487). Both amphibole and biotite appear stable from field observations and the rocks have a granular texture, suggesting intense post-kinematic recrystallisation. These observations require confirmation from petrography. Locally shear folds occur. Stretching lineations are not strongly developed, and plunge SE to ESE. Good kinematic indicators are scarce, but they are fairly consistent indicating an oblique top-to-west reverse shear sense. The ductile shear zone c. 1 km east of the Ataneq fault contains pegmatites which truncate the shear fabric, but which are subsequently folded (photo jvg2005-478). This suggests that the pegmatites intruded late in the shearing event, or that a phase of flattening strain postdates the shear event. This shear event may possibly be related to terrane juxtaposition. Locally, the shear zone fabric was folded by F3 folds. With the exception of the shear zone between the amphibolite belt and the Eoarchaeon gneisses at the eastern side of area 7, none of the shear zones separates obviously different rocks, although the homogeneous, bluish grey tonalitic orthogneiss was only observed west of the shear zone c. 1 km east of the Ataneq fault. Geochronology will be used to test the age of the shear zones and the age of gneisses on either side of them. None of the ductile shear zones was traced for more than a few hundred metres in the field, but they were interpreted from areal photographs to extend at least 2 to 3 km along strike.

Structure – west of the Ataneq fault

The structures west of the Ataneq fault have a significantly different orientation (Fig. A2_3), but have the same style and sequence. The S1 foliation is predominantly steeply NNE-dipping and is folded in F3 folds which have a range of orientations, but which predominantly plunge moderately to steeply to the northeast. The asymmetry of most of these folds is still consistent with the antiform to the east. This different orientation of the foliation is rather local, both to the south and north, the moderately to steeply ESE dipping orientation is again dominant. Only few isoclinal F2 folds were observed in area 6 (photo jvg2005-418).

The Taserssuaq tonalite truncates the S1 foliation in inclusions of orthogneiss and amphibolite (photo jvg2005-401), but locally has a weak foliation itself.

Structures common to both sides of the Ataneq fault

Retrograde shear zones occur on both sides of the Ataneq fault, and may well be associated with this structure. They form narrow zones mainly between 0.5 and 5 m wide, rarely up to 10 m, within which schistose shear bands form an anastomosing pattern (photo jvg2005-398, 405, 453). The Ataneq fault zone forms an exception, in that it is a c. 50 m wide shear zone. These zones are characterised by intense grain size reduction, and retrogression of amphibolites to biotite schist, while locally also chlorite and muscovite occur. Rust staining of the schistose bands is common, while some of the zones, e.g. the ones that lie in a zone 1 to 2 km east of the Ataneq fault form several m wide rusty zones that can be traced over many kilometres in the landscape, and in aerial photographs. Locations where these shear zones run into amphibolite belts, they contain disseminated pyrite and chalcopyrite in larger concentrations than anywhere else in the map area. Especially the latter zones show signs of cataclasis. Angular to sub-rounded fragments of feldspar and quartz lie in a very fine-grained, rusty brown matrix consisting of biotite, chlorite and quartz (photo jvg2005-354, 384). Seen on the foliation plane, these rocks have a chaotic character (photo jvg2005-381). Locally, the fragments are platy and have pronounced stretching lineations, which show a variety of orientations, due to fragment rotation during cataclasis. Locally, quartz ribbons occur. One of the cataclastic zones in the south-west of area 7 contains disseminated molybdenite (location jvg2005-278). Most of the shear zones in the map were traced from aerial photographs, since they have a marked topographic expression.

The fabrics in the retrograde shear zones are locally intensely folded (photo jvg2005-427, 429), but no clear indications were seen of the age of this folding relative to F2 or F3. Given the retrograde nature of these shear zones, and the lack of retrogression in association with F3 folding, it is assumed that the shear zones postdate the F3 folds.

Kinematic indicators are rather common and well developed in most of these zones. They consist of shear bands, asymmetric strain shadows around porphyroclasts and CS fabrics. Lineations are not always obvious, or not consistent, as in the cataclases. Commonly they plunge approximately southeast. Kinematics vary strongly, but the majority of the retrograde shear zones show oblique, top down-to-east normal displacement (photo jvg2005-455), while predominant dextral displacement is slightly less common. Assuming that the shear zones with normal displacement have not been rotated significantly since their deformation, they would represent a phase of extensional deformation.

Brittle faults occur predominantly in two sets, trending E-W and NW-SE. In the southern part of area 7, an E-W fault has a dextral offset of c. 100 m. Minor red staining and epidote mineralisation was observed along the larger faults. Small scale fractures and faults are widespread through the area, some with centimetre-scale offsets. The offsets in the conjugate sets of photo jvg2005-353 suggest that fracturing occurred under N-S compression of E-W extension. But small sinistral offsets along such small fractures appears dominant

(photo jpg2005-351, 352). Another set of west-dipping fractures occurs locally, spaced at 10 to 20 cm in dense swarms, and which have rusty surfaces (photo jpg2005-349, 350).

Ataneq fault

The Ataneq fault itself is poorly exposed in map area 4, and is characterised by a c. 50 m wide gap in the exposures (photo jpg2005-492). Signs of brittle deformation are virtually absent, and the few exposures at the margins and core of the zone indicate that the zone underwent a phase of retrograde shearing. Minor silicification occurs predominantly in a c. 100 m wide zone on the eastern side of the fault. Kinematic indicators are not consistent. Reverse, top-to-northwest, sinistral, and normal, top-down-to southeast, dextral shearing has occurred, but the latter appear to be the dominant phase. The Ataneq fault displaces both the large ultramafic dyke and the main metadolerite dyke with a dextral offset, indicating that it has been active during the Palaeoproterozoic. However, whereas the ultramafic dyke shows an offset of c. 4 km, the metadolerite dyke is offset by 440 m. This suggests 1) that the latest activity on the fault was Palaeoproterozoic or younger, and 2) that there are several periods of movement on the Ataneq fault, and 3) that the ultramafic dyke must be older than the metadolerite.

Discussion

Amphibolite belts

The amphibolite belts in both Kapisilik and Isukasia terranes are the oldest tectono-stratigraphic units of the terranes they appear in. The amphibolites have been so strongly deformed under amphibolite facies metamorphism, that protoliths have become impossible to recognise in most of the belts. Furthermore, widespread intense alteration has further hampered an evaluation of the original setting of the rocks in the amphibolite belts. The main exceptions are the metagabbros in areas 1, 7 and 9. Some of the more heterogeneous, calc-silicate rich amphibolites in areas 1, 7 and 9 could potentially be derived from pillow basalts. Although this belt is presumably continuous with the Ivisaartoq belt to the east, where pillow structures are commonly recognised, this interpretation is highly speculative. Geochemistry may provide more insight into the original environment of the belt. The agmatized amphibolite belts in Kangarsuaq may even be more difficult to interpret, because of the way the rocks are broken in fragments. The pervasively intruding melt may also have altered the rocks geochemistry. There is no obvious indication that these amphibolite belts are different from the one at the eastern margin of area 7.

The Eoarchaeon amphibolite belt in area 8 is distinct, in the occurrence of a metasedimentary unit, as well as the presence of the quartz-diorite. Especially the former strongly suggests a high crustal level origin for the belt.

Orthogneisses

The presence of the Ameralik dykes in the Eoarchaeon orthogneisses of the Isukasia provided a means of distinguishing these rocks from the dyke-free orthogneisses in the Kapisilik terrane. Based on the occurrence of the orthogneisses alone, such a distinction would be extremely difficult. Especially in area 1 and 9, the heterogeneous tonalitic orthogneiss was obviously intruded by a younger, more leucocratic granitic phase. This suggests that the orthogneisses form a complex of intruding phases of different generations. The difference in structural evolution of the two intruding phases may suggest that a significant age difference exists. Age determinations are required to determine the exact age relationship of these two rock types.

Structural history

With the exception of the rocks west of the Ataneq fault, the whole region has a consistent pattern of F3 folding, which is common to the Isukasia and Kapisilik terranes, likely also to the Tre-Brødre terrane, as proposed by Friend & Nutman (2005). F3 folding postdates terrane assembly around 2700 Ma. The regional S1 foliation, which appears common to all terranes, is a composite fabric which is likely the result of a series of events, presumably including thrusting during terrane assembly. The latest retrograde phase of shearing appears to culminate in the Ataneq fault. These late shear zones represent several phases of movement, of which the dominant one appears to be one of extensional deformation. These zones predate the Palaeoproterozoic dolerite dykes, but in the Ataneq fault, one of these retrograde shear zones was reactivated by dextral strike-slip movement after the intrusion of the dolerite dykes.

The interpretation of the retrograde shear zones being dominantly extensional is in contrast with the findings of Park (1986), who interpreted the network of shear zones in the area as thrusts. On the other hand, these structures may be related to the phase of extensional collapse, documented in the Isukasia area to the north-east by Hanmer & Greene (2002). The inconsistencies in kinematic indicators in these zones suggest that they were active under a variety of tectonic regimes, which allows for these structures to have been thrusts prior to reactivation during extension.

Ataneq fault

The actual nature of the Ataneq fault was difficult to assess, because of its poor exposure in area 6. It is a system of steeply dipping brittle faults with at least 4 km dextral displacement, but also retrograde shear fabrics occur within the fault zone, and indicate that the zone was active during the period of late, retrograde shearing. It displaces both the ultramafic dyke and a metadolerite dyke, both of which are unaffected by the retrograde shear zones outside the Ataneq fault. The metadolerite dyke is assumed Palaeoproterozoic, and therefore the dextral displacement is presumably the latest deformation and of Proterozoic age. The Ataneq fault must have been reactivated several times in its history. South of the mapping area, rocks of the Taserisuaq pluton occur also east of the Ataneq fault and the fault is not strictly a terrane boundary. Although it presumably separates the Akia terrane from the Kapisilik and Isukasia terranes along part of its length, it does not form the original fault structure along which the Akia and Kapisilik terrane were originally

juxtaposed. Based on field observations alone, there is no strong indication that the fault separates rocks with a different tectonic history in area 6. But this needs to be tested by using geochronology.

Appendix 3: Field report 2005 - Ujarassuit Nunaat Region – South (Nigel M. Kelly & Susanne Schmid)

Introduction and background

Mapping objectives for the 2005 field mapping season were to investigate the supracrustal belts in the inner Godthåbsfjord area between Ujarassuit Pavaat and Ilulialik, where detailed map data and understanding of Archaean and Proterozoic structures were felt to be lacking. Work represented a continuation of the GEUS 2004 project. Fieldwork during the 2005 season, which is summarised in this report, was carried out by Nigel Kelly (nmk) and Susanne Schmid (ssc) over the period 15 October to 16 August, working from 5 field camps in areas 1 to 5 (Fig. 2). Mapping focussed on the lithological and structural relationships in supracrustal belts, and between the supracrustal units and host felsic orthogneisses. An attempt was made to characterise the important structural features in order to relate these to the overall tectonothermal evolution of this part of the Godthåbsfjord region.

As mapping covered rocks of potentially 3 separate terranes (based on the nomenclature and terrane model of Friend & Nutman, 2005), observations and data from each terrane area will be presented separately, with a synthesis of common features and interpretations presented at the end of the report. In general, the resulting field maps match closely to that presented in the map of M.A. Crewe (64 V.2,49a) from mapping in 1981 and 1982.

Areas 1 to 3

Areas 1 to 3 covered an intensely deformed, linear and strike extensive supracrustal belt within felsic to intermediate orthogneisses lying immediately to the west of Ujarassuit Pavaat (Fig. 2; see also maps on the ArcView© project). The supracrustal belt, predominantly composed of mafic amphibolite with minor biotite-schist, forms a probable extension to more weakly deformed mafic and ultramafic rocks of the Ivisaartoq supracrustal belt. The area forms part of a new terrane segment proposed by Friend and Nutman (2005) called the Kapisilik Terrane, interpreted to be composed of Mesoarchaeon orthogneisses (~3070 Ma) hosting supracrustal belts of unknown age. The western part of areas 1 to 3 also covered the boundary, proposed by Friend & Nutman (2005) to lie between the Kapisilik and Færingehavn terranes. However, recent unpublished U/Pb zircon ages suggest this boundary may lie further to the west (C. Friend pers. comm. 2005). Mapping in these areas was conducted from 3 separate field camps (15/7-20/7, 21/7-27/7, 6/8-10/8), with a total of 14 days active mapping and sampling. Conditions were difficult with a high numbers of insects in some areas and extensive lichen cover on most outcrops.

Lithologies

Felsic Orthogneisses

Felsic orthogneisses in areas 1 to 3 are divided into two mappable units that correspond to the orthogneiss types that lie on either side of the formerly proposed 'Kapisilik' and Færingehavn terrane boundary (see lithological map). These are arbitrarily referred to as the *Heterogeneous* and *Migmatitic felsic orthogneisses*, respectively.

Heterogeneous felsic orthogneisses:

The heterogeneous felsic orthogneisses are further sub-divided into *banded* and *massive* types.

Banded felsic orthogneiss is a medium- to coarse-grained biotite-bearing orthogneiss with banding defined by distinct variations in biotite modal abundance (photo nmk2005-231). Locally, layer composition becomes more intermediate (photo nmk2005-041, 054). A well developed gneissosity is defined by elongate clusters of biotite, quartz-feldspar domains and by aligned and attenuated recrystallised leucosome (photo nmk2005-063, 066). Leucosome may be dismembered (photo nmk2005-041) and is commonly folded (photo nmk2005-017). Locally the *banded* felsic orthogneiss may be quite migmatitic (photo nmk2005-016, 037), although an 'in situ' versus 'injection' origin is not clear.

Banded felsic orthogneiss commonly contains discontinuous lenses and rafts of mafic (amphibolite) and ultramafic material. Amphibolite inclusions may be relatively undeformed (photo ssc2005-373, 374) or highly attenuated and folded (photo nmk2005-001 to 003, 042). Ultramafic inclusions occur on sub-metre to tens of metres scales (photo nmk2005-057, 058). These bodies are typically massive or weakly banded, and may be weakly or intensely deformed.

Coarse-grained, *massive* felsic orthogneiss is weakly banded and typically preserves a less well defined gneissosity (photo nmk2005-232, 038). This type commonly contains less biotite and lower leucosome volumes compared with the banded felsic orthogneiss. The weak banding that is commonly present is defined by minor variations in biotite modal abundance with spaced, layer parallel recrystallised leucosome. Where freshly exposed the orthogneiss is typically pale grey in appearance, but may appear white in some exposures. Locally the *massive* orthogneiss may have a higher abundance of biotite, becoming more intermediate in composition, and can develop an intense gneissosity defined by stringers of biotite- and feldspar-rich domains (photo nmk2005-093, 094).

In areas 1 to 3, *massive* and *banded* felsic orthogneisses are commonly affected by alteration related to moderately penetrative brittle to semi-ductile faulting that dissects all lithologies. Alteration is characterised by replacement of biotite with epidote (+/- chlorite) making the orthogneiss pale green in appearance (photo nmk2005-228). The orthogneiss is also locally silicified, appearing orange to reddish-orange in outcrop (photo nmk2005-072).

Migmatitic felsic orthogneiss:

Only observed on the western extremity of mapping area 3 (see maps on the ArcView© project on the DVD), this orthogneiss is characterised by abundant, attenuated and recrystallised leucosome interlayered on a centimetre scale with biotite-rich domains (photo nmk2005-068, 069). The rock is medium- to coarse-grained and composed of feldspar and quartz, with variable modal abundances of disseminated biotite. The orthogneiss contains a higher volume of leucosome compared with the typical occurrences of heterogeneous felsic orthogneiss mapped within the Kapisilik terrane area. The orthogneiss contains common inclusions of amphibolite, as attenuated (photo nmk2005-069) or rotated pods or boudins with layering and foliation oblique to the external layering (photo nmk2005-070).

Amphibolite

Two types of amphibolite were distinguished in areas 1 to 3, homogeneous (massive) and banded amphibolite. Outcrop quality was not sufficient to determine if these two types formed strike extensive units within the supracrustal belt, or defined any geologically significant geometry. Both types of amphibolite are variably migmatitic, with leucosome present in nearly all exposures. Leucosome, which may occur in high abundance, is typically recrystallised, attenuated parallel to foliation (photo nmk2005-011), and dismembered (photo nmk2005-045, 046, 047).

The dominant amphibolite type in areas 1 to 3, homogeneous (massive) amphibolite is typically fine- to medium-grained and composed of hornblende amphibole and plagioclase, with or without biotite (photo nmk2005-032). A foliation is weakly, moderately or strongly developed (photo nmk2005-233), defined by aligned amphibole and plagioclase aggregates, but may locally be close to L-tectonite (photo nmk2005-111). Leucosome, which varies from poorly to moderately abundant, is typically recrystallised and attenuated parallel to foliation and commonly folded (photo nmk2005-234). In area 3 massive mafic amphibolite may occur as strike extensive zones up to 20 metres wide. These outcrops are typically weakly to moderately foliated and cut felsic orthogneiss, leucosome veins and pegmatite (photo nmk2005-095, 107, 225). The leucosome abundance is locally high (photo nmk2005-076, 077). Within some sections this massive amphibolite may be coarse-grained (<1 cm, photo ssc2005-387), bordering on gabbroic in composition and texture (photo nmk2005-098, 099).

Banded amphibolite is layered on sub-centimetre to decimetre scales, with layering defined by variations in amphibole versus plagioclase content (photo nmk2005-009, 011, 015, 039, 059). Some layers are relatively leucocratic and locally coarse-grained (photo nmk2005-012, 014) and may preserve diopside. Intermediate to felsic zones are interpreted to reflect variations in the protolith, possibly volcanic, or in some cases represent recrystallised leucosome. Banded amphibolite may also preserve discontinuous layers and boudins of mafic to ultramafic material (photo nmk2005-030).

Both types of amphibolite are locally garnet-bearing. Garnet was commonly, though not exclusively, associated with recrystallised leucosome (photo nmk2005-036, 101) and is more common where amphibolite occurs adjacent to felsic orthogneiss (photo nmk2005-035). Garnet occurs as disseminated porphyroblasts or grain aggregates, locally up to several centimetres in size, though typically less than 0.5 cm.

Garnet-Biotite Schist

Biotite schists are nearly ubiquitously garnet-bearing and are typically associated with amphibolite. Garnet-biotite schist forms a strike extensive lense (over several kilometres) within the main amphibolite unit at its western boundary with felsic orthogneiss in areas 1 and 2. In addition, garnet-biotite schist occurs associated with amphibolite as isolated deformed lenses included within the felsic orthogneiss to the east of the main amphibolite unit in area 3.

Garnet-biotite schist is typically semi-pelitic in composition, predominantly composed of garnet, biotite, plagioclase and quartz, with or without graphite. Biotite abundance is highly variable, with compositions composed of up to 50% biotite, but also occurring as compositions that are more felsic and gneissic in character (photo nmk2005-092). Schists are locally more pelitic, with examples of sillimanite- and possibly staurolite-bearing assemblages. Garnet in the schists may occur as porphyroblasts and poikiloblasts up to 3cm in size, and as grain aggregates 4 to 5cm in size (photo nmk2005-091), typically enveloped by the biotite-feldspar-quartz foliation.

Garnet-biotite schist is commonly migmatitic, with locally high volumes of recrystallised leucosome. Leucosome may occur as nebulitic, ponded forms that interfinger with layering and layer parallel leucosome (photo nmk2005-022, 023), or as moderately to highly attenuated veins (photo nmk2005-027) that are parallel to layering and folded (photo nmk2005-024, 025, 026).

Ultramafic rocks

Ultramafic rocks occur as small rafts and boudins (<0.5 to several metres) and larger pods (up to 100 m+) within amphibolite and felsic orthogneiss. These rocks can be subdivided into two types: *green-brown ultramafite* (most common) and *black ultramafite*.

Green-brown ultramafite, named based on the typical colour of weathered outcrops, is typically composed of pale-green amphibole, serpentine and olivine, with or without talc and chlorite. In these rocks, pale amphibole may occur as rounded nuggets (possibly former orthopyroxene) that are typically 1 to 3 cm in size but as large as 15 cm in size (photo nmk2005-055, 056). Some ultramafite bodies preserve relic igneous textures characterised by randomly oriented phenocrysts (photo ssc2005-372) now pseudomorphed by pale-green amphibole (photo nmk2005-222, 223, 224).

Black ultramafite is predominantly composed of hornblende, with lesser amounts of diopside and actinolite, and commonly occurs as <10 to 15 metre sized rafts and boudins with felsic orthogneiss that may be weakly banded (photo nmk2005-057, 058). Where occurring as larger rafts, they are commonly cut by abundant leucosome.

Ultramafite is commonly cut by veins along which the rocks are altered to talc and chlorite-rich assemblages and domains rich in serpentine. Similar zones of alteration form rinds on many ultramafite bodies. In such alteration zones, large (3 to 5 cm) randomly oriented actinolite crystals may locally develop (photo nmk2005-219, 220). Some ultramafite pods that have undergone intense veining and alteration may appear banded, with talc- and chlorite-rich zones interlayered with the unaltered zones (photo nmk2005-104, 105). In some occur-

rences, where ultramafite is cut by leucosome, garnet and diopside form in the reaction zone (photo nmk2005-019, 020, 021).

Pegmatite

Pegmatitic dykes, as distinct from recrystallised leucosome within most lithologies, are composed of coarse- to very coarse-grained feldspar (K-feldspar + plagioclase) and quartz, with variable abundances of biotite. Pegmatite dykes cut all lithologies (e.g. photo nmk2005-050), but are themselves deformed. Pegmatite dykes occur in sizes varying from small veins up to large dykes, and can intrude in large volumes (photo nmk2005-110). Veins and dykes are variably deformed and recrystallised, and commonly sub-parallel to layering and foliation in amphibolite and orthogneiss. In these contexts the pegmatites may be folded (photo nmk2005-048, 049) or attenuated and boudinaged (photo nmk2005-062, 218). It is possible that more than one generation of pegmatite is present, although this was not clear based on composition or field relationships.

Structure-Metamorphism & Lithological relationships

Ductile structures, Fold-foliation relationships

Poor exposure (extensive lichen cover) coupled with similarity in grade between events, makes it difficult to unambiguously distinguish between overprinting ductile events. However, a number of key observations suggest that multiple events may have affected the rocks in areas 1 to 3. An event sequence is proposed in Table A3_1.

The preservation of a layer parallel foliation and minor aligned leucosome within amphibolite rafts in felsic orthogneiss (photo ssc2005-373, 374), suggests that this early foliation predates the intrusion of the heterogeneous felsic orthogneiss. However, this foliation may not reflect a distinct event – for example, the felsic orthogneiss may be a syn-deformation intrusion, with the foliation in the amphibolite representing an early phase of an orogenic event that continued to deform the rocks subsequent to intrusion.

More clearly, garnet-biotite schist in area 3 contains large garnet poikiloblasts that preserve aligned and folded inclusion trails that are oblique to the foliation external to the garnet (photo nmk2005-088 - 091). As these grains are partly enveloped by the dominant biotite-bearing foliation, and do not overgrow it, these textures indicate the presence of an earlier, folded foliation (i.e. one or more events predating garnet growth).

Table A3_1. Possible event sequence for areas 1 to 3.

Event	Characteristics	Conditions
D_{n-1}	layer parallel foliation in amphibolite	???
	<i>Intrusion of heterogeneous felsic orthogneiss</i>	
D_n	locally high-strain, ductile deformation and interleaving of amphibolite and orthogneiss, and tight to isoclinal folding; pre- or early syn-deformation leucosome	Amphibolite facies
	<i>Intrusion of pegmatitic dykes</i>	
D_{n+1}	moderate to high strain deformation (folding and HSZs), with localised attenuation, boudinage and recrystallisation of pegmatite	Amphibolite facies
D_{n+2}	open to tight folding of structures and lithologies, localised development of L4 mineral lineations, rotation of fold axes to F4 direction	Amphibolite facies
D_{n+3}	retrograde shear and fault zones: brittle-ductile deformation with development of chlorite & epidote assemblages	Greenschist Facies

Pre-pegmatite dyke structures - D_n

The first major ductile deformation event that can be recognised in both the amphibolite and felsic orthogneiss is characterised by moderate to high strain structures. It is not clear if these structures reflect the effects of a single event, or multiple overprinting events. Therefore, all structures that predate the intrusion of pegmatite dykes has been designated part of event ' D_n ', where 'n' may refer to one or more events. Event(s) associated with D_n locally produced well developed foliations. In amphibolite the foliation is defined by aligned amphibole (+/- biotite) and plagioclase (photo nmk2005-011), whilst in felsic orthogneiss, a medium to coarse-grained gneissosity is defined by feldspar, quartz and biotite. The presence of tightly folded gneiss veins in amphibolite within pockets of low strain (photo nmk2005-009), typically with only weakly developed or no gneissosity (photo nmk2005-010) suggests that this event produced the first foliation in the orthogneiss.

Quartzofeldspathic leucosome in both rock types is locally transgressive to layering, but commonly isoclinally folded, attenuated, boudinaged and aligned parallel to foliation. In addition, nebulitic and partial deformed leucosome in garnet-biotite schist (photo nmk2005-023 - 025), is suggestive of a pre- or early syn-deformation timing for these leucosomes. It is not clear from outcrop observation if metamorphism that accompanied this event reached conditions sufficient for partial melting, or if leucosome was injected into the terrane. However, mineral assemblages suggest that amphibolite facies conditions accompanied the development of structures.

Zones of highest strain are commonly focussed on boundary zones between felsic orthogneiss and supracrustal (amphibolite) units, but also within interlayered zones of amphibolite and felsic orthogneiss (photo nmk2005-028, 034, 039). Orthogneiss lenses within amphibolite are commonly intensely attenuated and boudinaged (photo nmk2005-042 -

046), whilst layers of amphibolite may be deformed by isoclinal (photo nmk2005-001) and sheath folds (photo nmk2005-061). The focussed nature of D_n deformation in such zones is well developed in area 3, where the mapped supracrustal 'package' in fact represents zones of massive and layered amphibolite interlayered with zones of dominantly felsic orthogneiss. At the base of SE-dipping packages of (dominantly) massive amphibolite are focussed zones of intense strain and mylonitisation (photo nmk2005-077). The high strain zones are characterised by intense attenuation of interlayered felsic orthogneiss and amphibolite (photo nmk2005-078), isoclinally folded layering and leucosome (photo nmk2005-079) and the occurrence of nose folds (photo nmk2005-080). The structures are indicative of extreme non-coaxial strain. Above these mylonite zones, amphibolite, which may be cross-cut by abundant leucosome, is only moderately deformed (photo nmk2005-077), but may also be cut by other zones of high strain where layers of felsic orthogneiss occur (photo nmk2005-076). In some cases the amphibolite package itself shows evidence for boudinage on tens of metres scales (photo nmk2005-081).

Post-pegmatite dyke intrusion – D_{n+1} & D_{n+2}

Felsic pegmatitic dykes cut across layer parallel foliations in both orthogneiss and amphibolite (photo nmk2005-050), but are themselves deformed and recrystallised. Pegmatite dykes are commonly folded (photo nmk2005-048, 051, 110), and are locally boudinaged (photo nmk2005-218), attenuated and rotated to be sub-parallel to a foliation in amphibolite or felsic orthogneiss (photo nmk2005-218). These observations suggest that two (amphibolite facies) events (D_{n+1} & D_{n+2}) affected the rocks, subsequent to the intrusion of pegmatitic dykes. An example of the structural style resulting from interaction between D_n, D_{n+1} and D_{n+2} is presented in Figure A3_1.

D_{n+1} produced high strain foliations in orthogneiss and amphibolite (photo nmk2005-218). The second event folded deformed and partially recrystallised pegmatite (photo nmk2005-048, 051, 110). Open, tight and isoclinal folds that deform foliations and foliation parallel leucosome (photo nmk2005-049, 117, 235), and boudinaged felsic orthogneiss layers in amphibolite (photo nmk2005-043 - 046), may be related to D_{n+1} & D_{n+2}. However, these events resulted in moderately S-plunging mineral and stretching lineations (hornblende in amphibolite, quartz + feldspar in orthogneiss) that are parallel to the axes of folds (Fig. A3_2a). The rare occurrences of fold axes oblique to this direction indicate that most fold axes and lineations observed in the area resulted from, or were rotated during D_{n+1} or D_{n+2}.

Poles to foliation measurements from felsic orthogneiss and supracrustal rocks form a main cluster in the northeast quadrant reflecting the dominantly SE-dipping fabric in the area, with a second minor cluster in the eastern quadrant. Poles to foliation in areas 1-3 also scatter across a girdle, interpreted to be related to open to tight folding of foliation a layering. The pole to this girdle ($27^\circ > 190^\circ$) is parallel to the general trend of moderately S-plunging mineral lineations and fold axes (Fig. A3_2a). When divided into geographical domains (Fig. A3_2b), the eastern cluster of poles to foliation reflects the west dipping layering/foliation that dominates in the northern part of area 1. This distribution reflects the change in orientation of the supracrustal belt from N- to NNE-trending, which can be observed in the lithological map.

Late brittle (+semi-ductile) faulting

Areas 1 to 3 are cut by numerous faults and fracture zones that are visible in outcrop and as linear features in air photographs. These fault zones define 3 broad trends: 1) NNE-SW and parallel to the trend of the supracrustal belt, 2) NE-SW, and 3) NW-SE (see maps on the ArcView© project on the DVD). The faults locally truncate and offset amphibolite units, although the total magnitude of offsets and their sense are not clear.

Within fault zones rocks are commonly brecciated (photo nmk2005-073, 236 to 238), with more ductile structures (chlorite-schists within amphibolite) locally developed. Rocks are retrogressed and altered to chlorite- and epidote-bearing assemblages, and may be silicified (photo nmk2005-072, 073, photo ssc2005-359). Disseminated pyrite and random splay of actinolite may also be developed (photo ssc2005-360, 361). Larger faults and fault zones may be represented as fault scarps (photo nmk2005-221) and eroded gullies (photo ssc2005-379) with rocks partially silicified and oxidised to a red-orange colour.

Away from faults, rocks may be cut by narrow zones of fracturing. Fractures occur on millimetre to centimetre scales, and commonly form anastomosing networks that are filled with epidote (photo nmk2005-063, 064, 074, 075) and/or silica (photo nmk2005-012 – 014, 086, 087, 226, 227). In some zones, rocks may be penetratively and statically retrogressed to epidote-bearing assemblages giving the rocks a green colour, without evidence of brittle or ductile deformation.

Contact relationship between supracrustals and felsic orthogneiss

The boundary between the amphibolite (or supracrustal) belt and felsic orthogneiss is typically a gradation of interlayered amphibolite and felsic orthogneiss (photo nmk2005-034, 035, 042, 062, 078), which may occur over a relatively wide area (e.g. east contact of amphibolite belt in area 1). In these zones intrusive relationships are not preserved, and layering is typically highly deformed and attenuated. It is possible that the contact between orthogneiss and amphibolite in these areas is a tectonised intrusive contact.

In some domains of the amphibolite, relatively narrow layers of grey orthogneiss are preserved. These are typically intensely deformed, attenuated and folded, but are locally wispy in character (photo nmk2005-009), cut across semi-rafted layers of amphibolite (photo nmk2005-059, 060) and may form ponding-like features (photo nmk2005-096, 097). These contexts suggest that these gneissic layers are intrusive into the amphibolite, and if related indicates that the main orthogneiss suite intruded into the amphibolite, possibly after the development of a layering and layer parallel foliation.

Location ssc2005-044 – notes in reference to Figure A3_1

Location ssc2005-044 is located in mapping area 1 (Fig. 2) within a 10 to 15m wide gorge (photo ssc2005-371) that defines the location of a late, brittle E-W-trending fault. The low cliffs on either side of the gorge display clear litho-structural relationships that reflect the structural and lithological complexity of the amphibolite belt in the Ujarassuit Nunaat area. The south side of the E-W gorge exposes intensely folded orthogneiss, ultramafite and pegmatite (photo ssc2005-365-368,370; Fig. A3_1), while the north side exposes well banded, biotite-rich orthogneiss with occasionally folded pegmatitic leucosomes (photo ssc2005-369). A number of distinctive features have been recognised:

- Felsic orthogneiss adjacent to ultramafite displays a gradual increase in modal abundance of amphibole over biotite with proximity to the ultramafite, taking on an appearance similar to banded amphibolite (photo ssc2005-376). From observations elsewhere in the belt, it is interpreted that the ultramafite, which forms part of the supracrustal package, was intruded by orthogneisses. Therefore it is probable that the amphibole-bearing orthogneiss is related to assimilation of ultramafic material during the intrusion of the felsic orthogneiss.
- The ultramafite consists of serpentine, talc and up to 3 cm long, black amphibole (actinolite) needles (photo ssc2005-372) that probably represent retrogression of a pyroxene- and olivine-bearing assemblage under greenschist to amphibolite facies conditions.
- Pegmatite, which cuts layering and foliation in both orthogneiss and ultramafite, but is also partly sub-parallel to a foliation in orthogneiss, indicates a deformation phase after the intrusion (Fig. A3_1).
- Orthogneiss, ultramafite and pegmatite are all folded but show several different deformation events (Fig. A3_1). Intense folding with roughly S-plunging fold axes deform ultramafite and orthogneiss. A slight variation in fold axes trend may reflect variations within a single event or the effects of two different events (Fig. A3_1). However, the lack of crenulation of foliations or lineations and other features for refolded folds might favour one event.

Interestingly, location ssc2005-044 represents a turning point in general direction of foliation from S-WSW north of the fault to mainly E south of the fault.

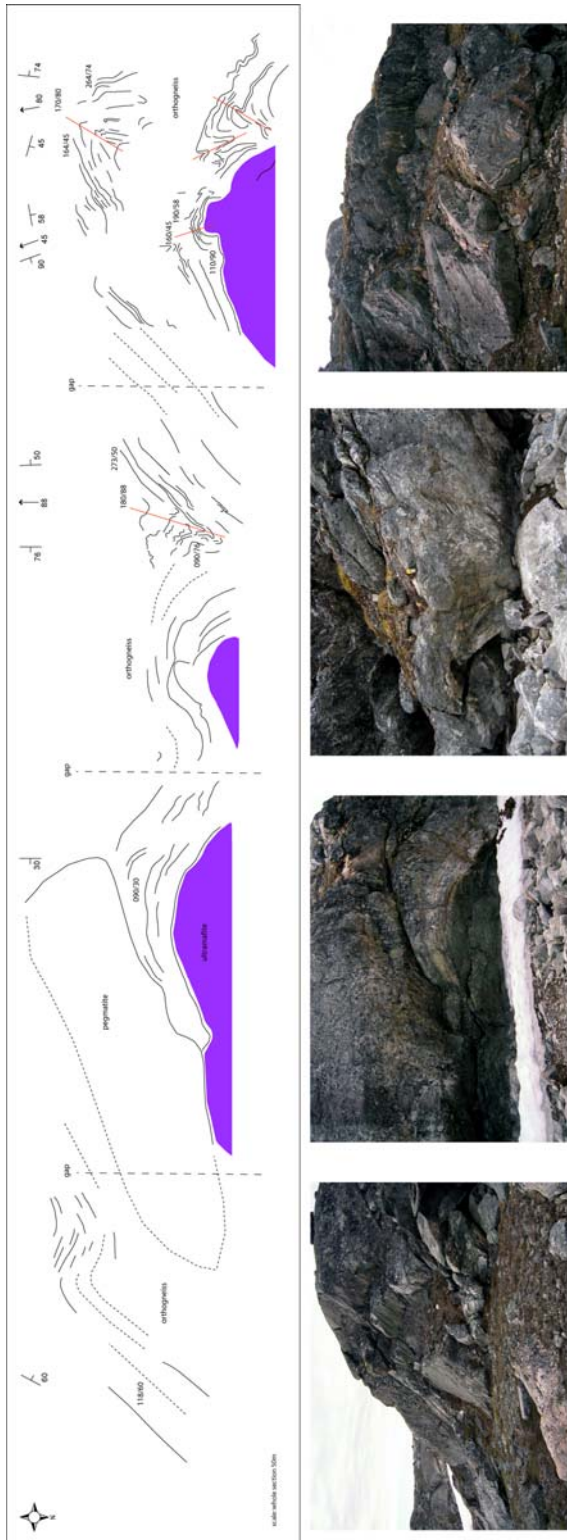


Figure A3_1. Structural cross-section through open to tightly folded, interlayered felsic orthogneiss, pegmatite and ultramafite in area 1. Note the broad asymmetry of folds suggests westward vergence during D_{n+2} deformation. F_{n+2} folds possible re-fold earlier folds in felsic orthogneiss (west end of the section). Location corresponds to observations presented for locality ssc2005-044.

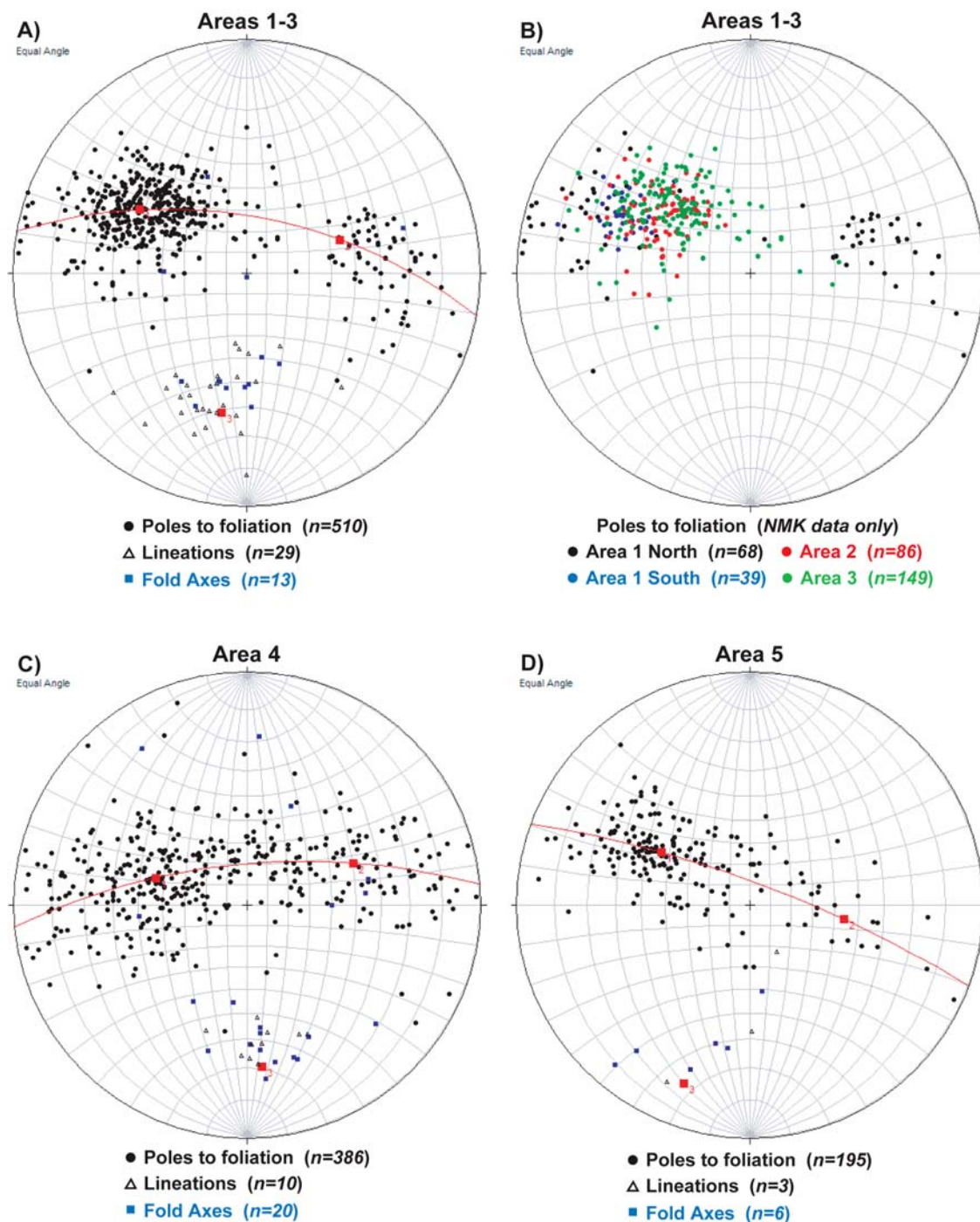


Figure A3_2. Equal angle stereonet for structural data from all field areas. Data include that collected by both nmk and ssc. N.B. Red lines represent great circles through girdles defined by poles to foliation in each area, with pole to the great circle (fold axis) depicted as a red filled square labelled '3'.

Alteration

Alteration affecting rocks in areas 1 to 3 may be separated into pre- or syn-ductile events, and alteration associated with late, brittle (and semi-ductile) faulting and fracturing. The latter has already been discussed in the structural section above.

Calc-silicate alteration: Within banded amphibolite, leucocratic veins and domains within the rock commonly preserve diopside, with or without garnet. These zones may reflect a degree of primary alteration of the protolith to the banded amphibolite, or metasomatic alteration associated with the injection of leucosome during metamorphism.

Alteration of Ultramafite: No ultramafic rocks observed in this area preserve primary igneous mineralogy. Whilst some exposures display features indicative of former igneous textures, these rocks have been pervasively hydrated and recrystallised during metamorphism. In addition, many exposures are cut by fractures and veins along which, and adjacent to, the metamorphic assemblages have been altered to variable percentages of talc, serpentine and chlorite (photo nmk2005-105).

Mineralisation

True mineralisation is rare in areas 1 to 3, with the most common feature being rusty surface coatings on amphibolite (photo nmk2005-052, 084, 085; photo ssc2005-380, 428) and garnet-biotite schist, and less commonly on felsic orthogneiss (photo ssc2005-346). These surface coatings do not result from a high percentage of oxide or sulfide minerals in the rocks, and tend to form as hydroxides (limonite, goethite) and oxides (haematite). Oxide alteration is locally more extensively developed (photo ssc2005-347, 348). In this example, rusty material occurs around a quartz vein in well foliated, flaggy amphibolite. The quartz vein is associated with coarse-grained amphibole (<3 cm) and biotite, with amphibolite altered to green-yellow-white coloured (hydr)oxide coatings and boxwork weathering patterns.

In addition, in some brittle fault zones, pyrite may be developed in altered rocks along with actinolite- (photo ssc2005-360, 361) and epidote-bearing assemblages. It is therefore possible that zones of (hydr)oxide development in other rocks result from alteration associated with late, brittle faulting. However, in areas clearly affected by brittle fracturing and alteration, oxidation is actually rare.

Preliminary Interpretations

Protoliths to supracrustal rocks

The intensity of deformation affecting the supracrustal belt during multiple overprinting ductile events has obscured unambiguous primary igneous or sedimentary features. Any interpretations must therefore be made with care.

Amphibolite: Within the supracrustal belt, amphibolitic rocks are dominated by relatively homogeneous types, with limited internal structure that may predate deformation, metamorphism and injection of leucosome. However, the less common banded amphibolite displays mafic and intermediate banding on centimetre to decimetre scales. Based on the relatively low grade of metamorphism that has affected these rocks, it is unlikely that this banding reflects metamorphic differentiation. The banding is most likely primary feature,

and may reflect part of the original volcanic protolith. Rare diopside within some layers may be a result of hydrothermal alteration of this protolith, although any such interpretation is purely speculative.

Garnet-biotite schist. Schistose rocks are found as layers within the amphibolite belt, or associated with amphibolite as layers or rafts in felsic orthogneiss. These rocks are dominated by semi-pelitic types, with rare pelitic (sillimanite-bearing) lenses. It is likely that these rocks have sedimentary protoliths.

Contact between heterogeneous and migmatitic felsic orthogneiss

In the western part of area 3 (in the vicinity of 64° 45.03' N, 050° 20.28' W) a lithological boundary is inferred between heterogeneous felsic orthogneiss and migmatitic orthogneiss, a boundary also inferred by previous mapping (Crewe 1981, 1982). On the basis of geochronological evidence elsewhere in the region (Friend & Nutman 2005) this boundary was originally proposed to be the boundary between the Kapisilik terrane to the east and Færingehavn terrane to the west, although this interpretation has been modified by subsequent dating by those workers. A contact was not exposed in this location. However, the intense character of deformation in rocks either side of the contact suggests that the lithological contact is at least highly tectonised.

Correlation of the 'Undifferentiated' orthogneiss

On 1:50,000 scale lithological maps, felsic orthogneiss to the east of the supracrustal belt and forming the dominant rocks of Ujarassuit Nunaat are labelled as 'Undifferentiated Granitic Gneiss'. Consistent with the map of Crewe (1981 1982), this orthogneiss does not significantly differ in appearance from that observed on the west side of the supracrustal belt. Minor variations in the orthogneiss do occur, including local bands of pale, massive orthogneiss close to the eastern boundary with the supracrustal rocks (area 1 only). However, these are interpreted to be local variations in the orthogneiss, and most likely do not represent a significantly different age component.

Outcrop pattern of amphibolite in area 3 – a fold axis?

Little evidence was found, either through the geometry of the regional lithological pattern or from mesoscopic (outcrop scale) fold asymmetries, to suggest that a regional scale anti-form controls outcrop style at the southern end of the supracrustal belt.

Overall, the amphibolite 'package' in the southern part of area 3 is characterised by inter-layered/interleaved amphibolite and felsic orthogneiss, with zones that are more or less dominated by amphibolite or orthogneiss. The boundaries between zones of dominantly amphibolite and dominantly felsic orthogneiss are commonly the focus of high strain deformation, inferred (see above, Dn) to be the result of tectonic reworking of intrusive boundaries. The minor to moderate repetition of such features with common geometry or facing throughout the southern area, may reflect one of a number of possible origins:

- thrust-related reworking and interleaving of the amphibolite and felsic orthogneiss during Dn

- isoclinal folding of a high-strain boundary between the felsic orthogneiss and amphibolite package during ductile event(s) that post-dates Dn

Another alternative may also be considered. Area 3 contains common NNE-trending brittle and semi-ductile faults and fault zones that dissect the amphibolite package. The repetition of high-strain felsic orthogneiss-amphibolite boundaries may reflect shuffling of the belt during this late stage brittle faulting.

Area 4

Area 4 encompasses a folded supracrustal belt within felsic to intermediate orthogneisses that occurs in an area called South Sallersuaq, central to the region being mapped (Fig. 2). The supracrustal belt is composed of mafic amphibolite with moderately abundant garnet-biotite-schist. According to the map published by Friend & Nutman (2005) the area formed part of the Færingehavn terrane. However, unpublished U-Pb data from a felsic orthogneiss sampled within the core of the regional fold structure suggests a Mesoarchaean age for these rocks, a possible indication of a Kapisilik or Akia terrane affinity (C. Friend & A. Nutman pers. comm. 2005). Mapping in these areas was conducted between 28/7 and 5/8, with a total of only 5 days active fieldwork due to bad weather over a number of days.

Lithologies

Felsic Orthogneiss

Felsic (biotite-bearing) orthogneiss in area 4 is dominated by coarse-grained felsic gneiss that contains abundant recrystallised leucosome (photo nmk2005-173). The orthogneiss typically preserves an intense gneissosity defined by alternating felsic- and biotite-rich domains, and sub-parallel leucosome (photo nmk2005-127, 128), which are commonly folded along with foliation (photo nmk2005-133). Locally, the gneissosity may only be weakly developed (photo nmk2005-120). In addition to the migmatitic orthogneiss, a massive felsic orthogneiss also occurs (photo nmk2005-184). It is most extensive on the northern boundary of the fold nose defined by the amphibolite belt, and is characterised by low volumes of leucosome. A coarse gneissosity may be developed in these rocks, which is locally folded (photo nmk2005-185).

Veins and layers of felsic orthogneiss may cut layering (photo nmk2005-142, 143, 194, 195) or be layer parallel in amphibolite (photo nmk2005-192). In addition, amphibolitic rafts occur within the orthogneiss (photo nmk2005-122, 123, 131, 174), which may be intensely deformed (photo nmk2005-125, 126). These observations suggest that the orthogneiss is intrusive into the supracrustal belt.

Amphibolite

The supracrustal belt in area 4 is dominated by amphibolite, with minor interlayered biotite (+/- garnet) schist, and defines a large isoclinal fold structure (see maps in the ArcView© project on the DVD). Amphibolite is composed of the assemblage hornblende amphibole,

plagioclase and biotite, with local occurrences of garnet and diopside, and may contain variable amounts of recrystallised, attenuated and dismembered leucosome (photo nmk2005-134, 146). Amphibolite is locally cut by leucocratic veins (plagioclase-rich) that may contain diopside and amphibole (photo nmk2005-152), with or without garnet. The amphibolite is locally intruded by felsic orthogneiss veins and more commonly occur as rafts within felsic orthogneiss that may be openly folded (photo nmk2005-123), or intensely deformed (photo nmk2005-125, 126). Amphibolite has been divided into two basic types, *homogeneous* (massive) and *banded amphibolite*, with homogeneous amphibolite being the most common.

Homogeneous amphibolite may be further sub-divided into massive mafic amphibolite and the homogeneous and weakly banded grey intermediate amphibolite. Massive mafic amphibolite (photo ssc2005-397) typically contains a lower modal abundance of plagioclase, and is commonly more coarse-grained, compared with grey intermediate amphibolite. Homogeneous and weakly banded grey intermediate amphibolite is by far the most abundant supracrustal lithology forming relatively thick packages with minor layers of banded amphibolite (photo nmk2005-162, 193). Foliation is typically well developed and defined by elongate trails of amphibole and plagioclase (photo nmk2005-163, 164) and attenuated leucosome that is elongate parallel to foliation (photo nmk2005-146). In zones of lower deformation intensity, grain size may be larger, with amphibole grains up to and larger than 5 mm (photo nmk2005-194).

Banded amphibolite forms discontinuous layers within homogeneous amphibolite, and preserves a lithological layering that is defined by variations in proportions of amphibole versus plagioclase on centimetre and decimetre scales (photo nmk2005-166, 167, 171, 189–191). Medium to well developed foliations in the banded amphibolite are typically parallel to layering, and defined by aligned trails and elongate domains of amphibole and plagioclase (<5 mm width; photo nmk2005-138). In addition, foliation may locally be characterised by aligned amphibole-rich segregations and trails of garnet porphyroblasts (photo nmk2005-147).

Biotite (+/- garnet) schist

Felsic schists occur as semi-continuous and discontinuous layers within amphibolite, varying from tens of centimetres to several metres in width. Some layers are garnet-absent (photo nmk2005-130), although most occurrences are composed of garnet, biotite, plagioclase and quartz, and are locally magnetite-rich (photo nmk2005-202, 203). They are typically medium- to coarse-grained (= 3 mm). Garnet commonly occurs as disseminated porphyroblasts up to 5mm in size (photo nmk2005-119), although larger grains do occur. Porphyroblasts are typically enveloped by the biotite-bearing foliation (photo nmk2005-119), and also occur in aggregates with leucosome >5 cm in size (photo nmk2005-180).

Many exposures are moderately migmatitic, hosting leucocratic segregations that are deformed into discontinuous ribbons (photo nmk2005-170) or envelope garnet porphyroblasts (photo nmk2005-134). Larger leucosomes occur, which are typically attenuated and dismembered (photo nmk2005-130).

Ultramafic rocks

Two distinct types of ultramafic rocks occur in area 4: 1) *Green-brown ultramafite*, and 2) *Black (dunitic) ultramafite*. Both are commonly associated, although type 1 pre-dominates.

Green-brown ultramafite occurs as discontinuous layers, small boudins and very large exposures (>100 m; photo nmk2005-149, 153, photo ssc2005-404, 413), that typically lie within openly folded layering in amphibolite. This type of ultramafite is identical to the typical green-brown ultramafic rocks found in other areas across the Godthåbsfjord region, and is composed of seed-like (\geq cm sized) nuggets of pale amphibole sitting in a matrix of amphibole, serpentine and olivine, with or without phlogopite. These bodies may be altered to talc- or serpentine-rich material, either within anastomosing networks (photo nmk2005-169) or within planar veins that dissect the rock.

Black (dunitic) ultramafite is predominantly composed of coarse-grained hornblende (2 to 5 mm) with disseminated olivine (1 mm) and rarer phlogopite, hosting millimetre to centimetre sized elongate aggregates (photo nmk2005-141) and discontinuous layers of pure-diopside (photo nmk2005-139, 140). Black ultramafite typically occurs in layers associated with green-brown ultramafite (e.g. on margins of large bodies), but contacts between the two types are not gradational (photo nmk2005-168). Moreover, they may occur isolated from the other ultramafites, and can occur as rafts in felsic orthogneiss (photo nmk2005-151). These layers are therefore interpreted to have distinct protoliths and do not represent alteration on the margin of green-brown ultramafite bodies.

Although also occurring as discontinuous inclusions in felsic orthogneiss, both types of ultramafite are most commonly found associated with amphibolite. These bodies are therefore interpreted to be related to the supracrustal sequence, either as part of the primary volcanic pile or as intrusive bodies.

Pegmatite

Felsic pegmatitic dykes intrude all lithologies and provide key structural markers. Pegmatites are composed of coarse- to very coarse-grained feldspar, quartz and biotite, and occur as centimetre-scale narrow veins or as dykes up to several metres wide (photo nmk2005-162). Locally, pegmatite may comprise greater than 50% of lithological exposure. This is pronounced in the northern part of the fold structural, although (for reasons discussed below) pegmatite intrusion must predate this fold.

Pegmatitic dykes intrude and cut layering and foliation in amphibolite and felsic orthogneiss (photo nmk2005-192, 193; photo ssc2005-414), but are typically deformed and partially to penetratively recrystallised. In zones of relatively intense deformation, pegmatite may be sub-parallel to foliation (photo nmk2005-179) but also folded (photo nmk2005-183). In some locations, pegmatite may cut layering and foliation, but be intensely boudinaged, folded and partially enveloped by a foliation (photo nmk2005-163, 164). In some zones of very high strain, pegmatites may be thoroughly recrystallised, developing a near-gneissic fabric that envelopes feldspar porphyroclasts (photo nmk2005-175, 176, 178). Locally, such fabrics in pegmatite are also folded (photo nmk2005-183).

Structure & Lithological relationships

The lithological distribution in mapping area 4 is predominantly controlled by a large multiply refolded fold structure (see maps on the ArcView© project on the DVD), with associated asymmetric, open to tight parasitic folds that occur on outcrop and larger scales. The presence of refolded folds on outcrop scales (e.g. photo nmk2005-137, 206), some of which have doubly plunging axes (photo nmk2005-211), and features described below, indicate that multiple ductile events affected the area prior to the development of the large fold structure. As most events either occurred at similar grade, or subsequent events thoroughly recrystallised earlier structures, it is difficult to distinguish between structures formed during different events, except where local cross cutting relationships are preserved. As such, structural features will be de-scribed as observed and possible event sequence proposed as a summary in Table A3_2.

Table A3_2. Possible event sequence for area 4.

Event	Characteristics	Conditions
D_{n-1}	layer parallel foliation in amphibolite	???
<i>Intrusion of migmatitic felsic orthogneiss</i>		
D_n	deformation of orthogneiss and amphibolite, tight to isoclinal folding of amphibolite rafts in orthogneiss; partial melting producing migmatitic layering in orthogneiss; leucosome development in amphibolite	Amphibolite facies
<i>Intrusion of pegmatitic dykes</i>		
D_{n+1}	deformation and recrystallisation of pegmatite dykes, development of high strain zones in orthogneiss and amphibolite	Amphibolite facies
D_{n+2}	Development of first phase of large scale fold structure - isoclinal F_{n+2} fold	Amphibolite facies
D_{n+3}	Development of second phase of large scale fold structure (F_{n+3}), refolding F_{n+2} ; characterised by E-dipping limbs and axial plane; associated asymmetric, S-plunging parasitic folds, east-dipping axial planes and W-vergent.	Amphibolite facies
D_{n+4}	Minor refolding (F_{n+4}) about E-trending open folds	???
D_{n+5}	retrograde shear and fault zones: brittle-ductile deformation with development of chlorite & epidote assemblages	Greenschist Facies

Ductile structures, Fold-foliation relationships

Felsic orthogneiss veins that cut a layer-parallel foliation in amphibolite, and discontinuous layers and rafts of amphibolite in felsic orthogneiss that contain foliations, suggest that the intrusion of the migmatitic felsic orthogneiss post-dated the development of a foliation in amphibolite. A feature also noted for areas 1 to 3, it is not clear if this foliation relates to a

distinct, pre-intrusion tectonothermal event, or if the felsic orthogneiss is a syn-orogenic intrusive.

Pegmatitic dykes cut intense layer-parallel foliations in amphibolite and felsic orthogneiss (e.g. photo nmk2005-192), indicating that one or more high strain events must have affected the rocks prior to the intrusion of the pegmatites. Felsic orthogneiss lenses within amphibolite that are parallel to the layering and intense foliation in amphibolite (photo nmk2005-192), and intensely deformed and interleaved amphibolite and orthogneiss (photo nmk2005-160), are indicative of a very high strain event affecting the rocks subsequent to the intrusion of the felsic orthogneiss. Tight to isoclinally folded lenses and rafts of amphibolite in felsic orthogneiss (e.g. photo nmk2005-125) that are within openly folded layers, suggests such deformation predates the development of the large synformal structure (see below) and may be related to this early, post-intrusion event. However, such intense folding also deformed layer parallel leucosomes within amphibolite rafts (photo nmk2005-126, 131). Moreover, an intense gneissosity is preserved in felsic orthogneiss that is in part defined by recrystallised leucosome (photo nmk2005-127, 128), indicating the occurrence of partial melting events prior to or during this high strain event, evidence for which is only locally preserved. These various structures, all of which are interpreted to predate pegmatite intrusion, are grouped together into a D_n event, and constitute the end result of multiple events.

Although they may cut layering and foliation in amphibolite and orthogneiss, pegmatitic dykes are commonly recrystallised (e.g. photo nmk2005-175) and have been extensively deformed. Pegmatites are locally boudinaged (photo nmk2005-163, 192) and may have foliation in amphibolite partially envelope them (photo nmk2005-164). In addition, pegmatite dykes may be rotated to be (sub)parallel to foliation/layering in the country rocks (photo nmk2005-179). These observations indicate that subsequent to pegmatite intrusion the terrane was affected by a further high strain deformation event (D_{n+1}). Associated with this high strain event is tight to isoclinal folding of foliation and banding in amphibolite (photo nmk2005-165, 191) and the development of sheath folds (photo nmk2005-189, 190), which have axial planes parallel to the intense foliation and general trend of layering. As the structures and fabrics associated with this ductile event are folded about the large fold structure, these high strain structures cannot be associated with the first phase of the large-scale fold, and as such predate that event.

The next recognisable ductile events to affect the terrane involved the development of the large refolded fold structure that dominates the area (D_{n+2} & D_{n+3}; see maps on ArcView© project on the DVD). The south-dipping northern and southern closure of this large fold (see below) and its outcrop pattern may give an impression of a large sheath fold. However, the low-strain character of parasitic folds on the limbs of this structure suggests that the intense strain typically associated with sheath fold development did not occur in this case. Instead, the geometry of this structure may be explained by an initial large-scale isoclinal fold (F_{n+2}) that was subsequent refolded about a second large-scale isoclinal fold (F_{n+3}; Fig. A3_3). Associated with this structure are open, tight and locally isoclinal folds, with upright to steeply dipping axial planes (e.g. photo nmk2005-136, 154, 157), which deform layering and high grade foliation (photo nmk2005-170, 171). They locally refold earlier isoclines (photo nmk2005-137) or other folds with recumbent axial planes (photo nmk2005-155, 158). Folds also deform recrystallised pegmatitic dykes (photo nmk2005-150, 182,

183). New fabrics that can be unambiguously associated with this event are extremely rare, although locally a foliation may be aligned parallel to the axial planes of folds. This may be defined in part by aligned, dismembered leucosome (photo nmk2005-197) and so reflect a rotated high strain foliation, or by recrystallisation of biotite fabrics in schist (photo nmk2005-198, 199). An example of the structural style associated with this folding is presented in Figure A3_4.

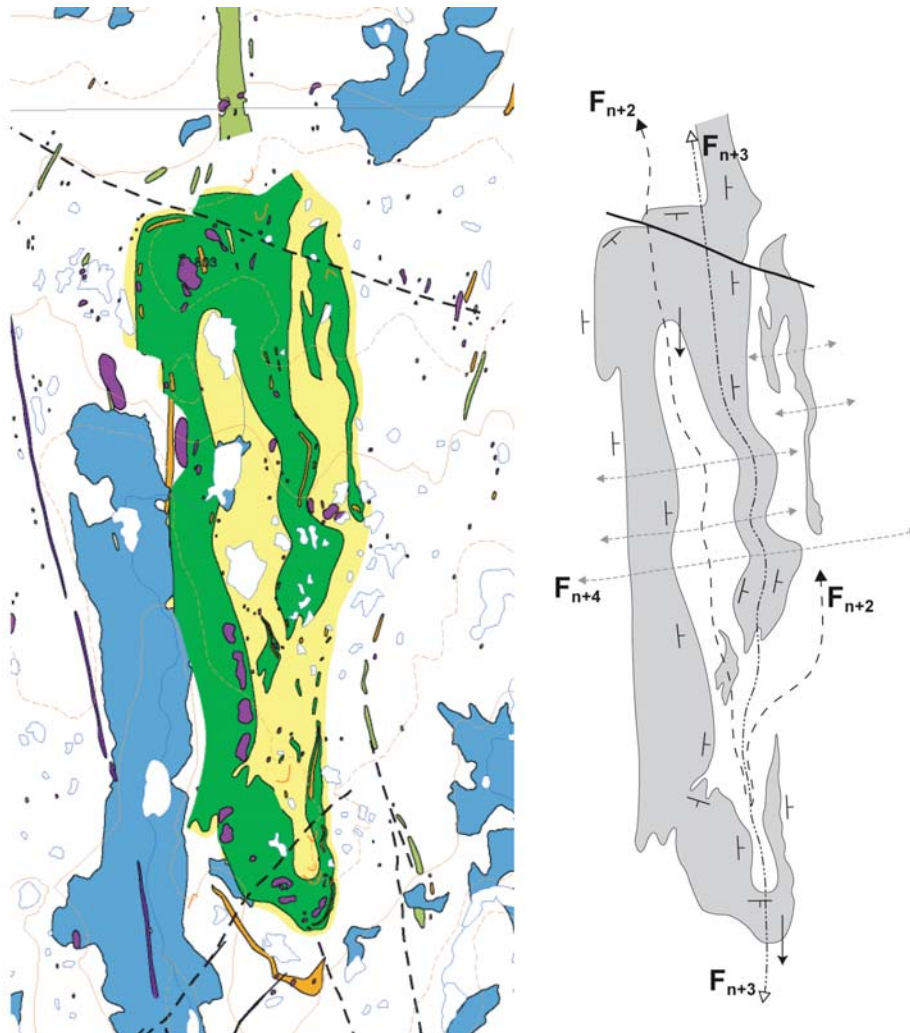


Figure A3_3. Schematic representation of a possible interpretation for refolding relationships in the large fold structure in area 4. Image on the left is the outcrop geometry of the supracrustal belt (green) in area 4, taken from compiled geological map. Image on the right are the inferred fold relationships: an initial (near-to) isoclinal fold (F_{n+2}) is refolded about a second large scale south-plunging isoclinal fold (F_{n+3}). These folds are subsequently partially refolded by minor F_{n+4} folds.

The distribution of structural measurements (Fig. A3_2c) reflects the effects of folding at regional and outcrop scales during this event. Poles to foliation define a girdle, the pole to which is parallel to fold axes and mineral (stretching) lineations in amphibolite and felsic orthogneiss. The large fold structure is characterised by east dipping limbs and closures in the north and south that are both south dipping. This geometry is coincident with the south-plunging open to tight asymmetric folds on outcrop scales, which have east-dipping axial planes, an observation that is consistent with them being parasitic to the F_{n+3} fold genera-

tion that refolds the earlier F_{n+2} isoclinal fold (see Fig. A3_3). In addition, the fact that fold axes and lineations measured and observed in the area are predominantly parallel to the F_{n+2} direction, indicate that earlier fold structures and lineations may have been rotated during this event.

Rare fold axes are oblique to the dominant trend, plunging to the west and to the north. It is possible that some of the folds reflect earlier fold generations, in completely rotated by the F_{n+3} generation. However, the presence of wobbles, best defined in the eastern limb of the large structure (Fig. A3_3), suggests that a subsequent (F_{n+4}) folding event affected the rocks. This fold generation would be defined by near E-W trending axes, and would result in minor refolding of south-plunging fold axes producing the rare north-plunging axes observed.

Late brittle (+ semi-ductile) faulting

Although not as abundant or penetratively developed as in areas 1-3, late, brittle (semi-ductile) faults cut through area 4. One fault is obvious on a region scale (see maps in the ArcView© project on the DVD) and has a sinistral offset of tens of metres. This fault is exposed as a low fault scarp (photo nmk2005-186) within which the rocks are partially oxidised and silicified (photo nmk2005-188). For up to 10 metres adjacent to the fault, amphibolite and orthogneiss are cut by numerous fractures and veins (photo nmk2005-187) and have assemblages retrogressed to epidote and chlorite.

Metamorphism

High strain foliations in amphibolite are composed of hornblende amphibole, plagioclase and biotite (photo nmk2005-138), with or without garnet (photo nmk2005-148). Garnet may occur as aggregates elongate in the fabric, or partially overgrow it (photo nmk2005-148), suggesting syn-deformation growth. Locally, garnet is rimmed by selvages of hornblende, indicating a degree of hydrous retrogression of the highest grade assemblages (photo nmk2005-159). In garnet-biotite schist, foliations are commonly partially defined by leucocratic segregations, with or without garnet (photo nmk2005-134). In addition, garnet may occur as rare porphyroblasts and aggregates within zones of more abundant leucosome (photo nmk2005-152). These indicate a degree of partial melting associated with metamorphism that affected these rocks, which may have been associated with peritectic garnet growth.

The presence of deformed leucosome within amphibolite, felsic orthogneiss and garnet-biotite schist suggests that conditions during the highest grade metamorphism were sufficiently hot to locally produce partial melts. In many exposures, it is not clear if all leucosome is in fact the result of in situ melting, instead being derived from elsewhere. However, some textures (e.g. photo nmk2005-134, 152) are interpreted to reflect in situ partial melting.

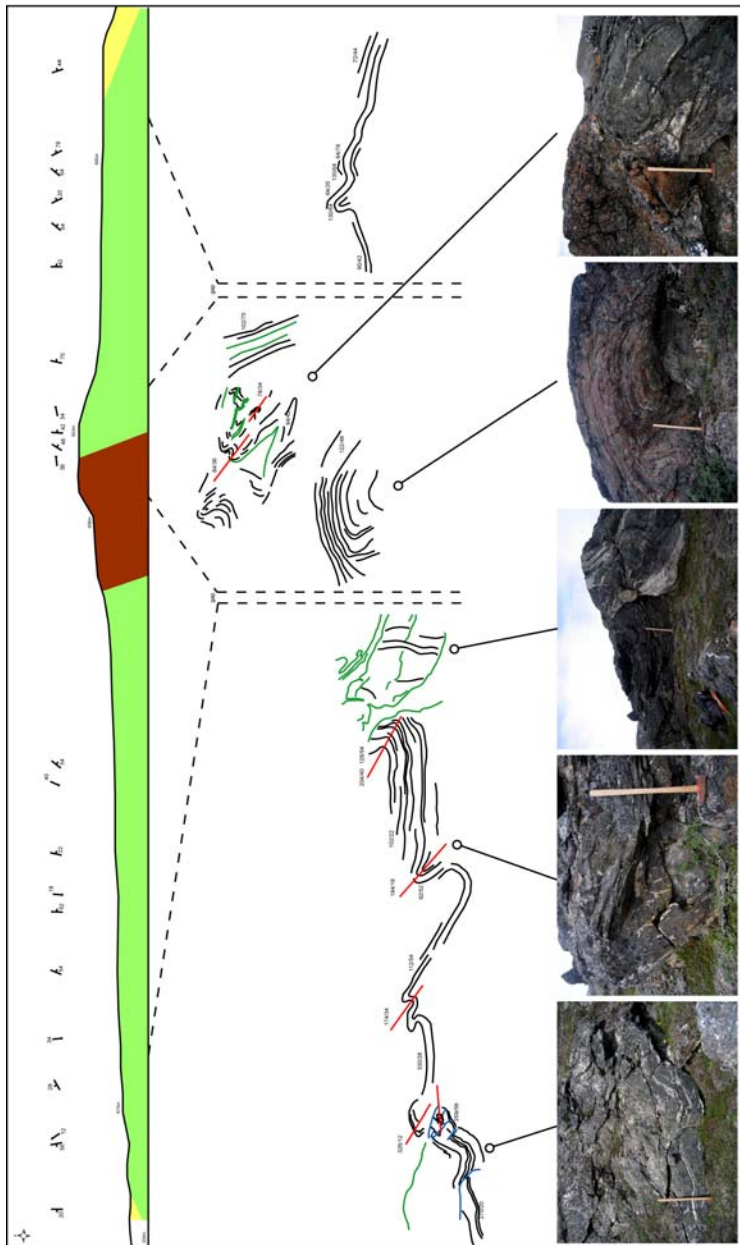


Figure A3_4. Structural section through the eastern limb of the fold structure in area 4 (location ssc2005-164 to 169), demonstrating the broad structural style associated with deformation. Fold asymmetries indicate westward vergence during open to tight folding associated with D_{n+3} . Green – amphibolite, Brown – garnet-biotite-magnetite rock, Yellow – orthogneiss.

The observations above, and the presence of biotite (instead of orthopyroxene) in felsic orthogneiss, are suggestive that the highest grades of metamorphism preserved by assemblages in area 4 are in the amphibolite facies. Although not always abundantly clear which structures relate to which event, the preservation of high strain amphibolite facies fabrics through the last (ductile) fold event, indicate that this event was most likely at conditions similar to those that accompanied the development of those fabrics.

The last, brittle faulting event is characterised by retrogression of amphibole and biotite-bearing assemblages, with replacement by epidote and chlorite. This suggests that greenschist facies conditions accompanied faulting.

Alteration

Alteration in area 4 is largely restricted to metasomatic alteration of ultramafite, and retrogressive alteration associated with brittle faulting, that have been described in the sections above.

Mineralisation

Typically limited to localised occurrences of rusty zones and coatings on amphibolite and pegmatite (photo ssc2005-414), area 4 also preserves a discontinuous layer of garnet-biotite schist (see maps on the ArcView© project on the DVD) that contains moderate to highly abundant magnetite, with or without quartz (photo ssc2005-405, 406, 407; photo nmk2005-202, 203). This layer is locally highly weathered, producing a highly oxidised, crumbly material that may preserve box-work weathering patterns. The latter suggests that the schist may also contain sulfide minerals. The protolith to this rock type is not clear prior to thin section petrography, but the high abundance of magnetite and association with garnet-rich, and locally quartz-rich zones suggest a possible banded iron formation origin.

Protoliths to supracrustal rocks

Consistent with supracrustal rocks in areas 1 to 3, the intensity of recrystallisation in area 4 affecting rocks during multiple overprinting ductile events, has obscured primary igneous or sedimentary features. As such, the interpretations discussed below are made with care. The supracrustal belt in area 4 is dominated by homogeneous, with subordinate banded, amphibolite. No primary igneous features are preserved in these rocks. However, the local occurrence of banded amphibolite and rare lenses of intermediate composition biotite schists within the amphibolite package is suggestive of a volcanic origin for these rocks. The intimate association of garnet-biotite schists of probable metasedimentary origin may reflect a volcanogenic and re-worked sedimentary component to the supracrustal package.

Area 5

Area 5 covered a supracrustal belt within felsic-intermediate orthogneisses immediately to the east of Ilulialik (Fig. 2), that is designated 'undifferentiated metasedimentary rocks' on existing 1:20,000 maps (Crewe 1981, 1982). Although dominated by garnet-biotite-bearing 'metasediments', the supracrustal belt also contains significant proportions of amphibolite (see maps in the ArcView© project on the DVD). The area forms part of the Tre Brødre Terrane (Friend & Nutman 2005) and interpreted to be composed of Neoarchean orthogneisses, although the age control of this interpretation is not known by the authors. Mapping in these areas was conducted between 11/8 and 16/8, with a total of 4.5 days active mapping and sampling.

Lithologies

Felsic Orthogneiss

Two types of biotite-bearing felsic orthogneiss were identified in mapping area 5 that correspond to the orthogneisses that occur either side of the proposed boundary between the Tre Brødre and Færingehavn terranes: 1) moderately migmatitic orthogneiss, with spaced leucosome, and 2) complex, migmatitic orthogneiss.

Moderately migmatitic felsic orthogneiss is characterised by low to moderate volumes of spaced leucosome (photo nmk2005-239, 268), and is typically homogeneous or weakly banded (photo nmk2005-267, 268; photo ssc2005-443). However, locally the orthogneiss is strongly banded, with banding defined by variations in biotite content, and can range from felsic to intermediate in composition (photo nmk2005-243, 264, 265; photo ssc2005-430). More rarely, mafic amphibole-bearing layers occur (photo nmk2005-266), which may reflect recrystallised amphibolite inclusions or part of an early igneous phase in the orthogneiss. Clearly defined rafts of amphibolite do occur (photo nmk2005-262). Gneissosity, where moderate to strongly developed, is defined by coarse-grained and aligned felsic (plagioclase + quartz) segregations enveloped by more biotite-rich domains (photo nmk2005-241). Leucosome within the orthogneiss is nearly ubiquitously deformed and partially or penetratively recrystallised. Where occurring as layers interleaved or interfolded with metasediment and amphibolite, or in boundary zones adjacent to the supracrustal belt, felsic orthogneiss is commonly garnet-bearing. As such, the rocks may be difficult to differentiate from biotite-poor schists.

Clear relationships characterising the early development of structures in the orthogneiss are apparent away from the supracrustal belt (e.g. location photo nmk2005-311), where the rocks are less affected by deformation events that post-date pegmatite intrusion. In higher strain domains, leucosomes may be weakly transgressive to layering, but are typically attenuated (photo nmk2005-239) or tightly folded (photo nmk2005-240). Within these zones, these folds do not fold a gneissosity, but have axial planes parallel to the high strain gneissosity and layering (photo nmk2005-240). In lower strain domains within the orthogneiss, open to tight folds deform compositional layer and leucosome, but not a foliation (photo nmk2005-242, 243). However, parallel to fold axial planes, a foliation and incipient gneissosity may be locally developed (photo nmk2005-243, 245, 246) or narrow (cm-scale) shear zones with or without leucosome may occur (photo nmk2005-244). These observations suggest that leucosome developed or was injected into the orthogneiss prior to, or during the development of the first gneissosity.

Complex, migmatitic orthogneiss differs from the moderately migmatitic orthogneiss by having a higher abundance of leucosome, and greater variation (on a small scale) in compositional layering (photo nmk2005-286 - 288). Layering includes variations in biotite content, but also the presence of amphibole-bearing layers.

Amphibolite

Forming part of the supracrustal sequence that is dominated by garnet-biotite rocks, amphibolite in area 5 comprises: 1) *Banded amphibolite*; 2) *Homogeneous grey intermediate*

amphibolite; and 3) *Massive mafic amphibolite*. Banded amphibolite is the most abundant of these types, with the other two types commonly forming layers within it.

Banded amphibolite is characterised by compositional layering on centimetre, decimetre and metre scales, mostly defined by variations in amphibole versus plagioclase modal abundance (photo nmk2005-254, 254, 261, 281) but also by interlayered garnet-biotite schist (photo nmk2005-259, 260). Compositions commonly vary between mafic and intermediate, although more felsic layers do occur, as do attenuated lenses and boudins of hornblende-rich (near ultramafic) material (photo nmk2005-254, 259). In leucosome-rich domains, which may cut foliation, very coarse hornblende may be developed along with diopside-rich fragments, aggregates and lenses (photo nmk2005-281 - 283). Banded amphibolite may also be locally garnet-bearing (photo ssc2005-436).

Homogeneous grey intermediate amphibolite is typically medium-grained and mafic to intermediate in composition (photo nmk2005-252, 284), and composed of amphibole, plagioclase and biotite. When associated with high leucosome volume, this amphibolite may be coarse-grained (photo nmk2005-253). Homogeneous amphibolite commonly occurs as layers within banded amphibolite, but may also be found as rafts within felsic orthogneiss (photo nmk2005-263). The rock is locally garnet-bearing, with porphyroblasts commonly disseminated through the rock (photo nmk2005-276) and not necessarily associated with leucosome.

Massive mafic amphibolite is composed of a high modal abundance of coarse-grained amphibole, with minor plagioclase, and a layer within layered supracrustal rocks (photo ssc2005-431, 438). This amphibolite also forms a distinct and mappable unit in the SW part of the mapping area within the axis of a large synform (see maps on the ArcView© project on the DVD; photo ssc2005-435). The rock may be garnet-bearing and locally garnet-rich, preserving large porphyroblasts (photo ssc2005-437, 439).

Garnet-biotite schist

Forming the dominant supracrustal lithology in area 5, these rocks mostly comprise garnet-biotite felsic schist (photo nmk2005-293, 296, 297) that are locally gneissic in appearance due to low modal abundances of biotite (photo nmk2005-292). Garnet occurs as disseminated porphyroblasts and poikiloblasts up to several centimetres in size, and as aggregates up to 15 cm in size (photo nmk2005-269) that are typically associated with leucosome (photo nmk2005-289 -291, 293). Rare aggregates appear to preserve a foliation (photo nmk2005-251). Garnet-biotite schist may be locally migmatitic (photo nmk2005-285).

Whilst dominated by garnet-biotite-plagioclase-quartz semi-pelitic assemblages, other more pelitic assemblages include:

- Sillimanite-bearing (with garnet-biotite-plagioclase-quartz +/- staurolite?)
- Orthoamphibole-bearing (with garnet-biotite +/- leucosome)

The latter assemblage occurs as part of a discontinuous lense within amphibolite-dominated rocks, and is composed of coarse-grained garnet and orthoamphibole, with or without biotite and minor leucosome (photo nmk2005-272). Garnet may form grains and aggregates between 2 and 15 cm in size (photo nmk2005-272, 275), with single crystals

and aggregates of orthoamphibole up to 20 cm in size (photo nmk2005-271, 273, 274). The largely ferromagnesian mineral assemblage and coarse grain sizes suggests this rock is restitic in composition.

Ultramafic rocks

Ultramafite is typically associated with amphibolite in the supracrustal sequence, occurring as discontinuous layers, small boudins and larger exposures that typically lie within folded layering in amphibolite. This type of ultramafite is identical to the typical green-brown ultramafic rocks found in other areas across the Godthåbsfjord region, as it is composed of coarse-grained pale green or brown amphibole in a matrix of finer grained amphibole, serpentine and olivine, with or without phlogopite. These bodies may be cut by metasomatic veins up to 2 metres across that alter the metamorphic assemblage to coarse-grained serpentine (antigorite; photo nmk2005-277), and locally chlorite and talc. Some ultramafite bodies preserve igneous crystal textures that have been pseudomorphed by pale green amphibole sitting in a serpentine-rich matrix (photo nmk2005-249).

Pegmatite

Felsic pegmatitic dykes are composed of feldspar, quartz and biotite, and intrude in variable abundances across area 5. Pegmatites cut layer parallel foliation in supracrustal rocks and felsic orthogneiss (photo nmk2005-247, 263, 266, 284) but are weakly to penetratively deformed and recrystallised. Locally the intensity of deformation has been high enough to produce a mylonitic (gneissic) foliation with development of feldspar porphyroclasts (photo nmk2005-270). Recrystallised pegmatites are also commonly folded.

Structural-lithological relationships

The lithological distribution in mapping area 5 is characterised by linear belts of metasedimentary and amphibolitic rocks interleaved with lesser bands felsic orthogneiss (see maps on the ArcView© project on the DVD). Whilst not simply defined, some evidence suggests that these parallel belts are juxtaposed as the result of interfolding during a late folding event (see below) that deformed all lithologies. As most events either occurred at similar grade, or subsequent events thoroughly recrystallised earlier structures, it is difficult to distinguish between structures formed during different events, except where local cross cutting or overprinting relationships are preserved. As such, structural features will be described as observed and an event sequence proposed as a summary in Table A3_3.

In many cases, it is not clear if high strain foliations in amphibolite, metasediments and orthogneiss rocks formed during single or overprinting events, and cannot be unambiguously related to a specific tectonothermal event. However, where local cross-cutting or overprinting relationships are present, the resulting structures give some clue as to the number and nature of individual events. For example, pegmatitic dykes locally cut a high grade foliation in amphibolite, metasediment and felsic orthogneiss, but are themselves deformed (folded and sheared) and recrystallised. Moreover, recrystallised pegmatitic dykes may be transposed parallel to layering in supracrustal rocks and folded by open to tight folds that are related to the final ductile deformation phase. As such, at least one duc-

tile structural event pre-dates the intrusion of these pegmatites, and at least two events post-date their intrusion. However, it is difficult to separate these events in the absence of pegmatite and other similar features.

Structures in area 5 are characterised by the development of high-strain foliations in most lithologies that are characterised by aligned trails of amphibole and plagioclase (amphibolite) and attenuated quartz-feldspar segregations in felsic orthogneiss and metasediment (photo nmk2005-279, 280). In addition, foliations may be characterised by attenuated and boudinaged mafic and ultramafic lenses in amphibolite, and attenuated leucosome in amphibolite, metasediment and felsic orthogneiss (photo nmk2005-268). Fabrics may also locally comprise a strong linear component (e.g. photo nmk2005-296, 297), with mineral lineations in amphibolite defined by elongate and aligned amphibolite, and mineral stretching lineations defined by quartz and feldspar in felsic orthogneiss and leucosome. Deformation that led to the formation of these high-strain foliations also developed tight to isoclinal folding of layering and leucosome (photo nmk2005-256, 257), and in overprinting events, foliations.

Dn

Evidence for this event is only unambiguously identifiable in moderately migmatitic felsic orthogneiss, although the fact that amphibolite occurs as rafts within felsic orthogneiss would suggest supracrustals were also affected by it. In low Dn strain domains, open to tight folds deform layering and leucosome, but not a foliation (photo nmk2005-242, 243), although an axial planar gneissosity may be locally developed (photo nmk2005-243, 245, 246). In moderate Dn strain domains, leucosomes are transgressive to layering and typically attenuated (photo nmk2005-239) or tightly folded (photo nmk2005-240). Folds in these zones deform a layering but not a foliation, but develop a weak to moderate axial planar gneissosity (photo nmk2005-240). In highest strain zones, gneissosity is layer parallel.

Table A3_3. Possible event sequence for area 5.

Event	Characteristics	Conditions
D_n	<i>Intrusion of felsic orthogneiss</i> deformation of orthogneiss, amphibolite and metasediment; development of first gneissosities recognised in orthogneiss, and foliations supracrustals; syn-deformation development of leucosome	Amphibolite facies
D_{n+1}	<i>Intrusion of pegmatitic dykes</i> deformation and recrystallisation of pegmatite dykes, supracrustal rocks and orthogneiss; localised development of high-strain zones, and mylonitic textures in pegmatite	Amphibolite facies
D_{n+2}	development of open to tight folds in supracrustal rocks and orthogneiss	Amphibolite facies

D_{n+1}

Evidence for this event is difficult to distinguish from previous or subsequent ductile deformation. However, local cross-cutting and overprinting events allow some insight into the character of D_{n+1}. D_{n+1} is characterised by the development of local high strain zones and layer parallel foliations that contain isoclinally folded leucosome. Tight to isoclinal folds that deform a foliation (e.g. photo nmk2005-256) - are refolded by D_{n+2} folds, suggesting that they were formed during D_{n+1}. In addition, hornblende + diopside-bearing leucosome may occur within the necks of boudins that contain a foliation (photo nmk2005-282), suggesting high-strain deformation during this event comprised a component of extension.

D_{n+2}

This event is characterised by open to tight, and locally isoclinal, folding of layering as well as layer-parallel foliation and leucosome in all lithologies (photo nmk2005-285). These folds locally refold tight to isoclinal folds in amphibolite (photo nmk2005-256, 257). Open to tight folds have consistent asymmetries across the area defined by east-dipping long fold limbs. Folds have predominantly S-plunging axes and steeply east-dipping axial planes. Poles to foliation measurements (Fig. A3_2d) form a dominant cluster in the NE quadrant, reflecting the dominantly ESE-dipping fabrics. The scatter of poles to foliation form a girdle, the pole to which (11°->200°) is broadly parallel to measured fold axes. These correlations suggest that the dominant folding event observed and resulting outcrop pattern is related to the D_{n+2} events.

Metamorphism

The preservation of garnet-biotite assemblages in metasedimentary rocks, hornblende + plagioclase in amphibolite and biotite defining foliations in felsic orthogneiss, suggest that peak conditions affecting rocks in area 5 were most likely in the amphibolite facies. Abundant leucosome in some lithologies, in some cases associated with large garnet aggregates (photo nmk2005-289, 290, 293) suggests conditions reached those appropriate for partial melting. Middle to upper amphibolite facies conditions are also supported by the local development of sillimanite in more pelitic compositions. The structural context of leucosome in orthogneiss (lithologies section) suggests that leucosome, at least in felsic orthogneiss, developed during the first deformation/metamorphic event to affect the orthogneiss (Dn). In addition, folded leucosome with asymmetries consistent with Fn+2 folds, indicates melting occurred during ductile events post-dating Dn, possibly during Dn+1 and Dn+2.

Within some rocks, large garnet porphyroblasts may be rimmed by hornblende selvages (photo ssc2005-436), indicating a degree of hydrous retrogression of these rocks during metamorphism. In addition, most garnet grains that occur in amphibolite are rimmed by plagioclase haloes (photo nmk2005-276; photo ssc2005-432, 439). These haloes did not contain any ferromagnesian phases identifiable by hand lens, therefore may not be unambiguously interpreted as decompression textures. However, rare resorbed garnet porphyroblasts that are embayed by fine-grained symplectic intergrowths of plagioclase and hornblende, where the grain-size is finer than that in the matrix (photo nmk2005-294, 295), may reflect decompression of the terrane late in, or after peak metamorphism. Alternatively this may reflect a lower pressure during successive metamorphic events.

Mineralisation/Alteration

No mineralisation of any significance was encountered in area 5. Localised rust zones, typically developed on weathered biotite-rich rocks do occur, although not associated with any visible oxide or sulfide minerals. Consistent with others areas (and described above in the lithologies section) the only significant alteration was associated with metasomatic veins that cut ultramafite. No brittle faulting and associated greenschist facies retrogression and silicification were observed.

Preliminary Interpretations & Discussion

Protoliths to supracrustal rocks

Consistent with supracrustal rocks in areas 1 to 4, the intensity of recrystallisation in area 5 affecting rocks during multiple overprinting ductile events, has obscured primary igneous or sedimentary features. As such, the interpretations discussed below are made with care.

Within the supracrustal rocks, amphibolitic rocks are dominated by banded types that display mafic and intermediate banding on centimetre to decimetre scales. It is unlikely that

this banding reflects metamorphic differentiation. In addition, the banded amphibolite commonly contains layers of garnet-biotite semi-pelite, which is of probable metasedimentary origin. As such, banding in amphibolite is most likely a primary feature, and may reflect part of an original volcanic protolith. However, dominating the supracrustal rocks in area 5 are garnet-biotite semi-pelitic schists and gneisses, with local occurrences of more pelitic sillimanite- and possibly staurolite-bearing assemblages. The layered nature of these rocks and occurrence of metapelite within the sequence is indicative of a metasedimentary origin.

Tre Brødre – Færingehavn Terrane boundary

The boundary between moderately migmatitic and complex migmatitic felsic orthogneiss in area 5 correlates with the previously mapped boundary between different orthogneisses in this area (Crewe 1981, 1982) and with the proposed terrane boundary between the Tre Brødre and Færingehavn terrane (Friend & Nutman 2005). In the area investigated this boundary does not outcrop and is therefore inferred. However, the outcrops on the Tre Brødre side of this boundary are dominated by intensely deformed felsic orthogneiss with abundant attenuated lenses of amphibolite and ultramafite, with layer parallel foliations that are steeply E-dipping. This outcrop character is suggestive of a high strain event affecting these rocks, and may reflect interleaving associated with a possible terrane amalgamation event.

Regional Structural Correlations

Despite having pre-amalgamation histories that by definition must be unrelated, some similarities are apparent when comparing the sequence of high-grade ductile events between terranes:

- Each terrane has pegmatitic dykes that cross-cut high-grade (D_n) foliations.
- Pegmatitic dykes are commonly deformed, recrystallised and transposed into parallelism with layering in supracrustal rocks and orthogneiss (D_{n+1}). In such cases, the pegmatites may develop a foliation.
- Recrystallised and partially to completely transposed pegmatitic dykes are deformed by open, tight and isoclinal folds related to further high-grade ductile deformation in each area (D_{n+2} , D_{n+3} , D_{n+4}).
- Each area preserves foliation geometries that reflect a dominant S-plunging fold event (Fig. A3_2), and a common west-vergent nature to the S-plunging fold generation across the region is apparent.

These similarities in structural character are possibly indicative of shared deformation histories, for at least one major deformation event across the three terranes. If these events are indeed common, they result from tectonothermal activity that must have been syn- and/or post-terrane amalgamation in the Godthåbsfjord region.

The age of pegmatite intrusion and subsequent tectonothermal events in the Ujarassuit Nunaat is not currently known. In addition, it is likely that each area was intruded by more than one generation of pegmatites with substantially different ages (C. Friend, pers. comm.). However, numerous pegmatites in the Godthåbsfjord region that have been dated

fall in the ~2630-2600 Ma age bracket, an age apparently post-dating the inferred timing of terrane amalgamation. If the age of pegmatites falls in the same bracket as other Godthåbsfjord region pegmatites, then the common events of the Ujarassuit Nunaat region must also have occurred post-terrane amalgamation. Alternatively, the timing and sequence of amalgamation events are somewhat more complicated than that expressed in the currently standing terrane model.

Appendix 4: Field report 2005 - Ujarassuit Nunaat Region – East, and Ivisaartoq (Ali Polat)

Field work for 2005 was undertaken in the Meso- to Neoarchaeon supracrustal belts in the Godthåbsfjord region, southern West Greenland, to better constrain their geological history. Mapping and sampling included area 1, area 9, area E2, and the Ivisaartoq supracrustal belt. Field work for the areas 1, 9 and E2 was mainly focused on field relations, lithological features, and structural characteristics. Sampling for these three areas were undertaken by Ph.D. student Carlos Calderon. Data points, major rock types, structural measurements, GPS coordinates, sample numbers, and photograph descriptions for all study areas are given in the Excel spreadsheet and in the ArcView© project on the enclosed DVD. New geological maps of the areas 1, 9, and E2 are presented in figures A4_1, A4_2, and A4_3, respectively.

In the area 1 banded amphibolites, heterogeneous orthogneisses, ultramafics (serpentinites, actinolite-tremolite-chlorite schists), and pegmatites have been recognised as major rock types (Fig. A4_1). In addition to these lithologies, there are garnet amphibolites, quartz-feldspar-mica schists, and mafic dykes in the area. Contacts between supracrustal rocks and orthogneisses are predominantly structural. Locally intrusive relations between gneiss and amphibolites are preserved near the contacts. Foliations in the amphibolites are generally parallel to those in the orthogneisses. Foliations generally strike in NE and NW, and dip SE and SW respectively. Mineral lineations and fold axes also plunge SE and SW. Orthogneiss and amphibolites are intruded by pegmatites. Pegmatites in turn are intruded by 2 to 4 m thick mafic dykes.

Banded amphibolites, orthogneisses, ultramafics, and pegmatites are the mappable types of rocks in area 9 (Fig. A4_2). Metagabbros, garnet amphibolites, and quartz-rich schists also occur in this area. Contact between orthogneisses and amphibolites are characterised by strong deformation. No intrusive relations between amphibolites and orthogneisses have been observed. The orientations of foliations and lineations in the area have similar to those of in the area 1.

In the area E2 banded amphibolites, orthogneisses, ultramafics, and pegmatites constitute the major rock types (Fig. A4_3). Calc-silicate formation (diopside-garnet-epidote) is locally well developed. Contacts between orthogneisses and amphibolites are tectonic in nature. Gneissic mylonites and migmatites are common near the green-stone gneiss contacts. In the southern part of the area the orthogneisses are structurally overlain by the supracrustal belt (Fig. A4_3). Kinematic indicators, including asymmetric folds, porphyroblasts, and reverse faults, at the contact suggest a south-southwest directed tectonic transportation.

Field work for the Ivisaartoq supracrustal belts was mainly focused on mafic to ultramafic volcanic rocks and gabbros for geochemical sampling in order to determine their tectonic settings and to understand their petrogenesis. Altered pillow basalts and calc-silicate formations were sampled to understand sea-floor hydrothermal alteration and post-magmatic metamorphic alteration. New ocelli structures in gabbros and pillow basalts have been rec-

ognised in several locations. A total of 48 samples were collected from the Ivisaartoq supracrustal belt. Samples will be analysed for major and trace (LILE, REE, HFSE) elements, and Lu, Nd and Pb isotopes.

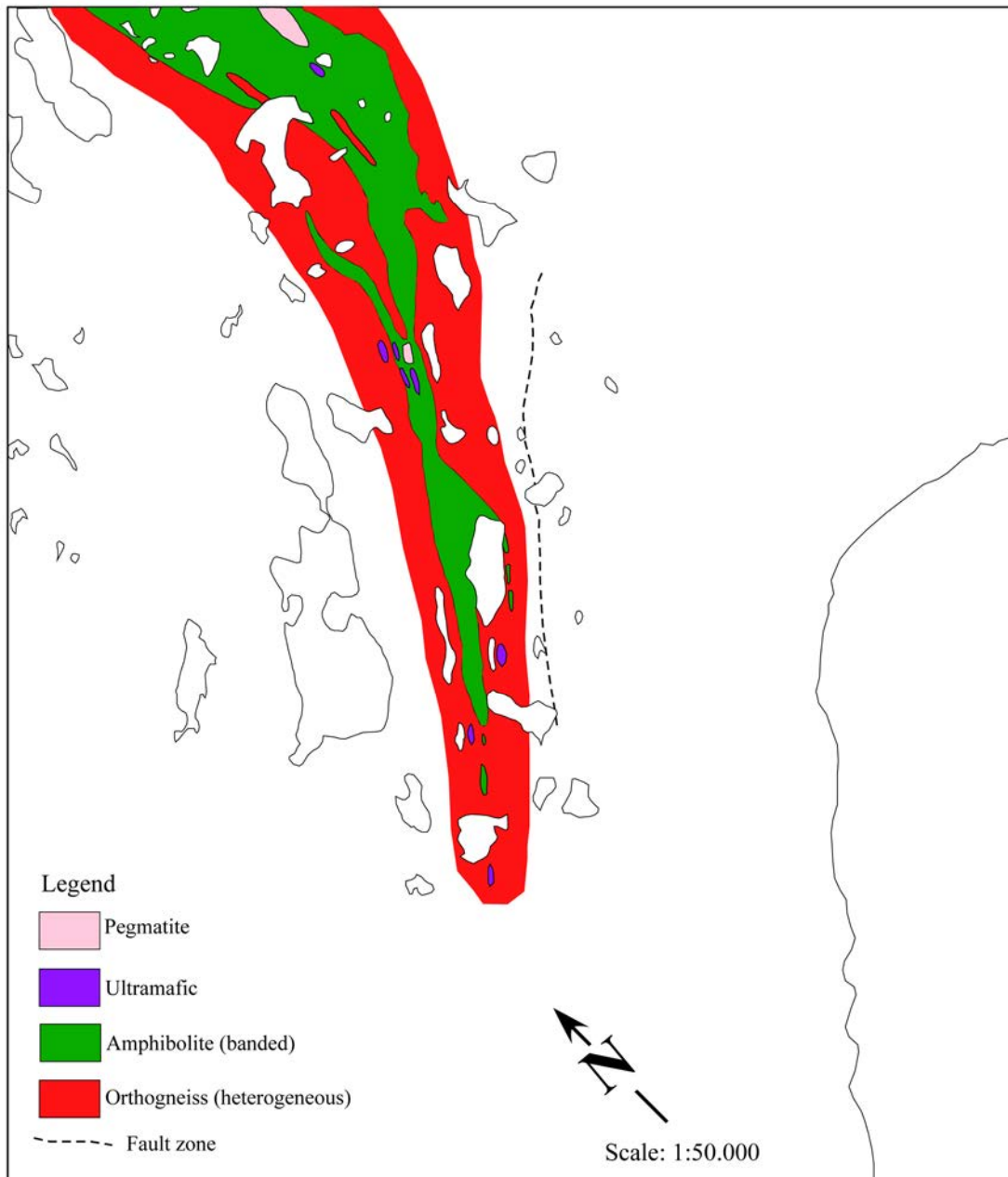


Figure A4_1. Simplified geological map of area 1.

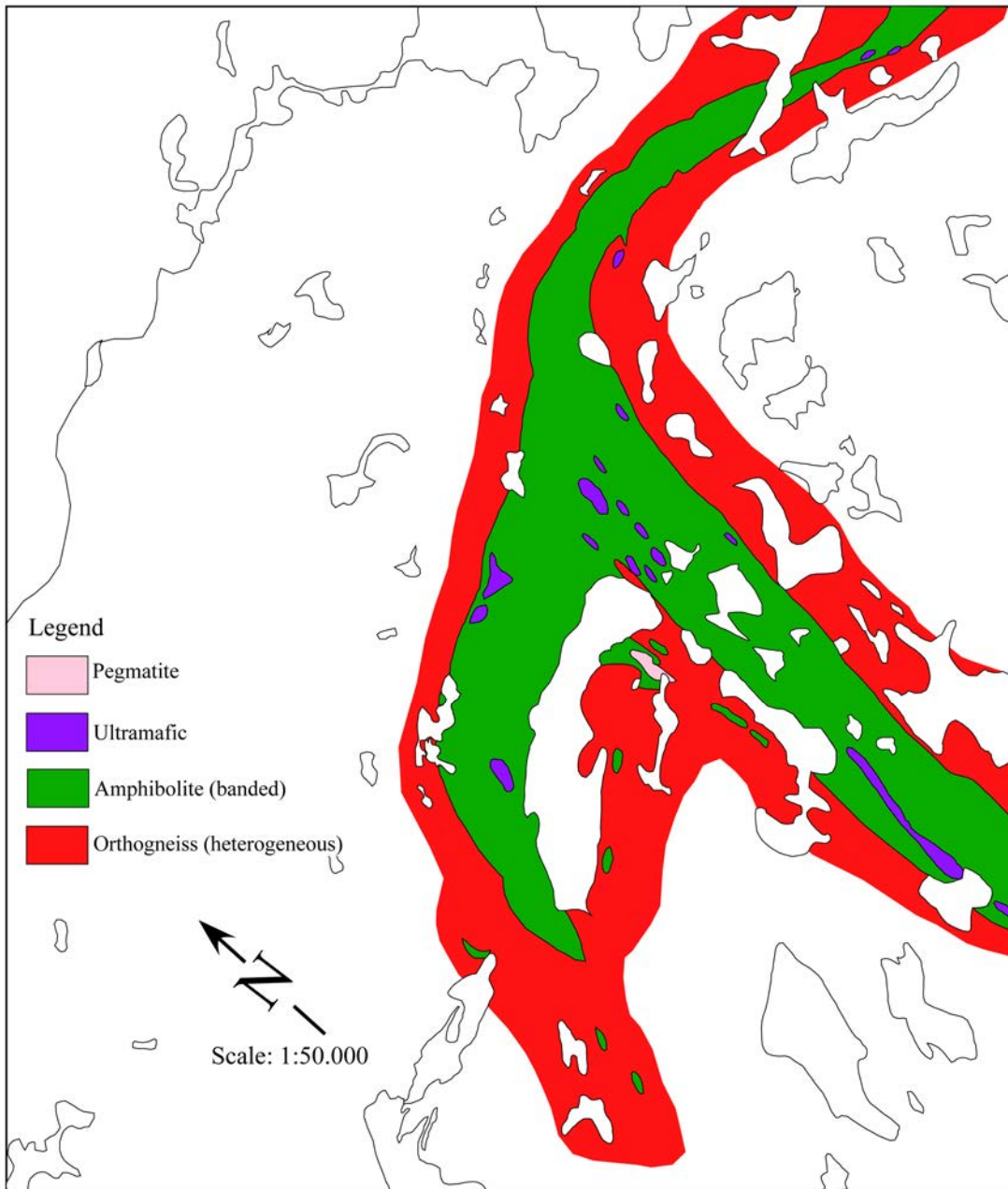


Figure A4_2. *Simplified geological map of area 9.*

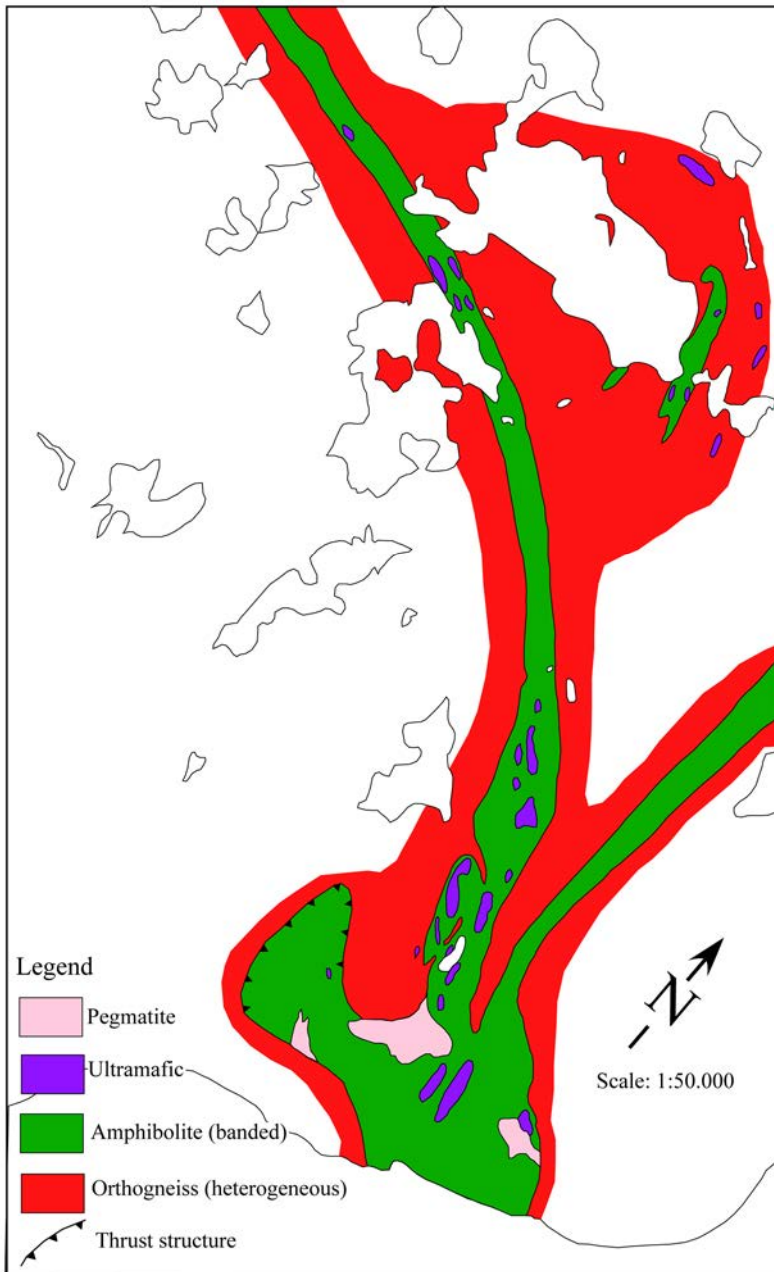


Figure A4_3. Simplified geological map of area E2.

Appendix 5: Field report 2005 - Ujarassuit Nunaat Region – East, and Ivisaartoq (Juan Carlos Ordóñez-Calderón)

Introduction

This progress report summarises the main geologic, stratigraphic and structural observations carried out during 6 weeks of field work in 2005. Detailed field work and sampling was conducted in Ivisaartoq supracrustal belt and other unnamed supracrustals in the inner Godthåbsfjord region.

The data presented in this report were gathered in three different localities labelled areas 1, 9, E2, and in western Ivisaartoq (Fig. A5_1). Most of the field work conducted in Ivisaartoq was carried in the western part of the belt, in the lower group of amphibolites (see Chadwick 1990). A total of 128 samples from amphibolites, metagabbros, metasediments, ultramafics, calc-silicates, and orthogneisses were collected. These samples will be analysed for their petrographic and geochemical characteristics. 287 structural measurements, including foliations, lineations, folds, and fault planes were taken for structural analysis.

The major objectives of this investigation are: 1) to establish the petrogenesis and geodynamic setting of some supracrustal belts in the area; 2) to investigate the structural characteristics of these belts; and 3) to understand the processes of element mobility associated with wide spread fluid flow and hydrothermal alteration in the area.

Lithological Units

Amphibolites and metagabbros

Areas 1, 9, and E2

These localities contain highly strained foliated amphibolites with tight isoclinal folds and widespread lineations. Primary structures such as pillows and volcanic clasts were not found in these areas.

On the basis of colour and grain size, the amphibolites exposed in these localities are mafic to intermediate. Mafic amphibolites (amm) are the dominant rock type. They are heterogeneous at outcrop scale, and are invariably foliated. The mafic amphibolites exhibit medium to fine grained textures. The main mineral components are hornblende + plagioclase + quartz. Garnet is also present, however, garnet-bearing amphibolites are either restricted to narrow layers (up to 1 m thick) or closely associated with calc-silicate alterations. Similar mafic amphibolites show gradation into pillowed amphibolites in the Ivisaartoq supracrustal

belt. By analogy, amphibolites in the areas 1, 9, and E2 are interpreted to represent deformed lava flows.

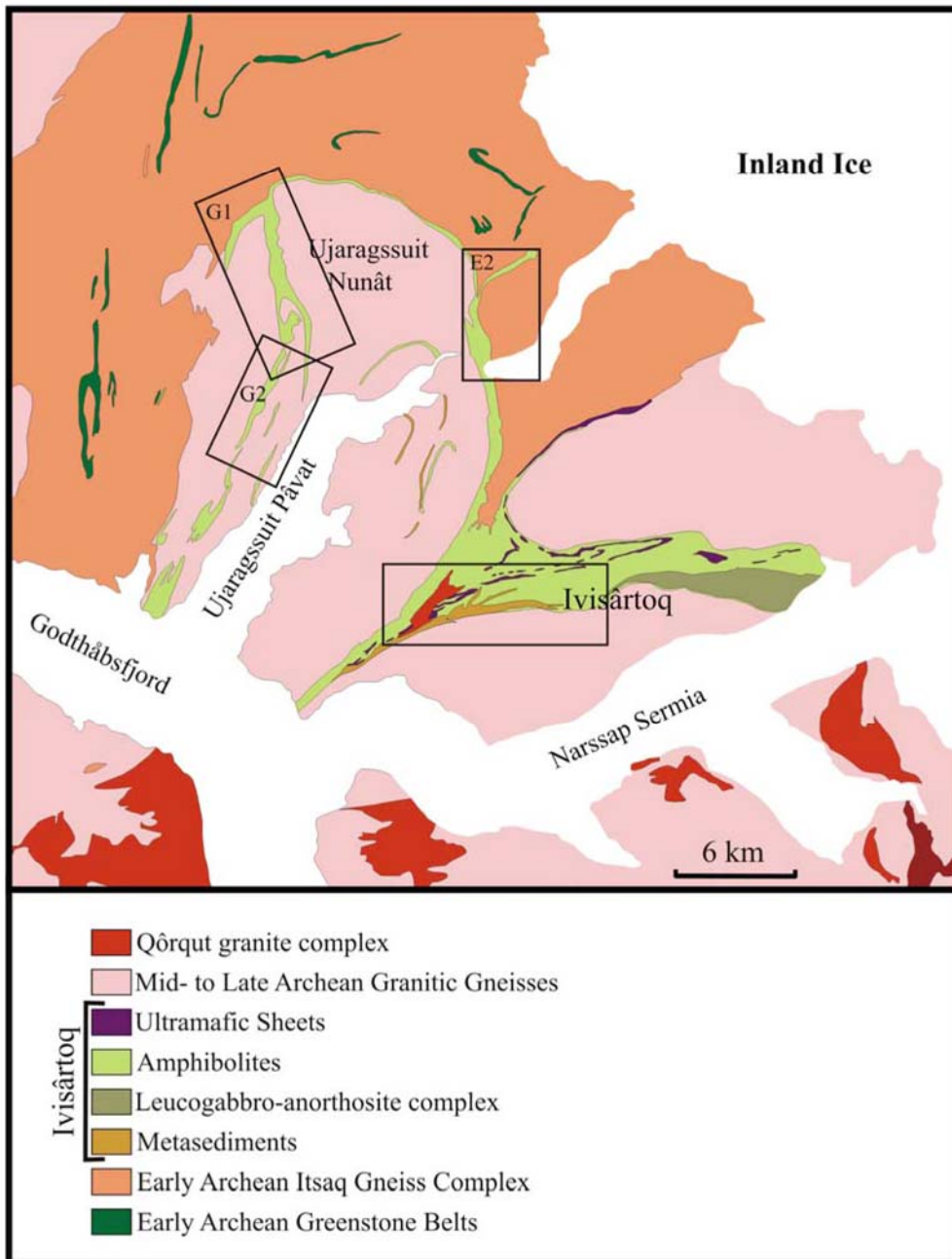


Figure A5_1. Simplified geological map of Ujarassuit and Ivisaartoq region showing the location of the field work areas (Insets). Modified from Chadwick and Coe (1988). Note G1 = area 9, G2 = area 1.

In the area 9 area, mafic amphibolites contain strained felsic lenses 1 to 10 cm long (photo co2005-044). These felsic lenses are primarily composed of fine grained plagioclase. Similar felsic lenses clearly change to ocelli structures in the least strained rocks of Ivisaartoq supracrustal belt. Therefore, felsic lenses found in area 9 are interpreted as strained ocelli structures.

Intermediate grey intermediate amphibolites (ami) are less abundant than the mafic amphibolites. They are foliated and exhibit centimetre-scale layering. The major minerals are hornblende + biotite + plagioclase + quartz ± garnet. The intermediate amphibolites are rarely associated with mafic amphibolites where they form layers of c. 0.5 m in thickness. More commonly they are associated with metasedimentary rocks. Close association with metasediments suggests a volcano-sedimentary origin for some intermediate amphibolites.

Well exposed metagabbros (mg) were found within the mafic amphibolites in areas 9 and E2. They were not found within the intermediate amphibolites or metasedimentary rocks. The metagabbros can be distinguished from the amphibolites by their coarser grained textures and more abundant plagioclase. Hornblende commonly exhibit augen textures. The metagabbros have concordant relationships with the amphibolites. Intrusive contacts were not observed, however, it is possible that the metagabbros represent remnants of dykes and/or small stocks that intruded the amphibolites and latter flatten and transposed during deformation.

Ivisaartoq supracrustal belt

Pillowed structures are well preserved in the upper group of amphibolites (photo co2005-079). The pillowed amphibolites are progressively more strained from north to south, resulting in heterogeneous foliated amphibolites with no pillowed structures in lower unit. The amphibolites of the lower amphibolite group have structural and mineralogical features similar to the highly strained mafic amphibolites of areas 1, 9 and E2. Ocelli structures are well preserved and are comparable to those strained ocelli found in area 9 area.

Metasedimentary rocks

Areas 1, 9, and E2

Metasedimentary units are commonly found within the mafic amphibolites; however, they are a minor component of the supracrustal belts exposed in these localities. The foliation of metasedimentary rocks is concordant with the amphibolites. Metasediments occur as single layers with less than 0.5 m in thickness. In some areas successive intercalations of metasediments with mafic and intermediate amphibolites form units up to 30 m in thickness (photo co2005-019).

The metasedimentary rocks are represented by aluminous paragneisses (pel), mica schists (ms) and quartzites. Paragneisses are composed of quartz + feldspars + garnet + biotite ± sillimanite ± kyanite. Schists are composed of quartz + feldspars + garnet + biotite ± muscovite ± sillimanite ± kyanite. Aluminous paragneisses are more abundant than mica schists.

No primary structures were found in the metasediments. However, fine layering and compositional variability of paragneisses and schists are interpreted as the result of primary compositional heterogeneity. Close association of metasediments with intermediate amphibolites suggest that some of these units could be of volcanosedimentary origin.

The metasedimentary rocks were sampled where no evidence for hydrothermal alteration was present. Some biotite-rich schists with large (3 to 4 cm) garnet porphyroblasts are closely associated with hydrothermal alteration and they might represent the alteration products of amphibolites.

Ivisaartoq supracrustal belt

A unit of metasedimentary rocks is exposed in the lower part of the lower amphibolite group (see Chadwick 1990). This unit is formed by paragneisses, mica schists, and quartzites. The paragneisses are commonly composed of quartz + plagioclase ± biotite ± garnet. Mica schists range from muscovite-rich to biotite-rich schists. Muscovite-rich schist commonly contains kyanite and garnet. Sillimanite, staurolite, and garnet are common in biotite schists, whereas hornblende is locally present. Mineralogical evidence suggests broad compositional variation, probably indicating diverse provenance for the metasediments.

No primary structures were found in the lower metasedimentary unit. However, in a single outcrop in the upper part of the unit, biotite schists contain elongated inclusions (10 to 15 cm in size) resembling clasts (photo co2005-082 and -083). These biotite schists are well exposed throughout the contact between the metasediments and the lower amphibolite group. Similar structures were not found along the strike of the biotite schists, and it is not clear if they are primary features.

Ultramafic rocks

Areas 1, 9, and E2

There are two dominant types of ultramafic rocks: 1) ultramafic enclaves, and 2) ultramafic schists. The ultramafic enclaves occur as massive reddish lenses generally hosted by the amphibolites or by the associated orthogneisses. These enclaves have ellipsoidal shapes making them easy to recognise and map (photo co2005-023). They range in size from 1 m to more than 50 m. They normally contain actinolite, however, the mineral components are difficult to determine in hand specimen. More rarely, olivine-rich ultramafic enclaves occur (e.g. in area E2). The ultramafic enclaves generally lack of foliation, however, enclaves with well developed crenulation cleavage were found.

Ultramafic schists occur as discrete layers, 0.5 to 1.0 m in thickness, intercalated with mafic amphibolites. They are composed of garnet + actinolite + chlorite + biotite. No primary structures were found in these rock units. Generally they are strongly altered as indicated by abundant hydrous phases such actinolite and chlorite. Close association with mafic amphibolites would suggest that these rock types represent metamorphosed ultramafic flows.

Ivisaartoq supracrustal belt

Ultramafic rocks in Ivisaartoq are the same type as in the localities described above. A remarkable difference is the occurrence of ultramafic schists with pillowed structures.

Late intrusives

Areas 1, 9, and E2

Late intrusives are represented by widespread pegmatites (peg) and dolerites (dolt). Pegmatites occur as undeformed stocks, dykes, and veins intruding the amphibolites. They are either concordant or discordant with the amphibolites. Pegmatites with concordant relationships generally parallel the foliation and fill fold hinges. The main mineral phases are quartz + plagioclase + biotite ± garnet. The grain size is variable, ranging from characteristic coarse-grained textures, with crystals up to 5 cm, to fine and medium grained textures. Fine grained textures are particularly found in thin dykes and around fold hinges and are the result of rapid cooling. Dolerites occur as undeformed dykes ranging from 0.3 to 4 m in thickness. These dykes clearly intrude the pegmatites and amphibolites (photo co2005-055).

Hydrothermal alterations

Areas 1, 9, and E2

Hydrothermal alterations are widespread in these areas. Two broad types of alteration are observed: 1) calc-silicate alterations, and 2) pyrite-bearing rusty alterations.

Calc-silicate alterations are developed as replacement in mafic amphibolites. These alterations consist of epidote + diopside + quartz ± garnet. They are parallel to the foliation forming continuous irregular layers several meters long. The timing of the alteration is not clear, however, calc-silicates layers are isoclinally folded (photo co2005-049).

Rusty, pyrite-bearing, quartz-rich layers are intercalated with the mafic amphibolites. These layers are brownish due to weathering of pyrite. There is no crosscutting relationship with the host amphibolites. It is possible that the pyrite-bearing quartzites are primary layers formed coeval with the amphibolite protolith.

Hydrothermally altered amphibolites give a similar rusty appearance, in which the brownish colour is due to alteration of amphibole. Altered amphibolites are composed of quartz + pyrite + chlorite + biotite ± garnet. This alteration forms discontinuous patches controlled by foliation planes. Field relationships suggest that this alteration postdates the calc-silicates and the pyrite-bearing quartz-rich layers.

Ivisaartoq supracrustal belt

Calc-silicate alterations occur in two styles: 1) replacing the pillowed cores, and 2) forming veins and lenses that are parallel or crosscut the foliation. The first type of alteration is probably of primary origin, coeval with the formation of pillowed structures (photo co2005-080). The second type of calc-silicate alteration is later and is controlled by the foliation suggesting that this postdates the regional metamorphism.

In addition to calc-silicate alterations, there is a wide spread hydrothermal alteration in the amphibolites and metasediments. This is a pyrite-bearing alteration occurring as discontinuous patches. Argillic alteration is developed in areas with intense alteration in the lower part of the metasedimentary unit (photo co2005-081).

Structures

Areas 1, 9, and E2

In general the foliation in these localities ranges from NS to N30E with variable dip direction. Isoclinal folds and lineations are wide spread, and show comparable orientation, consistently dipping NNE and SSE.

Amphibolites and orthogneisses exhibit concordant foliation. In several areas the contact between amphibolites and orthogneisses is clearly tectonic with well developed mylonites (photo co2005-070). Mylonitic fabrics range from blastomylonitic to ultramylonitic. Isoclinal and recumbent folding are more pronounced in areas near the contacts. Sheared amphibolite enclaves, up to 20 m long, commonly occur within the orthogneisses adjacent to amphibolite.

Ivisaartoq supracrustal belt

The foliation, mostly N60-70E, parallels the main trend of the belt. In general, the foliation of the lower amphibolite group dips NNW, whereas the upper amphibolite group dips SSE clearly defining a synform structure. Isoclinal folds and lineations are not as abundant as in the localities described above. The contact between the upper and lower amphibolite groups is highly strained with abundant quartz veins, secondary calc-silicate alterations, silicification, and development of mylonites.

Preliminary conclusions

The amphibolites in the areas 1, 9, and E2 are highly strained. The only primary features observed are deformed ocelli structures in metagabbros. Mafic amphibolites are the dominant rock type, with intermediate amphibolites restricted to thin layers within the mafic amphibolites and/or associated with metasediments. Metasedimentary rocks occur as thin layers or as units up to 30 m in thickness. The homogeneous amphibolites in areas 1, 9, and E2 show similar textural and mineralogical features to the amphibolites of the lower amphibolite group in Ivisaartoq.

The occurrence of shear zones with well-developed mylonites in the contacts between orthogneisses and the amphibolites belts suggest a tectonic contact between these units. Several types of hydrothermal alterations were observed. Calc-silicate alterations are the most prominent. Calc-silicates occurred as two distinctive types of alterations: 1) as replacement of pillowed cores, and 2) veins and lenses crosscutting and or paralleling the foliation of heterogeneous mafic amphibolites. The second style of calc-silicates clearly

postdates the pillowed replacements. Pyrite-bearing rusty alterations are commonly found in quartz-rich layers intercalated with amphibolites.

Patchy silicification and argillic alteration is well developed in the lower amphibolite group in Ivisaartoq. This alteration is pyrite bearing and could have a strong potential for gold mineralisation.

Appendix 6: Structural Geology of the supracrustal belts in the central Godthåbsfjord region, data collection for constraining tectonic cross-sections (Dave and Vincent Coller)

Introduction

The 2005 field program was aimed at gathering new structural data to use in the construction of regional tectonic cross-sections across the various terranes in the central Godthåbsfjord region. The field work areas concentrated on sections across the supracrustal packages and the different age gneissic panels in the Tre Brødre and the Akia terranes on Storø and Bjørneøen and focused particularly on the structural history of key contacts such as the Ivringuit Fault (Fig. A6_1).

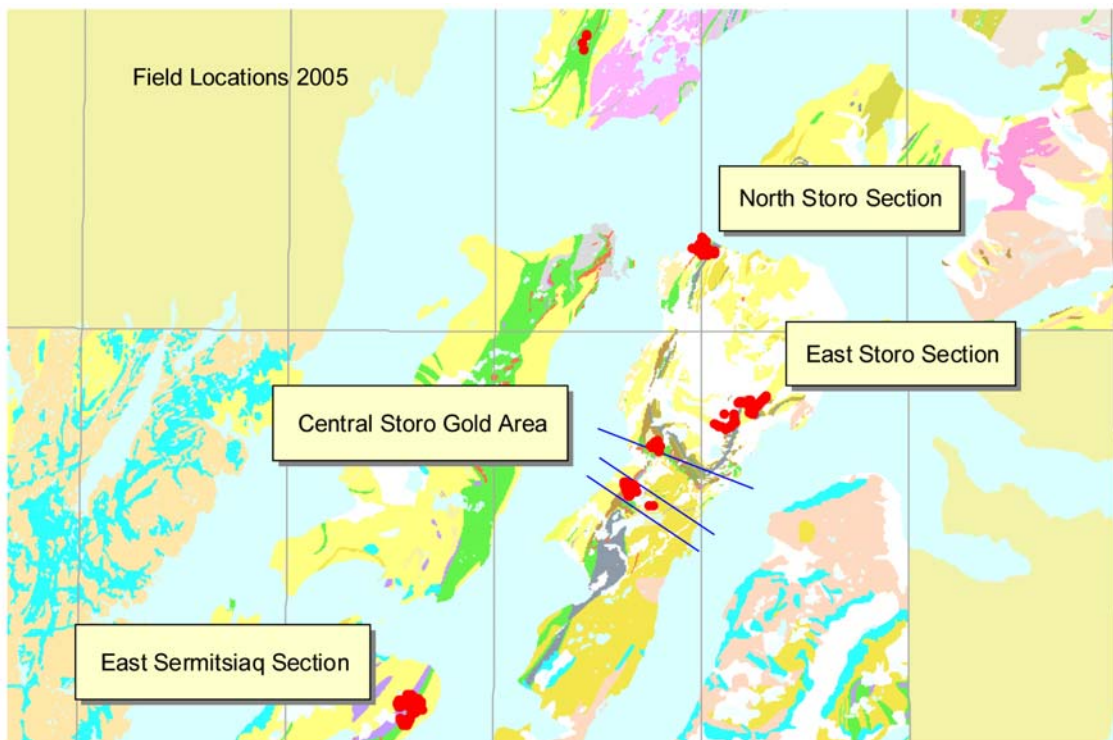


Figure A6_1. *Field locations for 2005.*

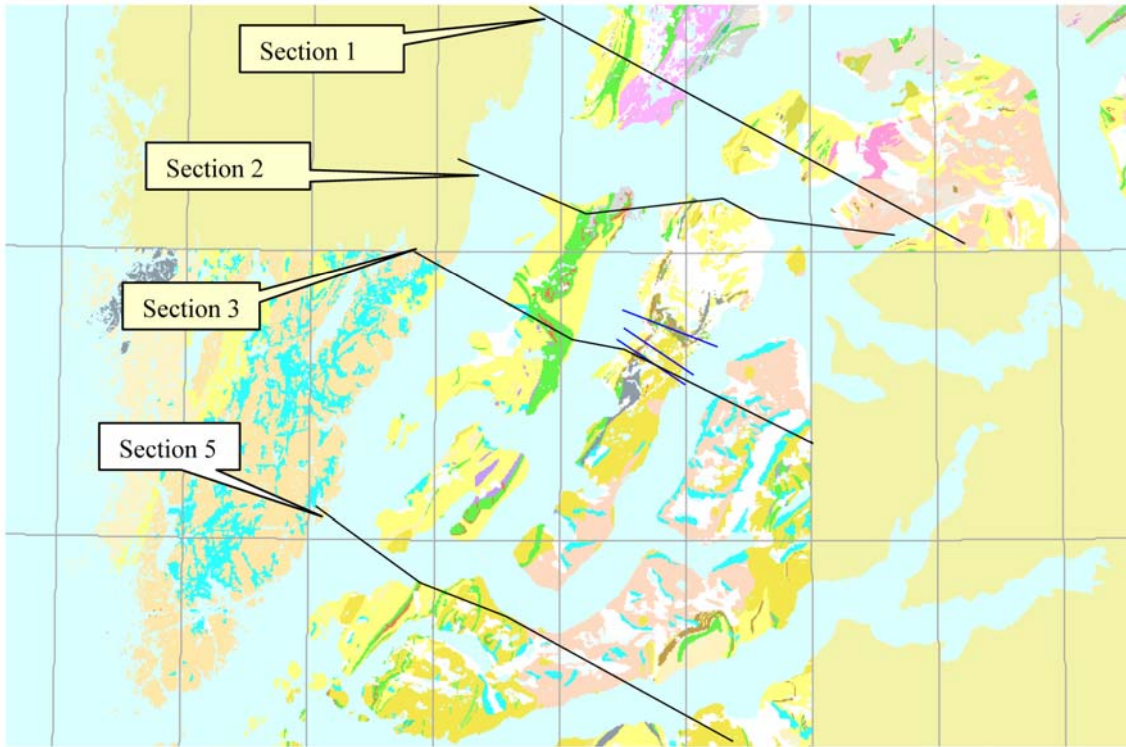


Figure A6_2. Location of planned regional tectonic sections.

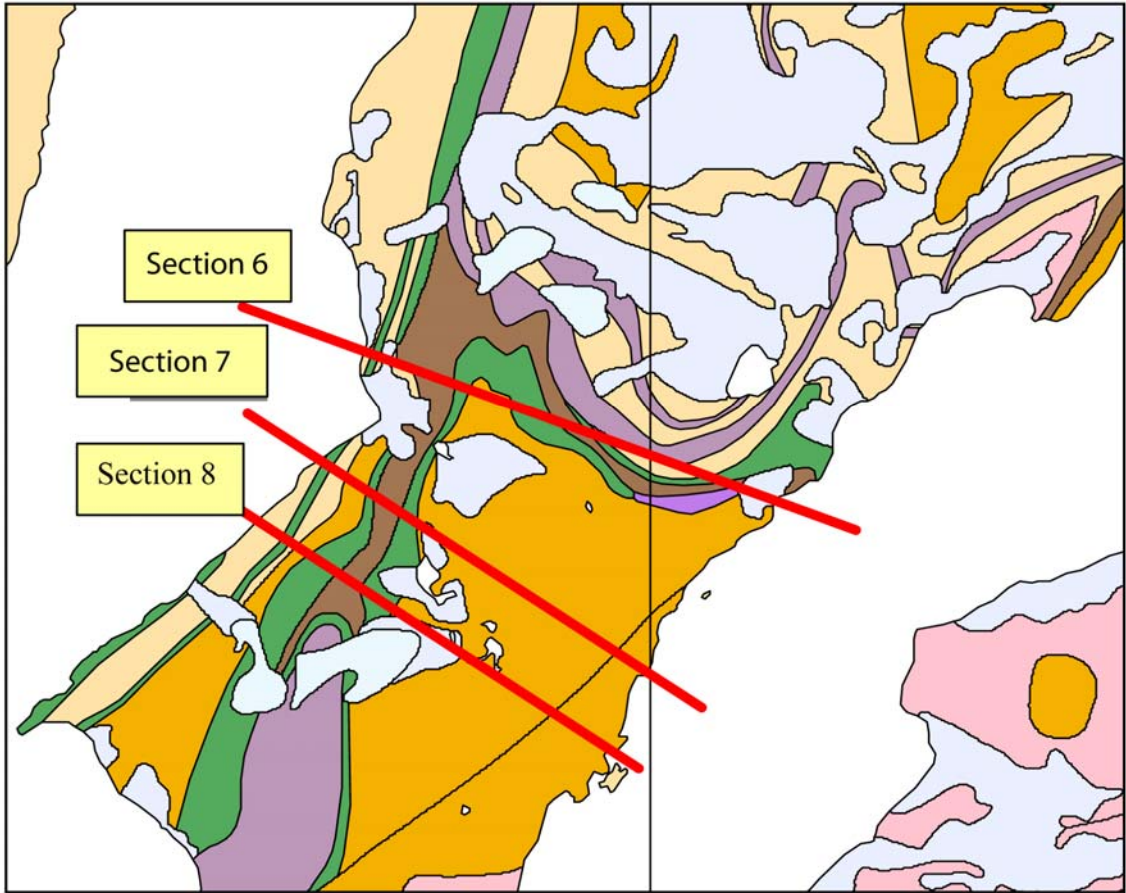


Figure A6_3. Location of Central Størø sections.

The location of tectonic cross-sections (Fig. A6_2) was based on the concentration of new data arising from the mapping and geochronology of the 2004 GEUS field program as well as previously published maps and age data. More local detailed sections are being constructed across Storø where detailed mapping of the supracrustal rocks and structure was undertaken by GEUS in 2004 (Fig A6_3).

The results of the 2004 program (Hollis et al. 2004) identified a complex interleaving of different age gneisses and juxtaposed Mesoarchaeoan and Neoarchaeoan supracrustal within the central Godthåbsfjord region and the aim of this current project is to examine the geometry of this region, the structural chronology of the main faults and their relation to the known mineralisation.

Field Results

Two detailed themes are selected from the field results so far, (1) the nature of the contact between the Ikkattoq Gneisses and (2) the supracrustal rocks on Sermitsiaq: The 'Ivinnguit Fault'.

Several detailed sections across the eastern boundary of the Akia terrane indicate a complex multiphase reactivation along the contact which was previously defined as the Ivinnguit Fault and terrane boundary (McGregor et al. 1991). The contact is defined on eastern Sermitsiaq by a multiphase fault rock which reveals a detailed structural history. The contact is well exposed for several kilometres in the Camp 4 area on eastern Sermitsiaq and defined by a continuous narrow zone (20 cm to 2 m) of cataclasite. The cataclasite appears to be largely derived from both amphibolites and mylonitic rocks in the supracrustal package (probably Mesoarchaeoan), however the fault rock also penetrate as zones within the Ikkattoq gneisses indicating formation during or after juxtaposition of the 'terrane'. The composition of the cataclasite is a quartz-biotite rock with tourmaline. There is no doubt that this rock is a fault rock which transects the supracrustals and gneisses with several other zones of the similar cataclasite, some, several meters wide, developed well within the amphibolite package which also constitute significant shear structures.

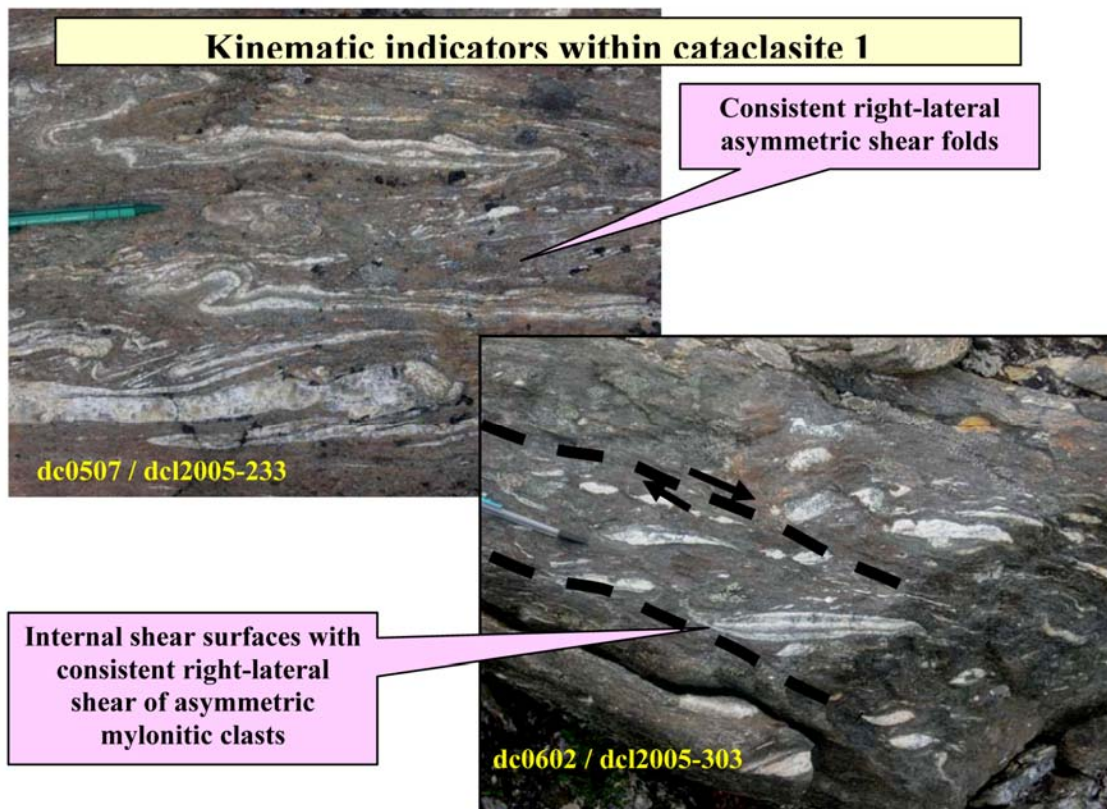
Three detailed sections across the supracrustals from the Ikkattoq to the Nûk gneiss on Sermitsiaq define a structural chronology and sense of displacement along the contact. The cataclasite contains field-scale mylonitic clasts indicating that it incorporates an earlier ductile fault rock (Fig. A6_4). The cataclasite also has a folded and sheared planar fabric which contains shredded quartz veins and aligned mylonitic fragments. The folds and shears consistently indicate an oblique dextral strike-slip fault movement indicating a significant ductile shear along the fault contact after the gneisses and amphibolites were juxtaposed. Further, coarse-grained garnets appear to overgrow the planar cataclastic fabric but may be deformed by the shear-fold strike-slip fault event. Close to the contact within the amphibolite are ductile blasto-mylonites developed within amphibolites and gabbros and these seem to be associated with the main shape fabric and stretching. No mylonites appear to be developed in the adjacent gneisses which have only moderate shape fabrics not too different from the gneiss fabrics 100 m east of the contact.

In summary the contact preserves is an early mylonitic shear and penetrative fabric within the supracrustals rocks which may represent the thrust imbrication of Meso- and Neoproterozoic supracrustals. The second clear event is a major shear generating a zone of cataclasis which juxtaposes the Ikkattoq gneisses and supracrustal packages.

The third event (which could possibly be a continuation of second shear event) is a ductile shear event which deforms the cataclasite fault rock. This is consistently an oblique dextral strike-slip ductile shear movement top to the east.

Several retrogressive chloritic shear zones several meters wide with mylonitic rocks are also developed within the supracrustals and this is presumed to post-date the third prograde ductile shear movement.

The implications for the Ivinnguit Fault in this area are that the contact has multi-stage movement – 2 to 3 prograde fault episodes, the earliest a reverse shear (thrust) and a later oblique ductile strike-slip.



The fault rock is 2-20m thick and composed of bio-tourmaline schist.

Figure A6_4. Structure of cataclasite along the 'Ivinnguit Fault' on Sermitsiaq.

Alteration within the supracrustal packages

There appears to be a growing possibility from the field work on Storø and the sections on Sermitsiaq that many of the silica-rich units within the supracrustals are rocks derived from amphibolitic protoliths and are not metasediments. We observed many pale-coloured quartz-rich units, many garnetiferous which are clearly within amphibolitic packages and derived from amphibolites. It is quite probable that these quartz-rich and aluminous rocks are metamorphosed altered assemblages, i.e. there may be very large scale layer-parallel fluid pathways through the package at some early stage or associated with a major deformation phase that has grossly altered the texture and mineralogy of large sections of the package. Also, some of the mica-schists are clearly fault rocks, specifically the cataclasites which are biotite-quartz-tourmaline assemblages.

Tectonic Cross-Sections

The construction of preliminary local and regional cross-sections was undertaken prior to the 2005 field program to highlight areas of poor data and tectonic problems. The new and revised sections are currently in progress. Seven sections have been captured in terms of tectonic units (see Fig. A6_8) with ArcView© and the contacts are being investigated. The progress on central Section 3 is illustrated in Figures A6_5, A6_6 & A6_7.

The sections are being constructed in ArcView© GIS package for ease of integration with other data (e.g. maps, magnetics and geochemistry) and also easy update as new age data and relationships become available from the 2005 program. Section 3 illustrates the index of 'Fault types' (Fig. A6_8) which are based on the age and structural relationships at contacts.

In the ArcView© tables each unit has an 'age attribute' which is based on the geochronology on or along strike of the section. This may be updated and displayed in the section view as new age data becomes available.

Central Storø Sections

The object of three detailed Central Storø Sections (Fig A6_1) is to try to understand the 3D geometry of the structure of the Storø supracrustal package and get a clearer understanding of how the gold mineralisation relates to the larger scale structure. These sections are in progress. The new field work in 2005 has clarified further the age of Storø shear fold-fault structures in relation to the post-terranic history. A second steep east dipping shear zone on Storø is developed in the eastern part of Central Storø between which are open folds of the same age.

Regional Sections

Four regional E-W sections are now being constructed across the main terrane boundary zone between the Akia and Tre Brødre terranes (Fig A6_2). Section 3 (Figs A6_5 to 8) illustrates the general geometry of the boundary zone with the various ages of gneisses and supracrustal packages and the much younger intrusive Qôrqut Granite. The faults are classified into different types and ages showing that boundaries such as the Storø shear zone contains multiple ages on certain sections (i.e. Storø shear zone – post terrane assembly overprinting an early thrust within the supracrustals).

This reactivation and overprinting of structures is more complex along some tectonic contacts such as between the supracrustals and gneisses on the north Storø section. This boundary incorporates three ages of structures within the same tectonic contact zone:

- Thrust imbrication of Meso- and Neoarchean supracrustals within the supracrustal belt on Storø.
- Terrane assembly shearing juxtaposing Nûk gneisses and supracrustals along the 'Ivinguit Fault' at c. 2700 Ma.
- Storø shear zone attenuation and shearing of earlier contact.

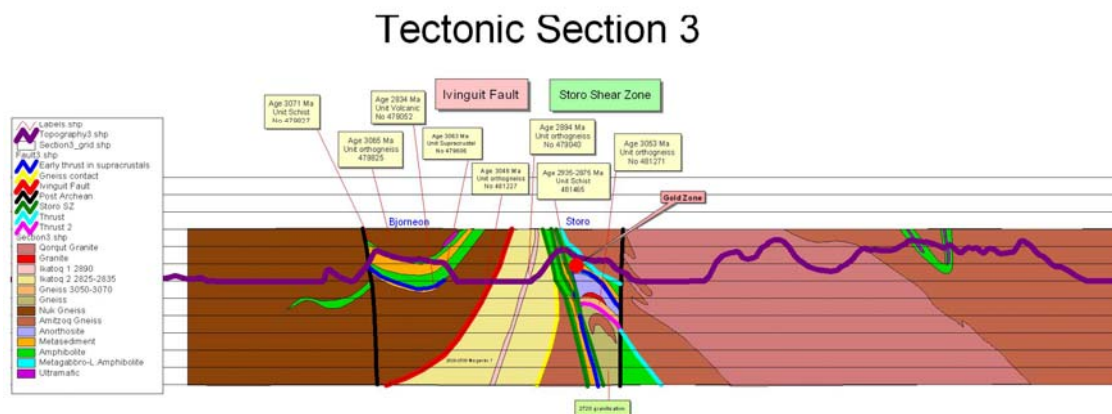


Figure A6_5. ArcView© based tectonic cross-section 3, central Godthåbsfjord.

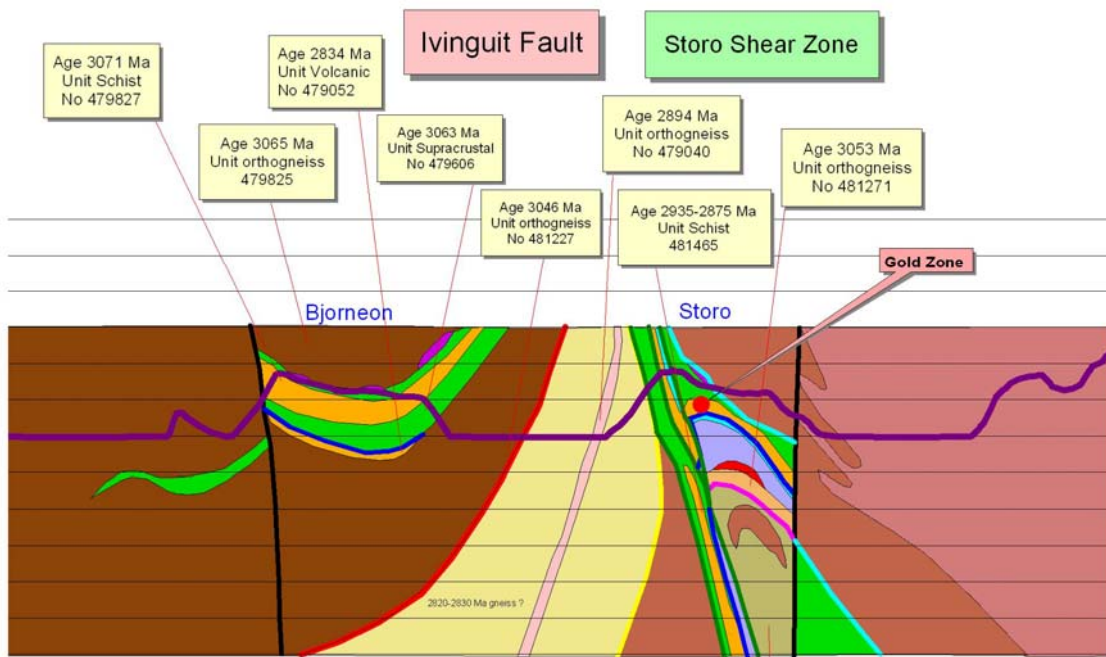


Figure A6_6. Detail of section 3 showing gold zone at 'tectonic triple junction'.

Tectonic Section 3

Mid Archean and Late Archean Supracrustal Packages

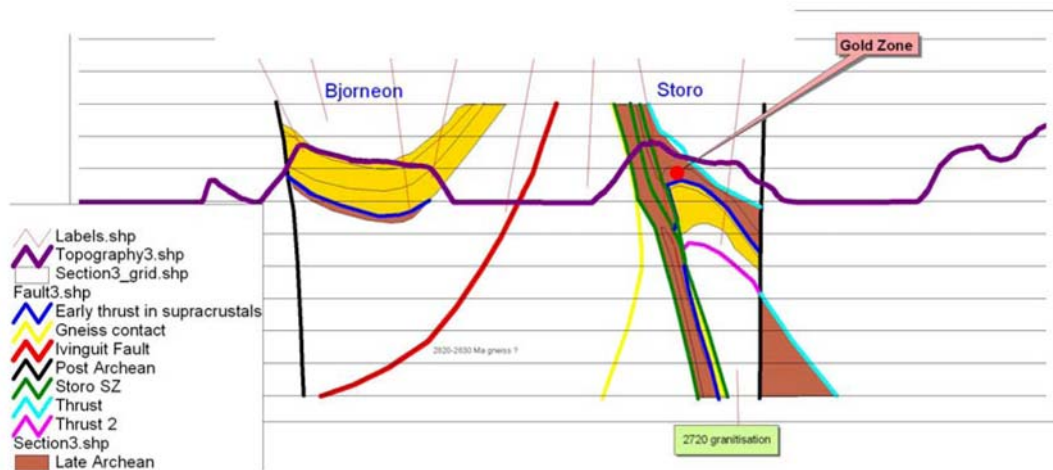









Figure A6_7. Supracrustal belts and main structures within the Akia and Tre Brødre terranes. Note: Brown – Neoarchaeon supracrustals; Yellow – Mesoarchaeon supracrustals; Red – Ivinguit Fault. Note the early 'thrust' contacts in dark blue between the two different age panels of supracrustals in both Akia (Bjørneøen) and Tre Brødre (Storø) terrane.

Tectonic Units

	Qorqut Granite
	Granite
	Ikatoq 1 2890
	Ikatoq 2 2825-2835
	Gneiss 3050-3070
	Gneiss
	Nuk Gneiss
	Amitzoq Gneiss
	Anorthosite
	Metasediment
	Amphibolite
	Metagabbro-L.Amphibolite
	Ultramafic

Fault Classification

	Early thrust in supracrustals
	Gneiss contact
	Ivinguit Fault
	Post Archean
	Storo SZ
	Thrust
	Thrust 2

Section3.shp

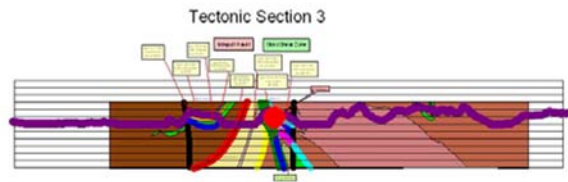


Figure A6_8. Units and fault legend for ArcView© tectonic sections (age and other legends not shown).

Appendix 7: Ore mineralogical examination of the Qussuk area (Britt Andreasen)

Introduction

During the summer 2005, field work in the Qussuk area was carried out by Gorm Thøgersen and Britt Andreasen. The work in the central part of the Qussuk peninsula was planned to take two weeks with 11 effective days in the field between the 19th of July and the 2nd of August. Henrik Stendal participated from the 19th to the 22nd of July. Adam Garde (GEUS) visited on the 21st and 22nd of July.

Furthermore a one-day reconnaissance on the 6th of August was used with half a day in the area north of the Qussuk bay and the second half in the western part of the Qussuk peninsula.

The work carried out in the field was based on the previous knowledge of gold anomalies in the area and it will result in a master thesis concerning a geochemical and ore mineralogical examination of the supracrustal belt. Henrik Stendal (GEUS) and Emil Makovicky (University of Copenhagen) are the supervisors connected to the project.

Previous work and geological setting

The Qussuk area has been covered by mapping for the Fiskefjord map sheet at scale 1:100.000 (Garde 1989) and discussed by Garde (1997). During the GEUS fieldwork in 2004 in southern West Greenland, Adam Garde examined and mapped the Qussuk peninsula in detail. Analysis of 57 rock samples from the Qussuk area showed anomalous gold content in several lithologies (Hollis et al. 2004; Appel et al. 2005). One sample (no. 477326, locality aag2004-109) collected at the head of the Qussuk bay yielded 2.2 ppm Au, and another sample (no. 477384, locality aag2004-187) collected in the central part of the Qussuk peninsula yielded 1.4 ppm Au.

The Qussuk area in the north-western Godthåbsfjord in southern West Greenland is located in the most eastern part of the Akia terrane (3.2 to 2.97 Ga ; Figs. A7_1 & A7_2). The Qussuk peninsula and Qussuk bay show two main supracrustal belts that form a sequence of NNE-trending, isoclinally folded and steeply dipping units with a thickness up to more than one kilometre (Garde et al. 1986, 2000). Variably deformed tonalitic and granitic intrusions crosscut and surround the supracrustal belts. Most of these intrusions belong to the Taserussuaq tonalite complex and the Qussuk granite, which have been dated at c. 2975 Ma and thus provide a minimum age for the supracrustals (Garde et al. 1986, 2000). The supracrustal belts are a sequence of amphibolites with local hydrothermal alteration and iron-sulphide occurrences. The amphibolites are leucocratic, rich in plagioclase and commonly contain biotite in addition to hornblende. In some areas the amphibolites show a fragmental texture of pyroclastic or volcanoclastic origin (Hollis et al 2004).



Figure A7_1. The Qussuk Camp.

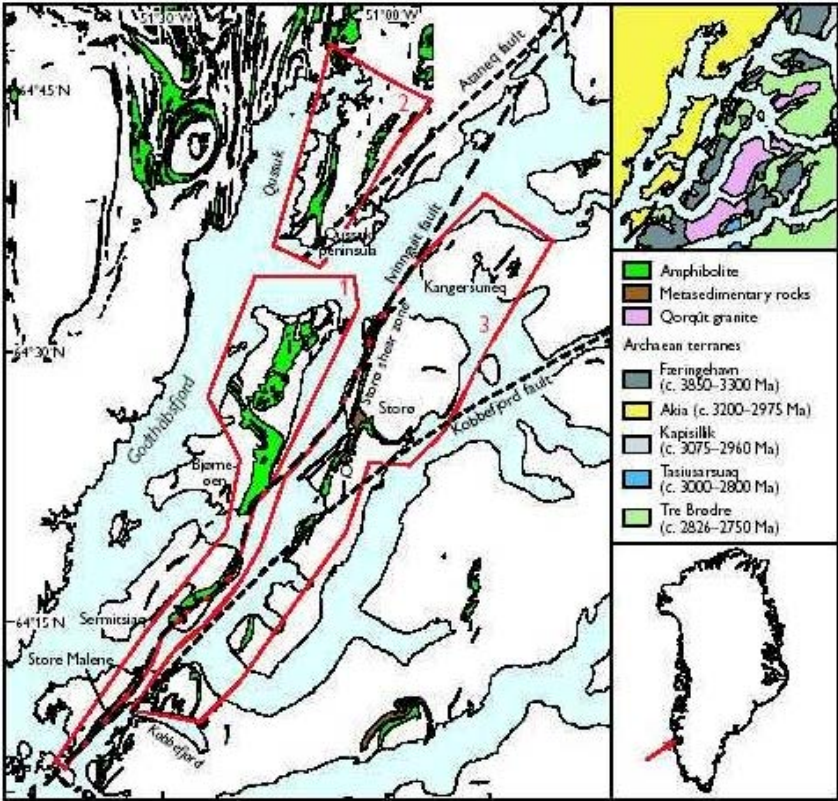


Figure A7_2. Overview map of the Godthåbsfjord region. The Qussuk area is encircled in red with the number 2. Shown in the map is the distribution of supracrustal belts in the area (from Hollis et al. 2005).

Methods

Samples were collected throughout the whole Qussuk area. A total of 89 samples in varying sizes from 300 grams to 1 kilo were collected and given the numbers 497601-497689 (Fig. A7_4; Table A7_1). From the central part of the Qussuk peninsula 75 samples were collected, nine samples were collected from the head of the Qussuk bay and five samples from the western part of the Qussuk peninsula. In several places the samples were collected systematically along cross sections to help the understanding of the stratigraphy of the area. Furthermore some modifications to the detailed map of the area, made by Adam Garde (in Hollis et al. 2004), were carried out (Fig. A7_3).



Figure A7_3. Detail geological map of the central part of the Qussuk peninsula, northern Godthåbsfjord with selected localities from the work done in 2005. Modified after Adam Garde in Hollis et al. (2004).

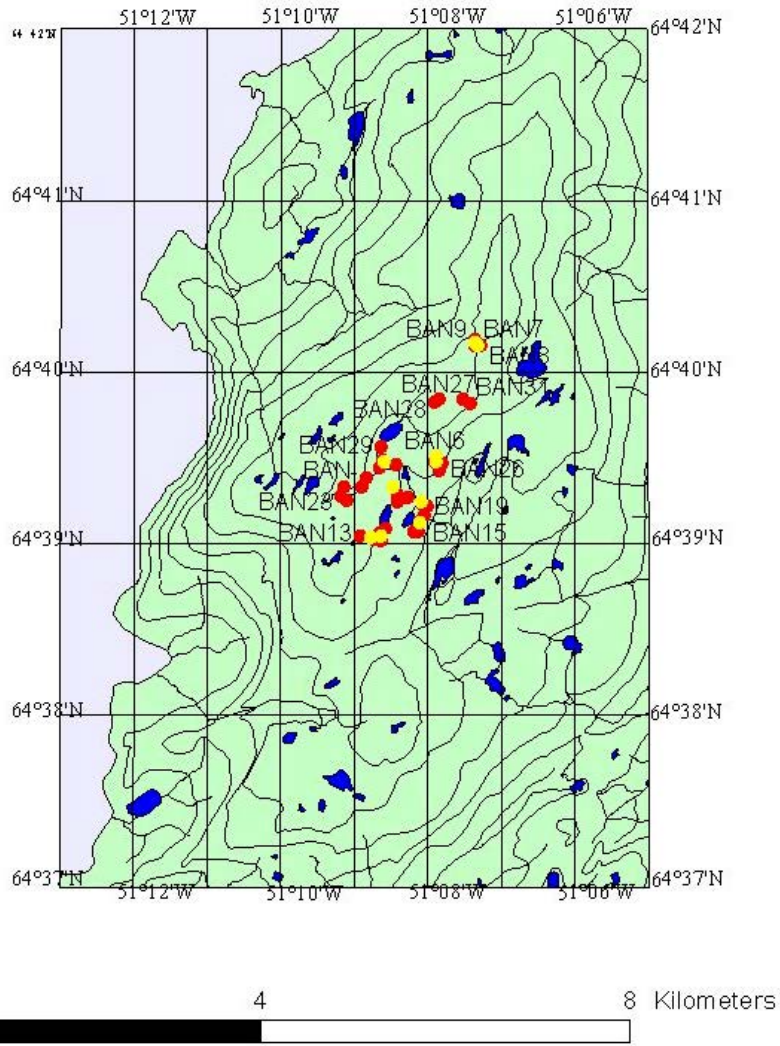


Figure A7_4. Map of the Qussuk Peninsula with BAN 2004 localities no. 01-39.

Table A7_1. *Rock sample data. Qussuk, central part of peninsula.*

Locality	Sample no.	Rock type	Mineral content	Colour	Grain size	Characteristics
BAN-01	497628	Extremely magnetic, Black rock	Magnetite <5% light minerals	Black	Fine	Massive
	497629	Non-magnetic black rock	~30% light minerals	Black	Fine	Surface chemical weathering
	497630	Non-magnetic black rock w. alteration clasts	~30% light minerals clasts: green + brown minerals	Black	Fine	Surface chemical weathering Foliation, lineation 1 malachite grain
	497631	Qz vein (1 cm) w. surrounding alteration	Quartz Green minerals	Black Greenish	Fine	Lineation
BAN-02	497627	Black amphibolite w. light minerals in veins/clods	Diopside/epidotite? Light minerals in cracks/clods	Black Greenish	Fine	Non-magnetic Chemical weathered surface w. oblong holes 1 malachite grain
BAN-03	497623	Qz-biotite-rich rock	Quartz Biotite Disseminated Fe-sulphides <2mm + few larger aggregates <1x0.5 cm	Light grey	Medium	Rust alteration surface
	497624	Light-coloured coarse grained rock	Albite Disseminated Fe-sulphides <2mm	Light	Coarse	Albitisation? Rust alteration surface and cracks in the rock
	497625	Garnet amphibolite	Biotite Garnet <3 mm Disseminated Fe-sulphides <2 mm + aggregates <0.5 cm	Grey	Fine	Rust alteration surface Lineation
	497626	Dark amphibolite	Biotite Aggregates of light mineral (Qz?) Disseminated Fe-sulphides <1 mm	Dark grey	Fine	

Table A7_1 continued. *Rock sample data. Qussuk, central part of peninsula.*

Locality	Sample no.	Rock type	Mineral content	Colour	Grain size	Characteristics
BAN-04	497601	Pyroclastic rock	Hornblende	Greenish		Distinct clasts w. different sizes and compositions
BAN-05	497602	Dark amphibolite	Disseminated Fe-sulphides <4 mm parallel w. lamination and in crack	Black	Fine	A c. 5 m wide layer next to grey intermediate amphibolite Lamination
BAN-07	497603	Dark amphibolite -sensu stricto	Hornblende	Black	Fine	
	497604	Grey intermediate amphibolite	Garnet <1 cm	Grey	Fine - medium	Poikiloblastic texture
	497605	Rust altered rock w. garnet crystals	Quartz Biotite Garnet <1 cm	Rusty brown-red	Medium - coarse	Most likely as boudins
	497606	Dark amphibolite	Fe-sulphides Hornblende Garnet	Black	Fine	Very little and few garnet grains
	497607	Garnet mica gneiss	Garnet <1.0 cm Mica		Medium	The garnets are metamorphic
BAN-08	497612	Biotite-rich amphibolite	Biotite Sulphides Quartz	Rusty		
	497613	Garnet amphibolite	Garnet Sulphides	Rusty		
	497614	Grey intermediate amphibolite	Sulphides	Rusty grey		
BAN-09	497608	Light-coloured rock in rust altered zone	Albite Disseminated Fe-sulphides	White and rusty		Albitisation
	497609	Garnet amphibolite	Garnet < 5mm Disseminated Fe-sulphides	Dark	Fine	Rusty surface Granite/quartz veins w. disseminated sulphides
	497610	Dark amphibolite	Quartz Sulphides	Black		Quartz vein ~2cm wide w. sulphides
	497611	Dark amphibolite	Sulphides	Black		
BAN-12	497615	Tonalite	Quartz Feldspars Dark minerals	Light grey	Coarse	Homogeneous Massive Intrusive in grey intermediate amphibolite
BAN-13	497616	Amphibolite sensu stricto	Amphibole Calcic plagioclase Epidote	Dark w. green and white spots	Fine	Heterogeneous Lineation

Table A7_1 continued. *Rock sample data. Qussuk, central part of peninsula.*

Locality	Sample no.	Rock type	Mineral content	Colour	Grain size	Characteristics
BAN-14	497617	Quartz-garnet-biotite rock	Quartz Garnet <1 cm Biotite Sulphides	Dark	Coarse	Rusty surface Much biotite
	497618	Quartz-garnet-biotite rock	Quartz Biotite Garnet <0.5 cm Sulphides	Dark	Medium	Rusty surface Less biotite than 497617
	497619	Sulphide-rich rock	Sulphides Biotite	Dark		Rusty surface No garnets
	497620	Sulphide-rich rock	Sulphides Biotite	Dark		Rust altered rock No garnets
	497621	Quartz-biotite gneiss	Quartz Biotite Sulphides			Disseminated sulphides + pyrite aggregates No garnet
BAN-15	497622	Quartz-rich rock	Quartz Sulphides	Grey		Rusty surface
BAN-16	497632	Black amphibolite w. light-coloured grains <7 mm	Biotite Andalusite?	Black	Fine	Found next to a granitic intrusive
BAN-17	497633	Dark amphibolite	Biotite Plagioclase	Dark grey	Fine	Massive
	497634	Dark amphibolite	Disseminated sulphides	Dark	Fine	Rust altered rock
	497635	Dark amphibolite	Quartz veins Biotite Disseminated sulphides	Dark grey	Fine	Massive Heterogeneous => Quartz veins <0.5 cm
	497636	Dark amphibolite	Quartz veins Fe-sulphides	Dark	Fine	Quartz veins <3 cm w. Fe-sulphides <0.5 cm in and along veins/grains
	497637	Dark amphibolite	Fe-sulphides Green minerals => tremolite/actinolite?	Dark	Fine	Pyrite aggregates in areas w. green minerals Disseminated sulphides in remaining rock Rusty surface
	497638	Dark amphibolite	Biotite Disseminated sulphides	Dark		Rust altered rock Pyrite aggregate <1.5 cm

Table A7_1 continued. *Rock sample data. Qussuk, central part of peninsula.*

Locality	Sample no.	Rock type	Mineral content	Colour	Grain size	Characteristics
	497639	Garnet amphibolite	Garnet <5mm Disseminated Fe-sulphides	Black	Medium	Porous
	497640	Grey intermediate amphibolite	Disseminated sulphides	Grey	Medium	Rusty surface
	497641	Grey intermediate amphibolite	Biotite Plagioclase	Grey	Medium	
BAN-18	497642	Garnet amphibolite	Garnet 1-15mm	Dark	Medium	Local rusty surface
	497643	Garnet amphibolite	Garnet 1-15mm Quartz veins Sulphides	Dark	Medium	Quartz veins (cm wide) w. sulphides <3mm
BAN-19	497644	Grey intermediate amphibolite	Quartz vein Sulphides <2mm	Light grey	Fine	Rust altered rock
	497645	Dark amphibolite	Biotite	Dark	Fine	
BAN-20	497646	Gabbro		Intermediate Grey/black	Medium	Spotted surface
BAN-21	497647	Dark amphibolite (sensu stricto?)	Hornblende (?) Biotite	Dark	Fine	A 2m wide band in grey intermediate amphibolite
BAN-22	497648	Amphibolite sensu stricto	Hornblende (?)	Dark	Fine	
	497649	Gabbro	Pronounced black grains	Intermediate	Medium-coarse	Spotted surface
BAN-23	497650	Dark amphibolite	Sulphides Light coloured grains	Dark	Fine	Rust altered surface The layer is <20cm wide
	497651	Amphibolite	Disseminated sulphides	Grey	Fine	Same layer as rock no. 497650
	497652	Grey intermediate amphibolite		Grey	Fine-medium	Rust altered rock No visible sulphides Representative for the rust altered zone
	497653	Intermediate rock w. green mineral bands	Light coloured Dark coloured Green minerals	Intermediate	Medium	Fall-out material
BAN-24	497654	Dark amphibolite	Disseminated sulphides	Dark grey	Fine	Rust altered surface
	497655	Dark amphibolite		Black	Fine	Rust altered plane through the rock
	497656	Grey intermediate amphibolite	Zone w. light coloured and green minerals	Intermediate	Medium-coarse	Rust altered surface

Table A7_1 continued. *Rock sample data. Qussuk, central part of peninsula.*

Locality	Sample no.	Rock type	Mineral content	Colour	Grain size	Characteristics
BAN-25		Pyroclastic rock				FALL-OUT MATERIAL
BAN-26	497657	Quartz-biotite rock	Quartz Biotite Fe-sulphides ~5-7mm	Intermediate	Medium-coarse	Rust altered surface and cracks
	497662	Garnet amphibolite	Garnet <0.5cm Sulphides?	Dark	Fine	Massive Rust altered surface
BAN-27						Qussuk's highest point
BAN-28	497658	Quartz-rich rock	Quartz Sulphides < 5mm	Rusty	Coarse	Hard dark centre w. Fe-sulphides in aggregates
BAN-29	497659	Grey intermediate amphibolite	Fe-sulphides <1mm	Dark	Fine	Foliation in lower part of sample w. light coloured layers Rust altered surface
	497660	Dark amphibolite	Fe-sulphides <1mm	Dark	Fine	Disseminated sulphides + aggregates of sulphides following foliation Rust altered surface
BAN-30	497661	Quartz-rich rock	Quartz Biotite Sulphides <2mm (Chalcopyrite ?)	Intermediate	Coarse	Rust altered surface
BAN-31	497663	Garnet amphibolite	Garnet <0.5cm Biotite	Dark	Fine	Rust altered surface Found in a 10m wide zone of dark amphibolite w local garnet
	497664	Grey intermediate amphibolite	Biotite Plagioclase One sulphide grain~1mm	Intermediate	Fine-medium	Rust altered rock sample
	497665	Dark amphibolite		Dark	Fine	From same zone as 497666
	497666	Garnet amphibolite	Garnet <1cm	Dark	Fine	Garnet grains are altered/pseudo-morph
BAN-32	497667	Dark amphibolite	Garnet <0.5cm	Dark	Fine	Rust altered surface

Table A7_1 continued. *Rock sample data. Qussuk, central part of peninsula.*

Locality	Sample no.	Rock type	Mineral content	Colour	Grain size	Characteristics
BAN-33	497668	Dark amphibolite	Quartz aggregate >3cm + vein <2mm	Black	Fine	Foliation
	497669	Dark amphibolite		Dark	Fine	Massive Rust altered surface
BAN-35	497670	Pyroclastic rock		Green	Fine w. bigger grains ~0.5cm	Hydrothermal altered rock w. clasts
	497671	Magnetic, black rock	Magnetite	Black	Fine	Massive Magnetic Few bigger grains~2mm – magnetite?
BAN-36	497672	Coarse-grained, dark rock	Magnetite (?) Pyroxene	Dark	Coarse	Uneven surface – pyroxene grains peep out
BAN-37	497673	Pyroclastic rock		Green	Fine w. bigger grains <0.5cm	Hydrothermal altered rock w. clasts – same as BAN-35 but more distinct layering
	497674	Magnetic, black rock		Black	Fine	In area w. hydrothermal altered rock - layering
BAN-38	497675	Pyroclastic rock		Green	Fine w. bigger grains	Hydrothermal altered rock w. clasts

Table A7_1 continued. *Rock sample data. Qussuk Bay and West Coast of peninsula*

Locality	Sample no.	Rock type	Mineral content	Colour	Grain size	Characteristics
HST225	497676	Grey intermediate amphibolite	Garnet <2mm Tourmaline (?)	Grey	Fine w. medium grained layer of garnet and tourmaline	
	497677	Quartz-tourmaline rock	Quartz Tourmaline layers 1-2cm wide	Grey and black	Quartz – coarse Tourmaline – fine	Quartz originally chert (exhalative)
	497678	Quartz-garnet-biotite gneiss	Quartz Garnet <2mm Biotite		Medium	Foliation 2 hand samples: 1 fresh, 1 rusty Metasediment (?)
	497679	Garnet amphibolite	Garnet <0.5cm Plagioclase Biotite	Dark	Medium	Foliation – few mm-wide plagioclase veins/layers
	497680	Garnet amphibolite	Garnet <4cm Tourmaline Plagioclase Quartz aggregates	Dark	Fine	Layers in grey intermediate amphibolite w. large garnet grains Crosscutting intrusions (granite-pegmatite) 0.5-1cm wide
HST226	497681	Sulphide-bearing exhalite	Quartz Biotite Disseminated Fe-sulphides		Coarse	Massive Rust altered surface Increasing biotite content and decreasing sulphide content towards the top
	497682	Intermediate amphibolite	Plagioclase veins mm-wide	Intermediate	Medium-fine	Spotted
HST227	497683	Dark amphibolite	Biotite Plagioclase	Dark	Medium-fine	Massive Spotted
HST228	497684	Dark amphibolite/ quartz exhalite	Biotite Plagioclase OR quartz (exhalite) Disseminated sulphides <1mm	Dark	Medium-fine	Foliation Rust altered surface

Table A7_1 continued. *Rock sample data. Qussuk Bay and West Coast of peninsula*

Locality	Sample no.	Rock type	Mineral content	Colour	Grain size	Characteristics
HST229	497685	Garnet amphibolite	Garnet <4cm Hornblende (cm) Biotite Calc-silicates (epidotite, diopside)	Black	Coarse	c. 25m wide – many intrusions (granite) ~1m crosscut Uneven surface – garnet + hornblende peep out Cm wide layers of boudinaged calc-silicates
HST230	497686	Quartz-rich rock	Semi-massive sulphides (chalcopyrite + pyrrhotite) Quartz	Rusty	Coarse	
	497687	Biotite-rich rock	Biotite Disseminated Fe-sulphides <1mm	Dark	Fine	Rust altered rock
	497688	Quartz + tourmaline? Rock	Quartz Tourmaline (?) Calc-silicates	Black and white (light coloured)	Coarse	
HST231	497689	Garnet amphibolite	Garnet <4cm	Dark	Medium	Layers with huge garnet grains (up to 10cm) in banded amphibolite

Main objectives

There are several 2 to 3 m wide sulphide mineralised horizons in the area and the main work was concentrated around these sulphide mineralised zones. All of them are NNE-trending. The zones are easily recognised by their characteristic brown-red-yellow rusty colour. The sulphide mineralised zones farthest towards the west of the area contain very small amounts of visible disseminated iron sulphides. The zones in the eastern and north-eastern parts of the area have high content of disseminated iron sulphides and aggregates of iron sulphides. Several zones have a medium to high content of garnet, with grain sizes of this mineral up to several centimetres.

Some attention was drawn to the hydrothermally altered grey intermediate amphibolite and an ultramafic body (Fig. A7_3). It is interpreted that the two rocks belong to the same system, i.e. an emplacement of the ultramafic rock could have happened simultaneously with the hydrothermal alteration of the grey intermediate amphibolite. A detailed E-W trending profile was made across the hydrothermally altered body. This body is interesting because there are, in fact, two different lithologies. One rock is non-magnetic and has many clasts. The other rock is homogenous (i.e. no clasts) and has a varying magnetic content from non-magnetic to extremely magnetic. The non-magnetic clast-filled rock is found where intense hydrothermal alteration has formed calc-silicate minerals (epidote, diopside?) occurring as clasts. The calc-silicate minerals give the rock a green colour. The rock is chemically weathered leaving holes with a brown zone encircling them in the matrix most probably after the calc-silicate minerals. The homogenous rock is found next to the clast-filled rock being non-magnetic closest to the boundary and becoming more and more mag-

netic further away. This rock is most likely an ultramafic rock with different degree of hydrothermal alteration.

At the head of the Qussuk bay the rocks are similar to those at the peninsula. The only true difference is the presence of tourmaline, which was not observed in the central part of the Qussuk peninsula. Tourmaline occurs as layers which are up to 2 cm wide found together with quartz and often garnet. Garnet crystals can be up to 10 cm in size but are generally not more than 4 cm. Besides the multiple garnet amphibolites two 2 to 3 m wide sulphide mineralised zones are present with the characteristic red-brown-yellow rusty colour at the surface (Fig. A7_5).



Figure A7_5. *Sulphide mineralised zone with the characteristic yellow-red colour.*

In the western part of the Qussuk peninsula several sulphide mineralised zones were present. One quartz-rich rock with a rusty weathering surface contained semi-massive chalcocopyrite and pyrrhotite. In a grey intermediate amphibolite thin veins of green minerals (most likely calc-silicates like epidote or diopside) are found equal to the calc-silicate minerals found in the central part of the Qussuk peninsula.

Figure A7_3 shows a detailed map of the central part of the Qussuk peninsula modified after Adam Garde. A large body mapped as amphibolite sensu stricto by Adam Garde is

now mapped mainly as grey intermediate amphibolite with a thin body of amphibolite sensu stricto. An extension of a sulphide mineralised zone south of the lake in the mid-west area has been observed and mapped. The area with the hydrothermally altered rock south of the camp was observed to be larger than it appears on Garde's map and in fact, was also found on the southern side of the ultramafic body. Furthermore the ultramafic body was observed to be a little smaller than shown on Garde's map.

Results

The Qussuk supracrustal belt is interpreted to represent an island-arc complex (Hollis et al. 2004). Nothing was found during fieldwork 2005 to contradict this interpretation. Generally the detailed map and the lithological units described by Garde are found to be correct with a few exceptions already mentioned according to the map. Since no results from laboratory analyses are yet available further work with the collected samples awaits.

Further work

The collected samples will be examined in several ways. Out of 89 collected samples, 63 have been sent for geochemical analyses. Polished thin sections will be made of about 10 samples with the possibility of a few extra samples when the results from the geochemical analyses are known. X-ray powder diffraction and single crystal diffraction will be applied to some of the samples to establish the mineral content of the clasts in the hydrothermal altered rock as well as the mineral content of samples that are very porous.

Appendix 8: Magnetic and geological profiling across the Ataneq fault (Pelle Gulbrandsen)

The aim of the fieldwork was to do a series of ground born magnetic and geological profiles across the Ataneq fault. With the later purpose of determining how the hydrothermal alteration has affected the magnetic minerals (mainly magnetite) in the original rock (tonalites), and how the intensity of the alteration decreases away from the fault zone.

The fieldwork was carried out between the 1st of August and 20th of August 2005, in the SW part of Greenland.

The work was carried out from three camps (Fig. A8_1):

Ataneq 1: N 64 45 050 W 50 48 600 (02-11 of August)

Ataneq 2: N 64 55 400 W 50 26 600 (16-18 of August)

Ataneq 3: N 65 07 182 W 50 14 057 (11-16 of August)

A total of five profiles were done, three from the first camp (Ataneq 1):

Camp 1 profile 1: (Ataneq 1.1)

Camp 1 profile 2: (Ataneq 1.2)

Camp 1 profile 3: (Ataneq 1.3)

One from the second camp (Ataneq 3):

Camp 3 profile 4: (Ataneq 3.4)

And one from the third camp (Ataneq 2):

Camp 2 profile 5: (Ataneq 2.5)

The GPS coordinates (in decimal degrees) for each profile can be seen in Table A8_1, along with the sample numbers and rock descriptions.

Geological mapping and sampling was done in proximity of the profiles. More extensive mapping of the area was carried out for the report by Gorm Thøgersen (Appendix 10).

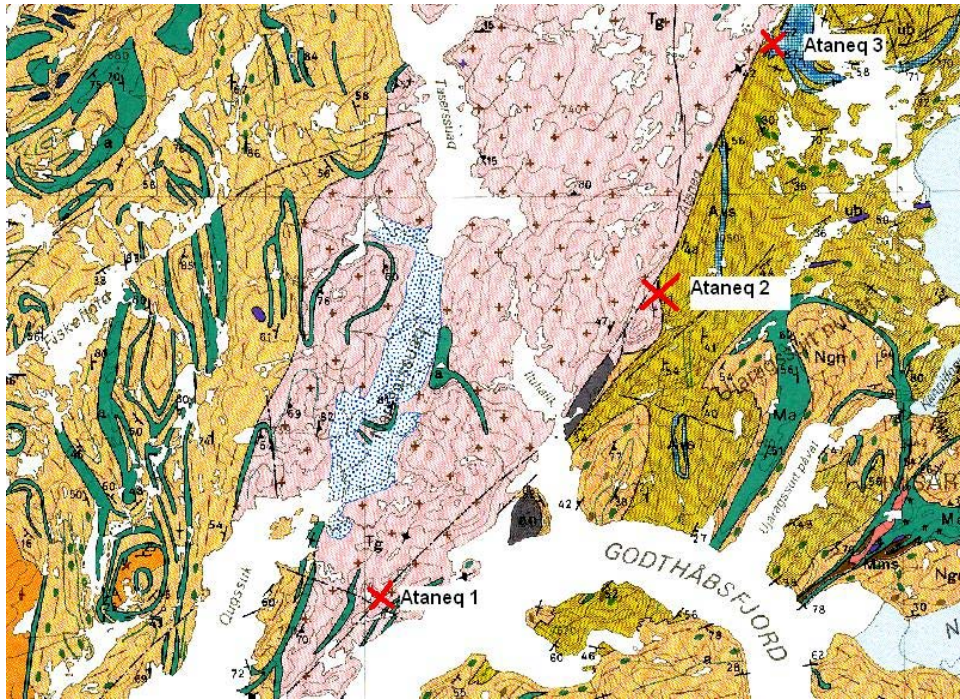


Figure A8_1. A part of the 1:500.000 scale map sheet *Frederikshåb Isblink–Søndre Strømfjord* (Allaart 1982). The entire fault zone from Ataneq 1 to Ataneq 3 is for the purpose of this report referred to as the Ataneq fault. Other texts may refer to the northern stretch of the fault zone as being part of the Ivinnguit fault.

Geological setting

The Ataneq fault is situated in the NE part of the Precambrian shield of the Godthåbsfjord region (1:100,000 scale map sheets Ivisârtoq 64 V.2 Nord and Isukasia 65 V.2 Syd).

The Ataneq fault, which is presumably Palaeoproterozoic in age, is characterised by extensive hydrothermal alteration of the host rock (tonalites; Appel et al. 2004). The alteration zone varies in width from about 500 m to 1000 m. The fault itself is mostly filled with boulders and sediments, but at the sides of the fault and on the plateau above it (Fig. A8_2), exposure is good.

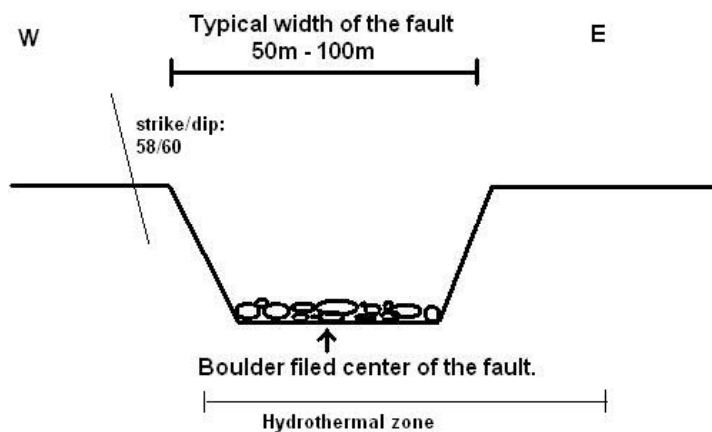


Figure A8_2. Typical cross-section of the Ataneq fault.

Most of the rocks within the alteration zone are thoroughly silicified and they have a fine-grained sugary texture dominated by milky quartz (Hollis et al. 2004). The quartz is in some places coloured green by epidote. Also red colouring (hematitisation) of the silicified rocks is seen along some fractures (Fig. A8_3; Appel et al. 2004).



Figure A8_3. Red colouring of silicified tonalite at Ataneq 1.1, locality 3.

Method

The geological/magnetic profiles were chosen with concern to good exposure and in particular accessibility, since the magnetometer was fairly heavy. Flags were set at appropriate intervals along the profiles. They were used to aim at, when walking with the magnetometer.

GPS positions were taken at each flag, and these positions were named as localities (i.e. the first flag, at the start of Ataneq 1.1 would be named locality 1, the next locality 2, and so on). Additional localities between two flags were named, locality number B (i.e. a locality between locality 3 and 4 would be named locality 3B). The geological mapping was done through observations and sample collection (see fig. A8_4, bottom).

The magnetic measurements were done using the G-858 magnetometer from geometrics. For each profile it was set to measure the vertical gradient. Before doing each profile, a base magnetometer was set up as well. For this the G-856 magnetometer from geometrics was used. The base magnetometer measured the variations in the total magnetic field. These values could then later be subtracted from the profile measurements, giving the actual magnetic properties of the profile rocks.

In Fig. A8_4 the magnetic measurements, along with the geological observations of the profiles can be seen. Additionally susceptibility and relative height measurements were done.

Results

The results from the geological and magnetic measurements have been summarised in the following figures (Fig. A8_4). The geological and the magnetic profiles are not precisely imposed on top of each other (e.g. locality 1 in the magnetic profile is not directly above locality 1 in the geological profile, they are a bit offset from each other).

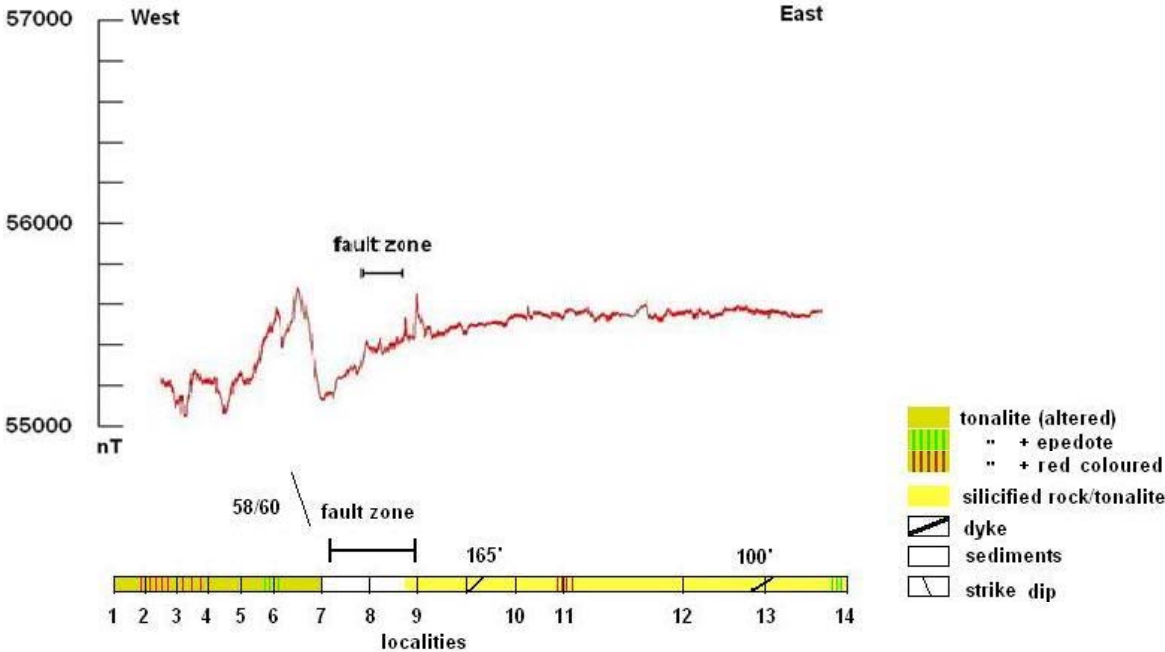


Figure A8_4a. Magnetic (top) and geological (bottom) profile of Ataneq 1.1.

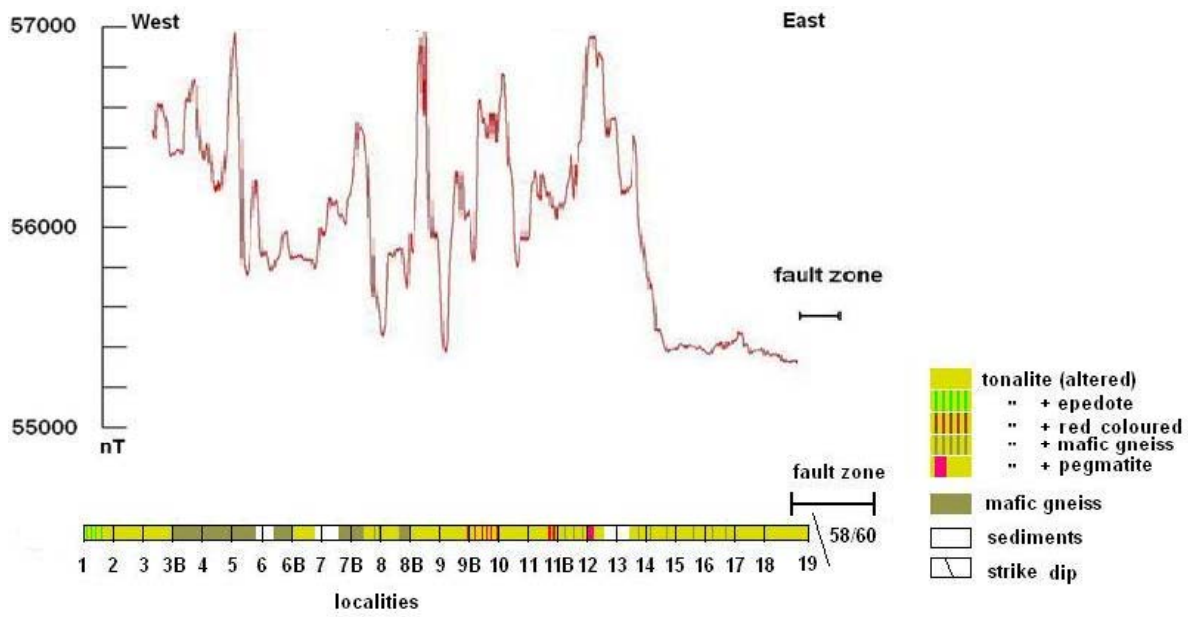


Figure A8_4b. Magnetic (top) and geological (bottom) profile of Ataneq 1.2.

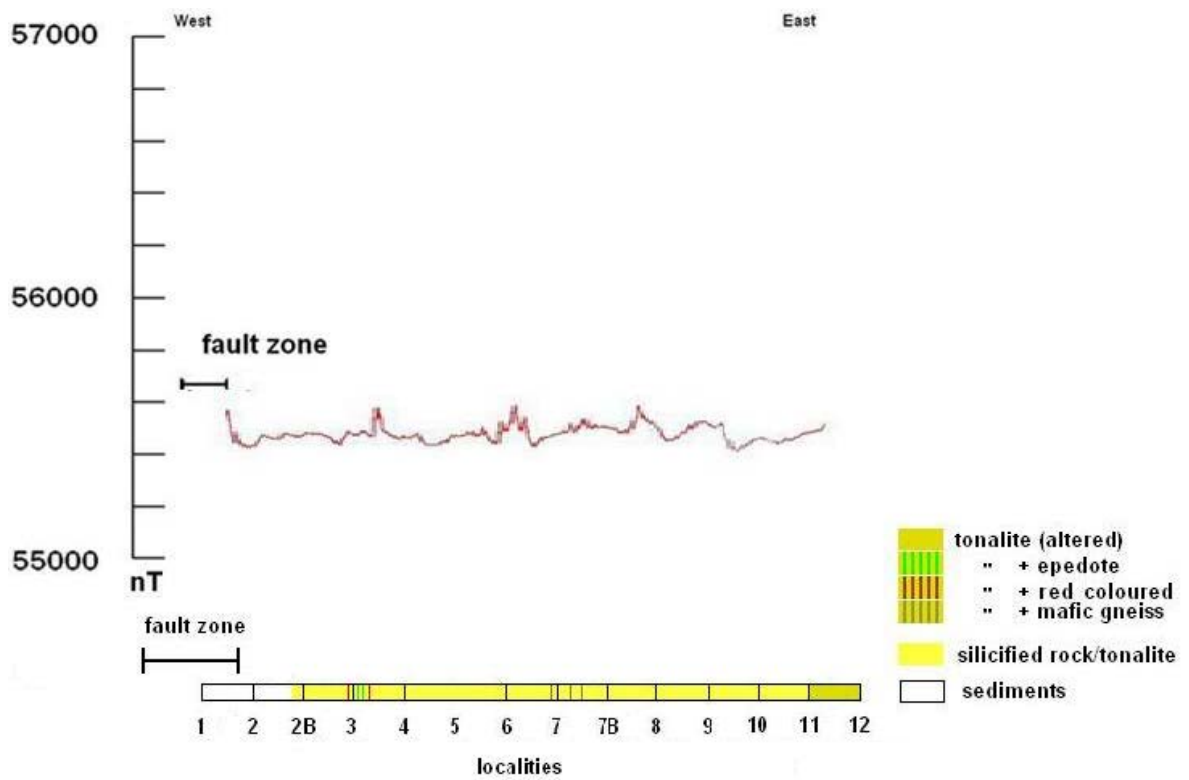


Figure A8_4c. Magnetic (top) and geological (bottom) profile of Ataneq 1.3.

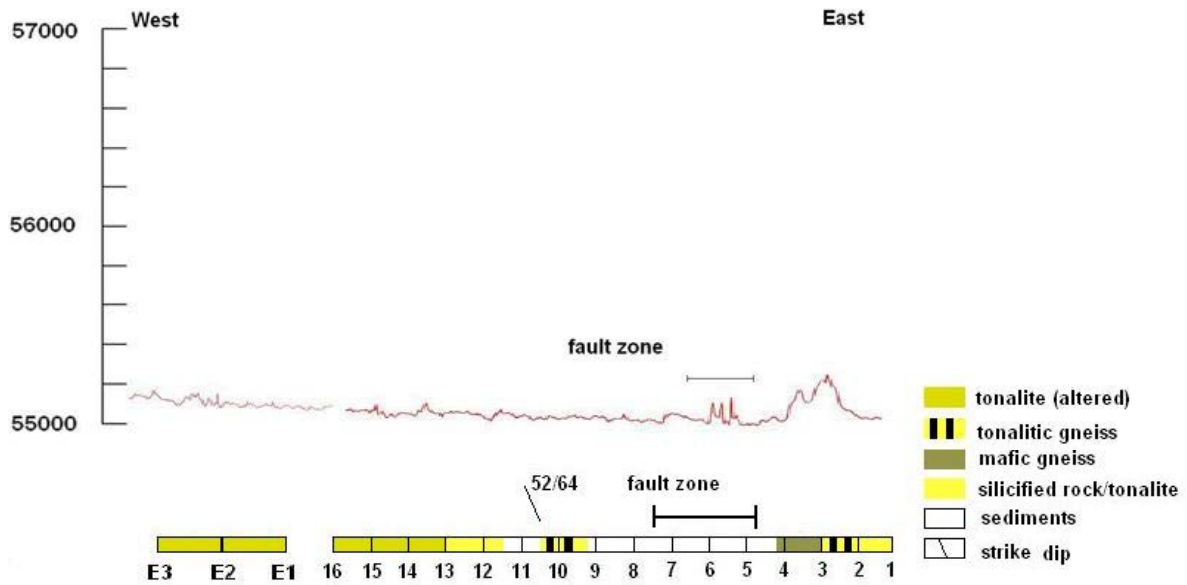


Figure A8_4d. Magnetic (top) and geological (bottom) profile of Ataneq 3.4.

Profile on the left is Ataneq 3.4 extra and the profile on the right is Ataneq 3.4.

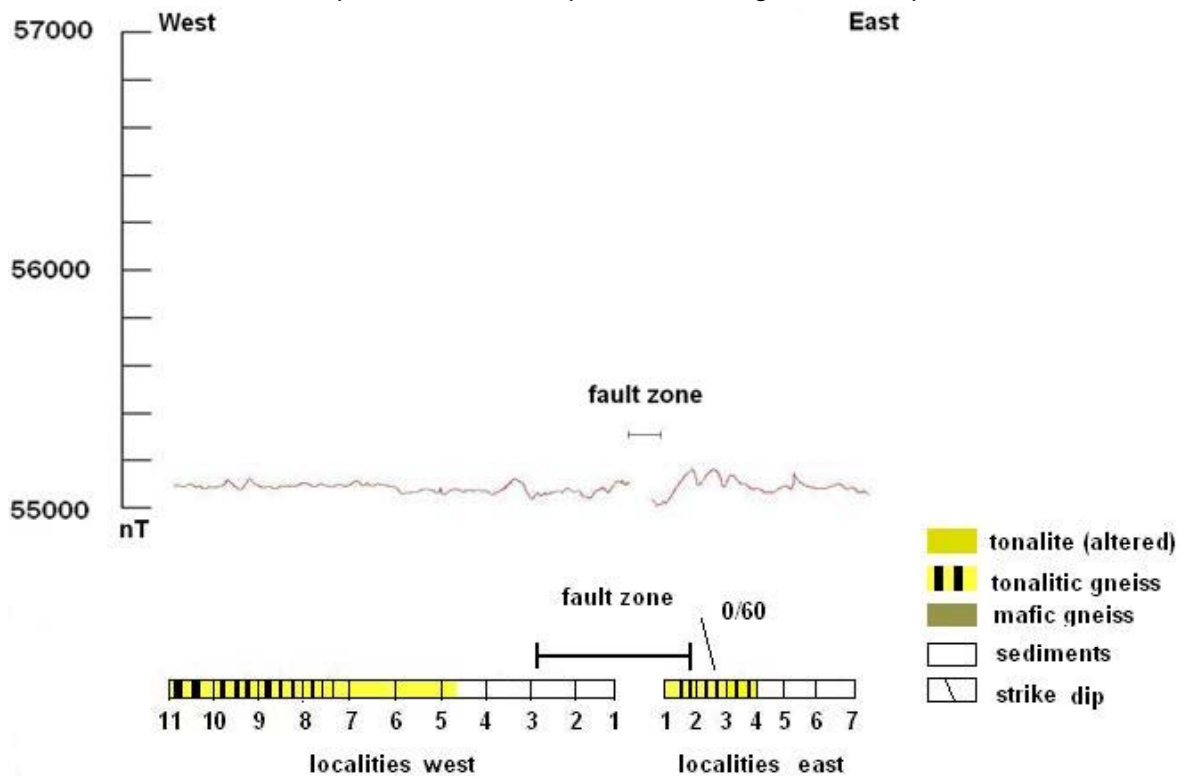


Figure A8_4e. Magnetic (top) and geological (bottom) profile of Ataneq 2.5. Profile on the left is Ataneq 2.5 West and the profile on the right is Ataneq 2.5 East.

Observations and conclusion

A list of all the samples collected can be seen in Table A8_1. In general, most of the rock observed was thoroughly silicified. The host rock was mostly tonalite or tonalitic gneiss. A few mafic lenses and dykes, ranging in width from about 5 cm to c. 5 m, were observed, as were a few areas with a fine grained dark gneiss (mafic gneiss).

It can be seen in the magnetic data, that the fault zone is represented by low magnetic properties. In most of the measurements the value in the fault is around 55000 nT. In some places high narrow spikes can be seen in the data (see Fig. A8_4), a narrow spike could mean that what causes the spike is close to the surface. The three narrow spikes in the fault zone at Ataneq 3.4 (see Fig. A8_4d) could be boulders.

In general, the magnetic properties of the rocks, increases away from the fault zone. It can be seen in all the profiles but profile 1.3 (see Fig. A8_4c), but is most obvious in profile Ataneq 1.1 (see Fig. A8_4a). The fact that the lowest magnetic point is located a little to the left of the fault zone (in profile 1) could be caused by the fault dip towards the northeast.

At a first glance there seems to be a good correlation between geological features and magnetic properties. Areas with tonalites have higher magnetic properties than the thoroughly silicified areas. And geological features like the pegmatite in Ataneq 1.2 have very high magnetic properties.

In future, work data and samples will be used in order to determine how the hydrothermal alteration has affected the magnetic minerals (mainly magnetite) in the original rock, and how the intensity of the alteration decreases away from the fault zone.

Table A8_1. List of all GPS positions and samples. Explanation: Ataneq (1.2) means, Campsite Ataneq 1, profile 2. Ataneq (3.4) means, campsite Ataneq 3, profile 4 (see start of report for further explanation). Localities 1, 2, 3 are the original flags for the geological/magnetic profile, localities with B (e.g. Locality 3B, would be a position between locality 3 and locality 4) are extra localities which were done if anything exciting showed up.

Locality	GPS		Sample nr.	Rock description
	N	W		
Ataneq(1,1)				
1	64,74895	-50,816829	497901	Altered tonalite (silicified)
2	64,7489	-50,816626	497902	Red coloured silicified tonalite
3	64,74885	-50,816384		
4	64,7488	-50,815912		
5	64,74869	-50,815488		
6	64,74857	-50,815094		
7	64,74828	-50,81493		
8	64,74807	-50,814631		
9	64,74772	-50,814508	497903	Heavily altered tonalite (silicified)
9B	64,74744	-50,813546	497904	Mafic dyke
10	64,74748	-50,814519	497905	Red coloured silicified tonalite
11	64,74706	-50,814204		
12	64,74635	-50,813399		
13	64,74607	-50,812502	497906+07	06=Mafic dyke, 07=silicified tonalite
14	64,74577	-50,811831	497908	Silicified tonalite

Table A8_1 continued. List of all GPS positions and samples. Explanation: Ataneq (1.2) means, Campsite Ataneq 1, profile 2. Ataneq (3.4) means, campsite Ataneq 3, profile 4 (see start of report for further explanation). Localities 1, 2, 3 are the original flags for the geological/magnetic profile, localities with B (e.g. Locality 3B, would be a position between locality 3 and locality 4) are extra localities which were done if anything exciting showed up.

Locality	GPS		Sample nr.	Rock description
	N	W		
Ataneq(1,2)				
1	64,75191	-50,804797	497909	Heavily altered tonalite (silicified)
2	64,75192	-50,804798		
3	64,75206	-50,804926		
3B	64,75231	-50,804621		
4	64,75235	-50,804926	497910	Fine-grained, dark Gneiss with quartz-
5	64,75247	-50,80502	497911	Fine-grained, dark Gneiss
6	64,75268	-50,805212		
6B	64,7528	-50,805064	497912	Altered tonalite
7	64,75294	-50,805433		
7B	64,753	-50,805596	497913	Fine-grained, dark Gneiss
8	64,7532	-50,805677		
8B	64,75329	-50,806162	497914	Fine-grained, dark Gneiss
9	64,75343	-50,805357		
9B	64,75363	-50,805294	494715	Red-coloured tonalite (silicified)
10	64,75365	-50,80526		
11	64,75382	-50,805466		
11B	64,75379	-50,80652	497918	Heavily red-coloured tonalite (silicified)
12	64,75418	-50,805651	497916	Coarse-grained quartz-vein with mag-
13	64,7544	-50,805858		
14	64,75468	-50,806268		
15	64,755	-50,80666		
16	64,75525	-50,806878		
17	64,75552	-50,807175		
18	64,75573	-50,807432	497917	Altered tonalite
19	64,75602	-50,80779		

Table A8_1 continued. *List of all GPS positions and samples. Explanation: Ataneq (1.2) means, Campsite Ataneq 1, profile 2. Ataneq (3.4) means, campsite Ataneq 3, profile 4 (see start of report for further explanation). Localities 1, 2, 3 are the original flags for the geological/magnetic profile, localities with B (e.g. Locality 3B, would be a position between locality 3 and locality 4) are extra localities which were done if anything exciting showed up.*

Locality	GPS		Sample nr.	Rock description
	N	W		
Ataneq(1,3)	N	W		
1	64,75813	-50,785481		
2	64,75796	-50,785286		
2B	64,75785	-50,785118		
3	64,75781	-50,784917	497919	Altered tonalite (silicified)
4	64,75758	-50,784666		
5	64,75722	-50,784195		
6	64,75699	-50,784235		
7	64,75679	-50,783965		
7B	64,7567	-50,783873	497920	Altered tonalite (silicified)
8	64,75659	-50,78378		
9	64,75646	-50,783706		
10	64,75641	-50,78326		
11	64,75643	-50,782876		
12	64,75632	-50,782553		

Table A8_1 continued. List of all GPS positions and samples. Explanation: Ataneq (1.2) means, Campsite Ataneq 1, profile 2. Ataneq (3.4) means, campsite Ataneq 3, profile 4 (see start of report for further explanation). Localities 1, 2, 3 are the original flags for the geological/magnetic profile, localities with B (e.g. Locality 3B, would be a position between locality 3 and locality 4) are extra localities which were done if anything exciting showed up.

Locality	GPS		Sample	Rock description
	N	W	nr.	
Ataneq(2,5)				
west 1	64,92228	-50,443759	4979-29-30-31	3 rock samples: altered tonalite (silicified) amphibolites? And dark Gneiss
west 2	64,92218	-50,444053		
west 3	64,92196	-50,444269		
west 4	64,92182	-50,444089		
west 5	64,92146	-50,445176		
west 6	64,92137	-50,445473		
west 7	64,92118	-50,445996		
west 8	64,92127	-50,446124		
west 9	64,921	-50,446514		
west 10	64,92094	-50,446917		
west 11	64,92073	-50,447362	497932	Pale silicified gneiss
east 1	64,922	-50,443232	497933	Clearly pale dark banded gneiss
east 2	64,92206	-50,442798		
east 3	64,92222	-50,442637		
east 4	64,92223	-50,442278		
east 5	64,92218	-50,442132		
east 6	64,92204	-50,441769		
east 7	64,92193	-50,441606		

Table A8_1 continued. List of all GPS positions and samples. Explanation: Ataneq (1.2) means, Campsite Ataneq 1, profile 2. Ataneq (3.4) means, campsite Ataneq 3, profile 4 (see start of report for further explanation). Localities 1, 2, 3 are the original flags for the geological/magnetic profile, localities with B (e.g. Locality 3B, would be a position between locality 3 and locality 4) are extra localities which were done if anything exciting showed up.

Locality	GPS		Sample nr.	Rock description
	N	W		
Ataneq(3,4)	N	W		
1	65,11785	-50,243116		
2	65,11767	-50,243743	497926	
3	65,11767	-50,244355	4979-24- 25-27	(24)Fine grained quartzitic rock (25) Dark gneiss with green alteration (epi-dote) (27) a rock sample from a rust zone
4	65,11761	-50,244798	497923	Fine-grained, dark Gneiss
5	65,11755	-50,245649		
6	65,11759	-50,246149		
7	65,11767	-50,246473		
8	65,11766	-50,246802		
9	65,11775	-50,247019		
10	65,11797	-50,247613		
11	65,11802	-50,248313		
12	65,11801	-50,249447		
13	65,11818	-50,249943	497922	Silicified tonalite
14	65,11826	-50,250837		
15	65,11838	-50,251538		
16	65,11872	-50,251544	497921	Silicified tonalite
Ataneq(3,4) Extra 1	65,11933	-50,252896		
Ataneq(3,4) Extra 2	65,12014	-50,25672	497928	Medium grained tonalitic rock
Ataneq(3,4) Extra 3	65,12106	-50,257052		

Appendix 9: A geological and geochemical interpretation of mafic and ultramafic rocks and their economic mineral potential, Fiskefjord region, southern West Greenland (Tine Kristensen)

This project is a collaboration between GEUS and the Department of Earth Science, Aarhus University, and is part of the GEUS Hydrothermal project, Nuuk 2005. The project forms the basis for a speciale (cand.scient.) at Aarhus University under the joint supervision of Henrik Stendal and J. Richard Wilson. Fieldwork was carried out in July and August 2005. The aim of the fieldwork was to investigate the geological setting and evolution of supracrustal belts with respect to their economic mineral potential in two areas in the Fiskefjord region (Fig. A9_1). The main target was to map the two areas and collect samples for further investigations. A total of 49 samples (1 kg hand specimens for geochemical investigations) were collected (Table A9_1 + Fig. A9_2 + Fig. A9_3).

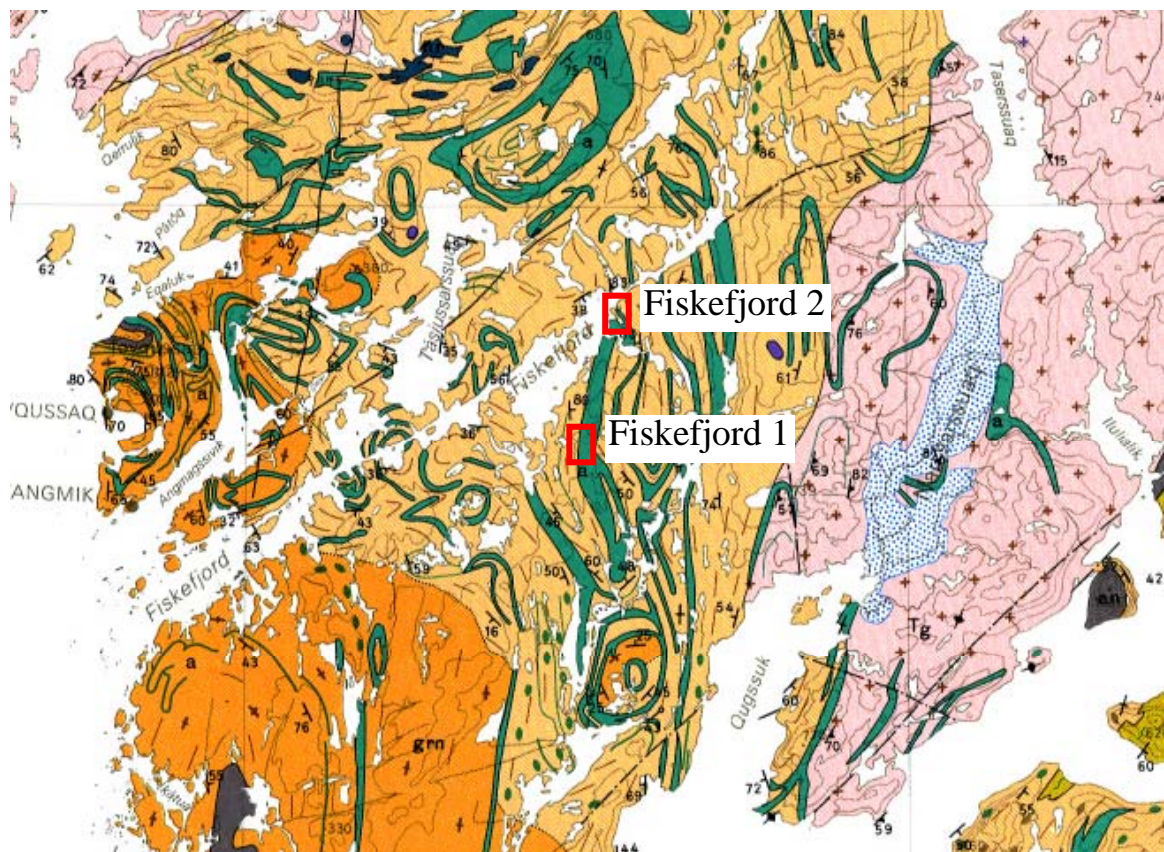


Figure A9_1. Geological overview map of the Fiskefjord region. The locations of the two investigated areas are shown (modified from Allart 1982).

Table A9_1. *Description of collected samples in the Fiskefjord 1 and Fiskefjord 2 areas.*

Sample	Locality	UTM E	UTM N	Locality	Description	1H	1C-EXP 2
497801	TIK001	476981E	7189232	Fiskefjord 1	Rusty amphibolite	x	x
497802	TIK002	476812E	7189587	Fiskefjord 1	Peridotite with chrom-diopside and magnetite banding	x	x
497803	TIK002	476812E	7189587	Fiskefjord 1	Peridotite/dunite		
497804	TIK003	476781E	7189661	Fiskefjord 1	Pyroxenite		
497805	TIK004	476811E	7189675	Fiskefjord 1	Ultramafic mica schist with fuchsite		
497806	TIK007	476546E	7190366	Fiskefjord 1	Dark, homogeneous gabbro/amphibolite		
497807	TIK008	476637E	7190613	Fiskefjord 1	Banded amphibolite		
497808	TIK009	476677E	7190630	Fiskefjord 1	Dark, homogeneous orthomagmatic amphibolite		
497809	TIK010	477861E	7188480	Fiskefjord 1	Rust band with disseminated sulphides in banded amphibolite	x	x
497810	TIK011	478052E	7187939	Fiskefjord 1	Banded amphibolite	x	x
497811	TIK013	477792E	7187499	Fiskefjord 1	High-strain gneiss with quartz pegmatites	x	x
497812	TIK015	477820E	7187676	Fiskefjord 1	Dark peridotite with disseminated sulphides	x	x
497813	TIK017	478070E	7188932	Fiskefjord 1	Massive banded amphibolite	x	x
497814	TIK020	477221E	7188722	Fiskefjord 1	Dark, massive norite	x	x
497815	TIK020	477221E	7188722	Fiskefjord 1	Dark norite		
497816	TIK047	476978E	7188681	Fiskefjord 1	Rust band in norite with disseminated sulphides and chromite	x	x
497817	TIK051	476735E	7189094	Fiskefjord 1	Peridotite with magnetite/chromite and fuchsite	x	x
497818	TIK021	476989E	7188575	Fiskefjord 1	Norite		
497819	TIK069	477346E	7188726	Fiskefjord 1	Dark, banded amphibolite		
497820	TIK073	476857E	7189095	Fiskefjord 1	Peridotite with magnetite/chromite	x	x
497821	TIK074	476762E	7189028	Fiskefjord 1	Norite		
497822	TIK075	476704E	7189050	Fiskefjord 1	Light, banded amphibolite		
497823	TIK077	477103E	7188554	Fiskefjord 1	Dark norite/pyroxenite	x	x
497824	TIK078	477017E	7188622	Fiskefjord 1	High-strain norite with bands of magnetite	x	x
497825	TIK081	476993E	7188652	Fiskefjord 1	Norite with bands of magnetite	x	x
497826	TIK081	476993E	7188652	Fiskefjord 1	Norite with bands of magnetite	x	x
497827	TIK084	477373E	7188808	Fiskefjord 1	Dark, homogeneous amphibolite with bands of rust	x	x
497828	TIK085	477444E	7188760	Fiskefjord 1	Homogeneous amphibolite		
497829	TIK086	479851E	7200473	Fiskefjord 2	Rust band with disseminated sulphides in norite	x	x
497830	TIK087	479822E	7200547	Fiskefjord 2	Rust band with disseminated sulphides in high-strain norite	x	x
497831	TIK091	479730E	7200769	Fiskefjord 2	Rust band with disseminated sulphides in dark, banded norite	x	x
497832	TIK101	479693E	7200697	Fiskefjord 2	Dark norite	x	x
497833	TIK108	479586E	7201134	Fiskefjord 2	Peridotite/dunite with magnetite/chromite	x	x
497834	TIK107	479560E	7201114	Fiskefjord 2	Light norite		
497835	TIK109	479720E	7200848	Fiskefjord 2	Rusty metasediment with garnet	x	x
497836	TIK092	479661E	7200486	Fiskefjord 2	Rust band with disseminated sulphides in dark, banded	x	x
497837	TIK096	479820E	7200449	Fiskefjord 2	Brown, coarse-grained pyroxenite		
497838	TIK111	480040E	7200417	Fiskefjord 2	Fine-grained peridotite with magnetite/chromite	x	x
497839	TIK112	480021E	7200542	Fiskefjord 2	Fine-grained peridotite with magnetite/chromite and chrom-	x	x
497840	TIK113	479709E	7200818	Fiskefjord 2	Rust band with disseminated sulphides in dark, banded norite	x	x
497841	TIK114	479652E	7200930	Fiskefjord 2	Homogeneous amphibolite		
497842	TIK108	479586E	7201134	Fiskefjord 2	Peridotite		
497843	TIK118	479933E	7200672	Fiskefjord 2	Rust band with magnetite in dark norite	x	x
497844	TIK119	480031E	7200597	Fiskefjord 2	Rust band with magnetite in dark, banded norite	x	x
497845	TIK120	479870E	7200338	Fiskefjord 2	Rust band with disseminated sulphides in banded norite	x	x
497846	TIK122	479712E	7199981	Fiskefjord 2	Banded amphibolite with garnet and magnetite	x	x
497847	TIK123	479745E	7199976	Fiskefjord 2	Rust band in dark amphibolite with magnetite	x	x
497848	TIK123	479745E	7199976	Fiskefjord 2	Banded amphibolite	x	x
497849	TIK124	479780E	7200513	Fiskefjord 2	Light norite	x	x

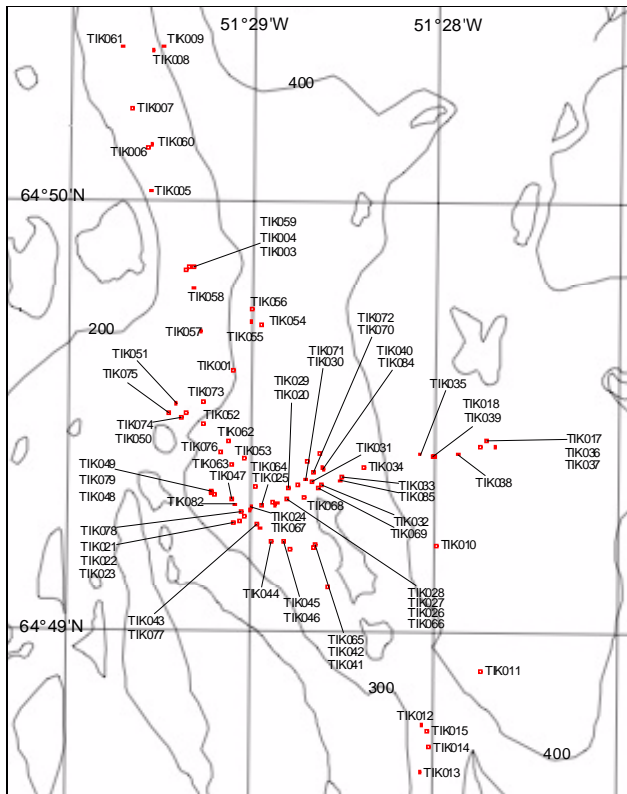


Figure A9_2. Localities in the Fiskefjord 1 area (TIK001-085).

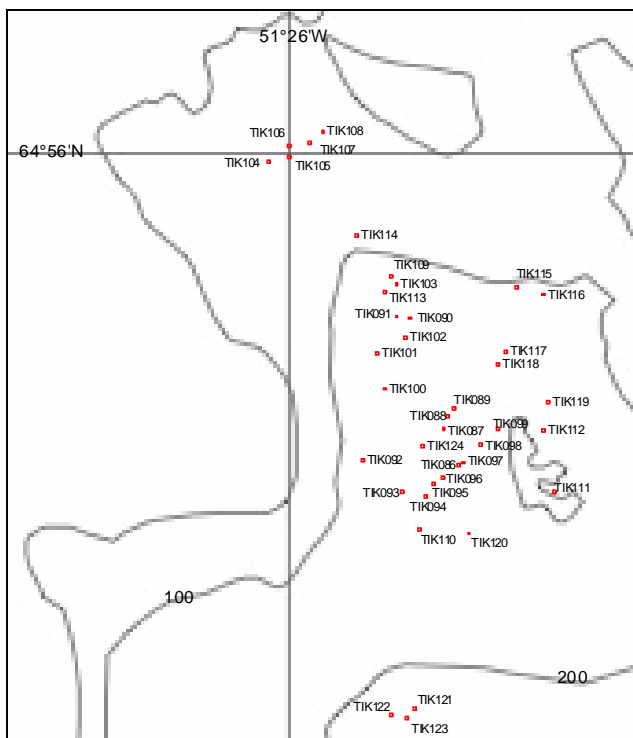


Figure A9_3. Localities in the Fiskefjord 2 area (TIK086-124).

Samples and analyses from fieldwork in the area in 2004 indicate that the ultramafic to mafic rock sequence in the area represents fragments of a layered intrusion with high contents of Cr, Mg and Ni (Appel et al. 2005). The area was previously studied by Garde (1997) in a regional context.

Geologically the Fiskefjord region is located in the c. 3.2 to 2.97 Ga Akia tectonostratigraphic terrane of southern West Greenland. The Akia terrane comprises a supracrustal association that forms layers and enclaves in grey orthogneiss. Homogeneous amphibolite associated with cumulate noritic and dunitic rocks represent fragments of layered complexes. Heterogeneous amphibolite, (basaltic) andesitic amphibolite, leucogabbro-anorthosite and minor pelitic metasediments also occur. The grey orthogneiss belongs to the tonalite–trondhjemite–granodiorite (TTG) association. They were generated during continental accretion at around 3000 Ma. Most of the dioritic gneiss is c. 220 Ma older. Intense deformation and metamorphism accompanied the 3000 Ma magmatic accretion and obscured the primary origin of the supracrustal association (Garde 1997).

Fiskefjord 1 area

The study in the Fiskefjord 1 area was carried out around N 64°49.054' and W 051°28.356' at ~300 m elevation. The area covers about 8 km² (Fig. A9_4; Table A9_1). The focus was an ultramafic to mafic sequence including peridotite, norite and amphibolite. The ultramafic bodies in the Fiskefjord 1 area are mainly peridotites, with some very olivine-rich sections where olivine sand is present. They have a characteristic brown alteration colour and some of the bodies are cut by pyroxenite veins of cm-size. The bodies are up to 50 m wide and can be followed for over 2 km along strike in a N-S direction (Fig. A9_5). The dip is close to vertical. The peridotite bodies are commonly relatively fine-grained in the centre and grade into a more coarse-grained variety toward the margin. In addition to olivine and pyroxene the peridotites also contain fuchsite, magnetite and chromite. Some of the ultramafic bodies show modal layering on a cm-scale. An interesting feature is that most of the bodies are only magnetic (due to magnetite) on one side, varying between east and west. The transition from peridotite to norite is characterised by a coarse-grained pyroxenite. The peridotite becomes more coarse-grained toward the norite and there is locally a gradual development in grain size and mineralogy in the norite. The contact is probably of magmatic origin. The norites are medium- to coarse-grained and crumble easily. They are generally homogeneous but some show local modal layering of cm-size. The norites vary in colour from pale to dark grey. The transition from norite to amphibolite is mainly characterised by sharp contacts, but gradual transitions are also observed. The norites change from being crumbly near the contact with the ultramafic bodies to being more massive at the contact with the amphibolites. Locally the norites are banded in the transition to banded amphibolite. There are two kinds of amphibolite in the Fiskefjord 1 area: homogeneous amphibolites and banded amphibolites. The homogeneous amphibolites are black, massive and fine-grained. The banded amphibolites are typically medium-grained and vary in colour from very dark to pale grey. They are cut by up to 25 cm-thick plagioclase-rich veins and are locally intruded by granitic veins. The banded amphibolites are often crumbly and strongly weathered. Some of the amphibolites are magnetic due to magnetite. Isoclinal folds are developed in some of the amphibolites. A medium-grained garnet biotite gneiss, up to 50 m wide, can be

followed over more than one kilometre in the Fiskefjord 1 area. The gneiss is strongly foliated and is cut by granitic pegmatitic veins.

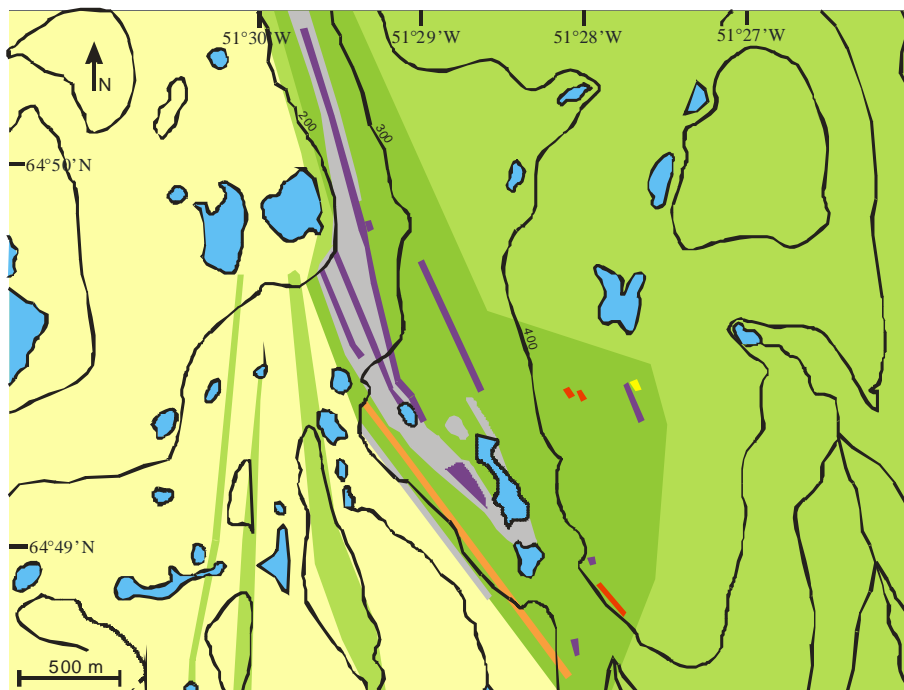
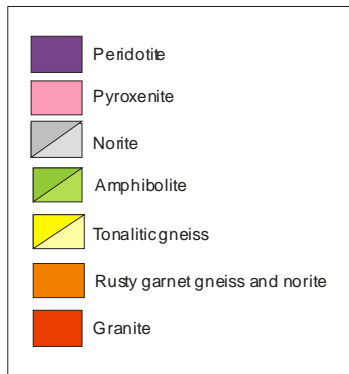


Figure A9_4. Detail of the geological map of a supracrustal belt in the Fiskefjord 1 area.



Figure A9_5. *Ultramafic body (rusty rocks) in the northern part of the Fiskefjord 1 area. The light grey rocks are norite. The dark grey rocks are amphibolite.*

Fiskefjord 2 area

The Fiskefjord 2 area is located at N 64°55.688' and W 051°25.657' at ~125 m elevation. The size of the area is about 0.5 km² (Fig. A9_6: Table A9_1). The focus in this area was an ultramafic to mafic sequence corresponding to the sequence in the Fiskefjord 1 area. The ultramafic bodies in the Fiskefjord 2 area are also mainly peridotites. They are fine- to medium-grained and olivine sand is locally present. In the centre of the largest ultramafic body the peridotite weathers in aggregates, probably reflecting the presence of large pyroxene oikocrysts. The ultramafic bodies are all magnetic (due to magnetite) on the west side but not on the east side. Stratabound pyroxenite is present on either one or both margins of the peridotites. The pyroxenite is brown, medium- to coarse-grained and weathers in aggregates. The pyroxenite is always located between peridotite and norite or between two norites. The transition from pyroxenite to norite is locally marked by a sharp boundary but elsewhere there is a gradation from crumbly to massive norite and a gradual change in the mineralogical composition. There are two kinds of norite in the Fiskefjord 2 area. One is dark grey, medium-grained, banded and magnetic in zones. The other is pale grey, medium- to coarse-grained and crumbles easily. The norite is generally homogeneous but, in connection with the pyroxenite in contact with the largest ultramafic body, it is banded and folded, pyroxenes are concentrated in streaks and there are large lenses that are rich in biotite and pyroxene. The transition from norite to amphibolite is mainly sharp. There are three different kinds of amphibolite in the Fiskefjord 2 area. One is black, medium-grained, homogeneous and crumbles readily. The other is pale grey, banded, magnetic and cut by pegmatite veins. These two types of amphibolite are similar to those in the Fiskefjord 1

area. The third kind of amphibolite, only found in the Fiskefjord 2 area, is banded, fine- to medium-grained and strongly magnetic. It contains garnet and is cut by veins of an unidentified white mineral. Folds are also present. A garnetiferous gneiss is also present in the Fiskefjord 2 area. The gneiss is fine- to medium-grained, rusty and weathered.

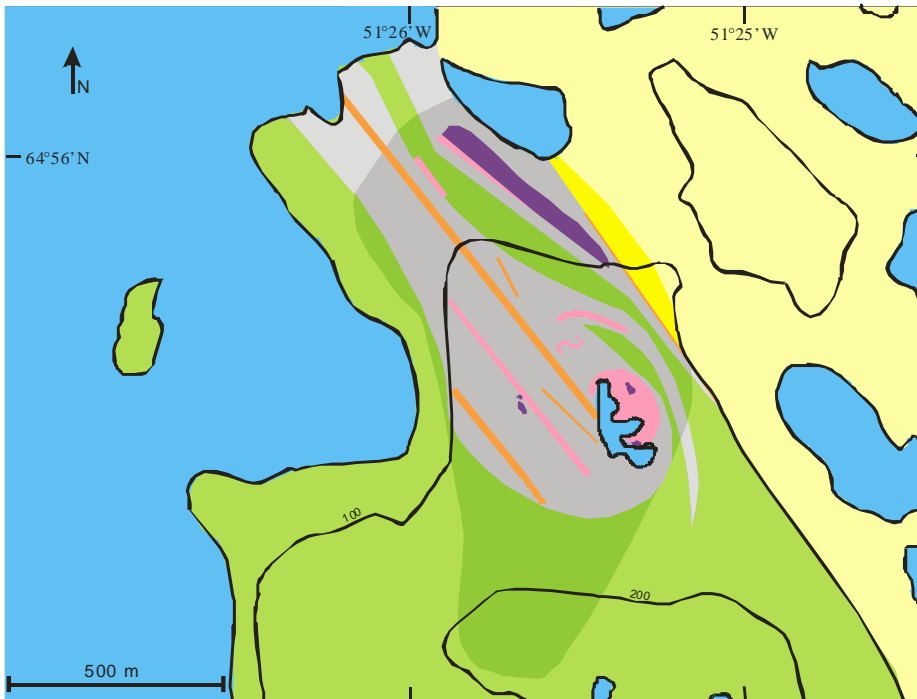
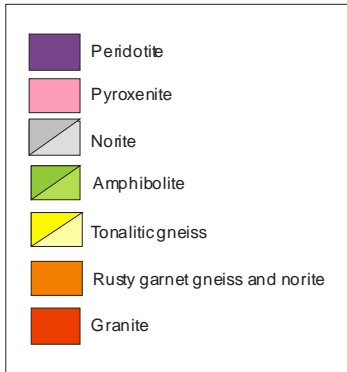


Figure A9_6. *Detail geological map of a supracrustal belt in the Fiskefjord 2 area.*

Sulphide mineralisation

The norites and amphibolites in both the Fiskefjord 1 and 2 areas contain several rusty bands (20 to 40 cm thick) or zones of disseminated sulphides. The sulphides are typically pyrite but chalcopyrite and pyrrhotite are also observed. The sulphide-mineralised zones seem to be associated with dark grey, medium-grained banded norite and amphibolite. In the Fiskefjord 2 area disseminated sulphides also occur in a rusty band (2 m thick) in the garnetiferous gneiss.

It seems likely that the mafic and ultramafic rocks in the Fiskefjord region represent a layered intrusion and one of the main aims is to find out whether or not this is true. In this context it is important to establish the role of the amphibolitic unit(s). The mafic precursor must either have been basaltic/gabbroic rocks unrelated to the peridotites and norites or represent gabbroic rocks in a peridotite - norite - gabbro sequence. In the latter case the question arises as to why the gabbros are far more extensively metamorphosed than the peridotites and norites.

Another main aim is to examine the mineralisations with respect to their economic potential and find out how they were formed. Samples from previous fieldwork in the Fiskefjord 1 area (Appel et al. 2005) show enhanced values of copper and nickel in the mafic rocks with 0.1 to 0.2% Cu and up to 0.12% Ni. The ultramafic rocks show high contents of Cr, Mg and Ni with 0.24 to 1.27% Cr, up to 26% Mg and up to 0.31% Ni. The geological environment indicates that PGE-metals may be present and sediment samples from the southern Fiskefjord area taken by NunaMinerals A/S in 2005 show enhanced values of platinum. The sulphur content is under 1% S in most of the samples. It is most likely that the sulphide mineralisations formed by one or more hydrothermal events.

Future work will be concentrated on petrographic investigation of the rocks together with mineral chemical (microprobe) analyses and whole rock chemical (XRF) analyses.

Appendix 10: Ataneq fault – hydrothermal alterations (Gorm J.-P. Thøgersen)

Introduction

This report gives an overview on fieldwork carried out by GEUS around the Ataneq fault, Godthåbsfjord region, West Greenland - summer 2005. Two GEUS teams were involved in this work: (1) Gorm J-P Thøgersen & Britt Andreasen and (2) Pelle Gulbrandsen & Lizette Apel Jensen (see Gulbrandsen Appendix this report). The first team mapped, described and sampled rocks at and around the Ataneq fault paying special attention to possible mineralisation along the fault zone. The second team collected geophysical magnetic data. Along. The fieldwork was concentrated on three locations along the Ataneq fault Fig. A9_1). The coordinates of the study areas are:

- Ataneq 1, N. 64°44'934; W. 050°48'647, altitude: 687 metres.
- Ataneq 2, N. 64°55; W. 050°26
- Ataneq 3, N. 65°07'204; W. 050°14'024, altitude: 694 metres.

At each of these locations, field observations were carried out within a perimeter of two kilometres. The most detailed study concerns Ataneq 1. The investigations of 29 samples from this very area constitute the main part of my M.Sc. project begun last year. The 2005 field work is an extension of this project. Work at Ataneq 2 and 3 was less detailed.

The geological setting

Regional geology

Geologically, Greenland can be subdivided into: 1) infracrustal regions, 2) supracrustal regions, 3) magmatic provinces and 4) sedimentary basin regions (Stendal et al. 2005). The Godthåbsfjord region mainly consists mainly of infracrustal rocks 2600-3700 Ma old intercalated with minor supracrustal belts. The lithology constitutes mainly of tonalite-trondhjemite-granodiorite (TTG) belonging to the North Atlantic Archaean craton (Garde 1989, 1997; Hollis et al. 2004, 2005). In addition, there are granitic intrusions, mafics and ultramafics rocks. The Godthåbsfjord region comprises several terranes: the Akia terrane in the north; the Kapisilik, Tre Brødre, Færingehavn, and Isukasia terranes in the central region, and the Tasiusarsuaq terrane in the south. The Ivinnguit fault is a major tectonic boundary structure which trends NE-SW and defines the southern boundary of the Akia terrane. The Ataneq fault is a conjugating fault to the Ivinnguit and along some of its length lies within the Akia terrane. In the northern part Ivinnguit and Ataneq faults are merged in the same lineament.

Local geology

The Ataneq fault trends similar to the Ivinnguit fault NE-SW and can be followed over a distance of 50 km. The Ataneq fault is first traced on the Qussuk peninsula, here it trends parallel with the Ivinnguit fault. After crossing the Ilulialik fjord the Ataneq and Ivinnguit faults coincide until they reach Isukasia. From here it is difficult to see which way the Ataneq fault is striking.

The Ataneq fault probably formed during a Palaeoproterozoic orogen within the Archaean craton. The Ataneq fault is characterised by a substantial hydrothermal alteration of the TTG rocks which have completely changed them into quartzite where the alteration was most intensive. In the ranges of lesser alteration the original lithologies are still recognisable.

Methods and results

Ataneq 1

During the mapping of this area 25 GPS positions of rock boundaries and other structural features were taken, and 16 samples of various rock types were collected in order to supplement the samples collected during field work in 2004. Figure A9_2 shows the GPS positions of structural features and figure A9_3 shows the GPS positions of the 16 samples. Figure A9_4 shows the geological map of the area, which is based on data collected during the field campaign and the cross section data by Pelle Guldbrandsen (Appendix 8). The main lithology is tonalite which has undergone hydrothermal alterations. These alterations have resulted in five different kind of hydrothermal alterations products. To the east on the map, special attention should be paid on the mafic and ultramafic rocks in the high strain/shear zone.

Description of the structural features at Ataneq 1

Ataneq is a highly complex fault system. This means that there are many cross-cutting conjugating faults to the Ataneq fault. In the mapping process the strike of six conjugating faults were measured. It was impossible to make dip measurements because the walls and bottom of the faults were filled with loose blocks. The largest of these faults is the one closest to cross section 3 (Fig. A9_3). This fault is approximately 50 to 75 m wide; the others measure only half that wide. In addition to the conjugating faults a high strain/shear zone is observed. It strikes almost north-south and varies from 5 to 40 m across. It can be followed for at least one kilometre.

Lithological description of the Ataneq 1 area

The 16 samples collected in this area represent at least eleven different rock types, where the first five belong to the TTG sequence resulting from hydrothermal activity (Fig. A9_1; Table A9_1).

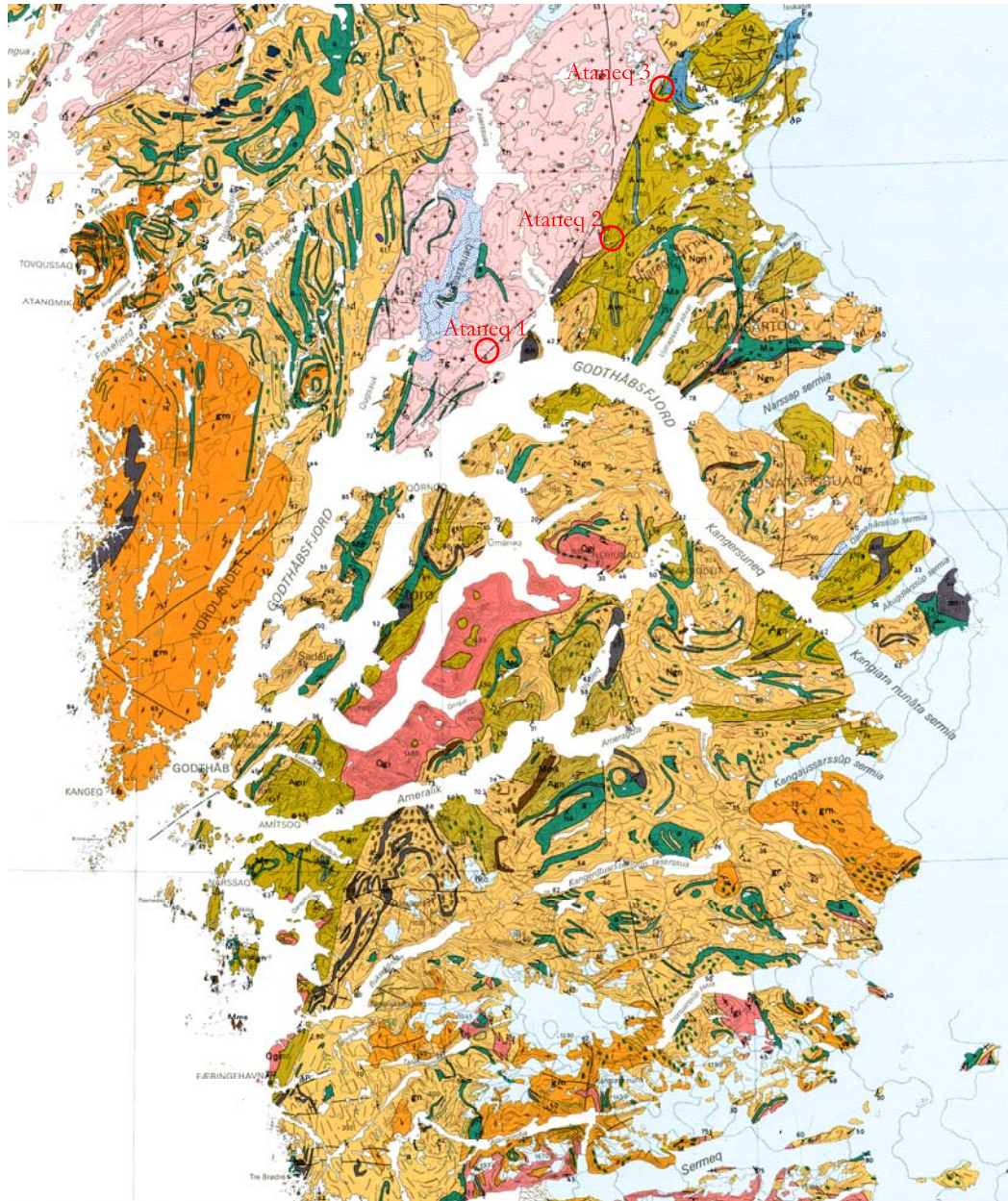


Figure A9_1. Regional map of West Greenland, red circles indicate campsites.

Table A10_1. Rock sample list.

Sample #	Locality #	Locality	Description	Latitude	Longitude
497701	BAN 12	Ataneq fault camp 1	Unaltered coarse-grained tonalite	64.390190	-51.087260
497702	Pelles profile 1 and loc. 1, Ataneq 1	Ataneq fault camp 1	Hydrothermal altered tonalite with quartz-veins	64.449370	-50.490100
497703	Pelles profile 1 and loc. 8, Ataneq 1	Ataneq fault camp 1	Hydrothermal altered sheared quartzite	64.448480	-50.488780
497704	GOT 3	Ataneq fault camp 1	Fine-grained altered dike - greenish	64.448570	-50.488300
497705	GOT 5	Ataneq fault camp 1	Fine-grained altered dike - greenish with disseminated sulfides	64.447530	-50.486290
497706	GOT 6	Ataneq fault camp 1	Hydrothermal altered silicified tonalite	64.447530	-50.486290
497707	GOT 9	Ataneq fault camp 1	Fine-grained dark amphibolite with quartz-veins	64.451790	-50.473020
497708	GOT 9	Ataneq fault camp 1	Ultra-mafic body with quartz-veins	64.451790	-50.473020
497709	GOT 10	Ataneq fault camp 1	Rust-weathered plutonic rock with disseminated sulfides	64.450310	-50.475010
497710	GOT 11	Ataneq fault camp 1	Brittle hydrothermal altered coarse-grained tonalite	64.448220	-50.496270
497711	GOT 12	Ataneq fault camp 1	Medium-grained plutonic rock	64.451290	-50.495010
497712	GOT 12	Ataneq fault camp 1	Coarse-grained plutonic rock	64.451290	-50.495010
497713	GOT 13	Ataneq fault camp 1	Fine-grained dark foliated gneiss with quartz-veins	64.451420	-50.482950
497714	GOT 14	Ataneq fault camp 1	Total hydrothermally altered coarse-grained tonalite - hematitised	64.452230	-50.484090
497715	GOT 16	Ataneq fault camp 1	Fine-grained hydrothermal altered tonalite with disseminated sulfides	64.453250	-50.476030
497716	GOT 17	Ataneq fault camp 1	Soapstone	64.453800	-50.470580
497717	GOT 25	Ataneq fault camp 1	Medium-grained gneiss with quartz-veins	64.452440	-50.471730
497718	GOT 26	Ataneq fault camp 3	Silicified, almost quartzitic, medium-grained tonalite	65.070990	-50.150460
497719	GOT 27	Ataneq fault camp 3	Rust-weathered plutonic rock with disseminated sulfides	65.068520	-50.150980
497720	GOT 27	Ataneq fault camp 3	Rust-weathered plutonic rock with disseminated sulfides	65.068520	-50.150980
497721	GOT 28	Ataneq fault camp 3	Rust-weathered fine-grained gneiss with disseminated sulfides	65.067920	-50.154070
497722	Camp Ataneq 3	Ataneq fault camp 3	Brittle dark fine-grained glimmer schist	65.072040	-50.140240
497723	Pelles profile 1 and loc. 5, Ataneq 3	Ataneq fault camp 2	Dark fine-grained tonalite	Har Pelle	Har Pelle
497724	Pelles profile 1 and loc., Ataneq 3	Ataneq fault camp 2	Dark medium-grained tonalite	Har Pelle	Har Pelle

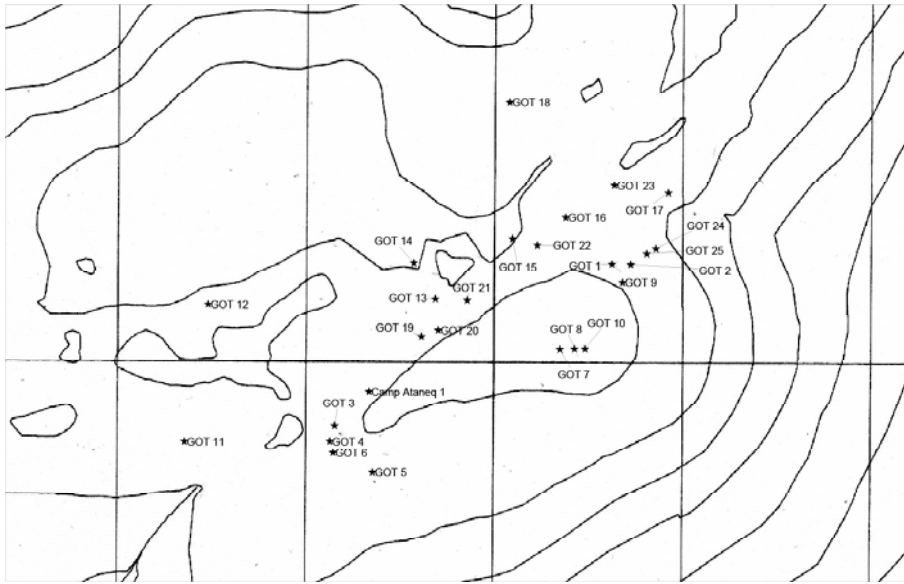


Figure A9_2. GPS-positions of structural features at Ataneq 1.

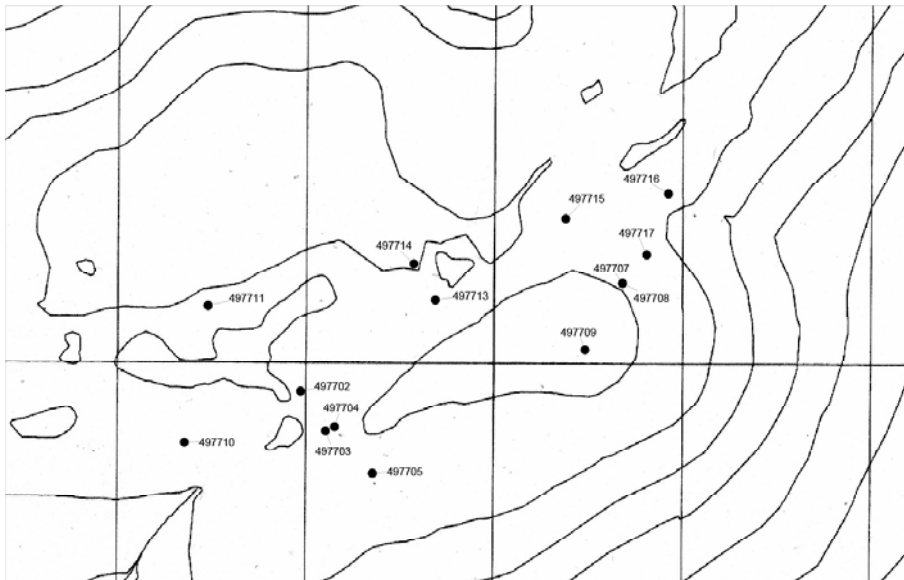


Figure A9_3. GPS-positions of the 16 samples at Ataneq 1.

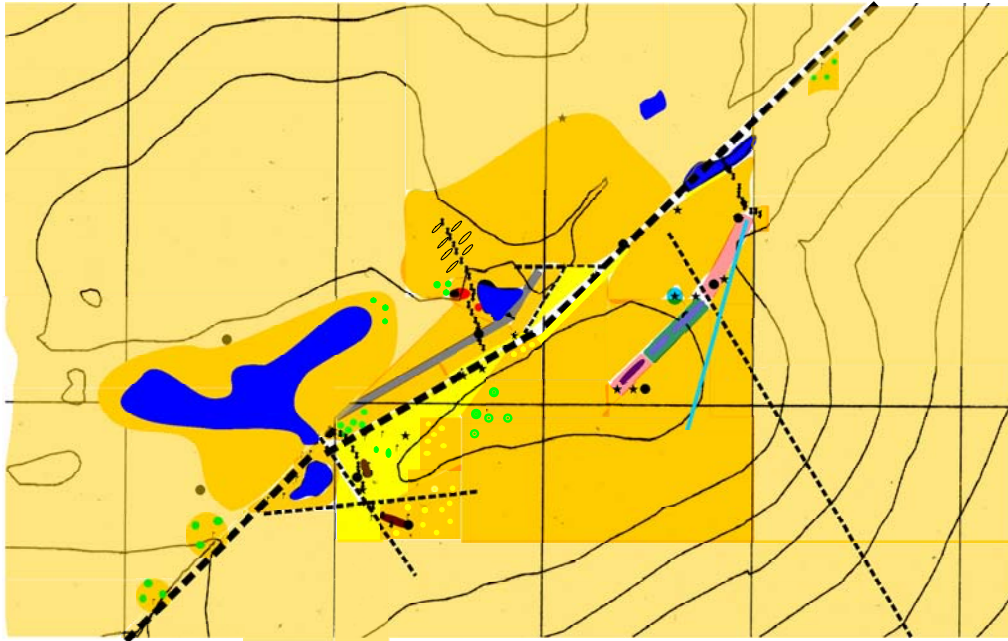


Figure A9_4. Geological map of Ataneq 1.

1) TTG sequence

1.1) Slightly altered tonalite

This rock is coarse grained and consists of equigranular light and dark coloured minerals. Furthermore, the rock exhibits clearly cross-cutting, 10 to 15 cm wide quartz veins. Besides, red and green alteration surfaces a slight foliation can be observed in the rock.

1.2) Altered tonalite with epidote and chlorite

This rock shows small 1 to 3 cm veins of greenish minerals (epidote and chlorite); quartz and plagioclase are seen as medium sized aggregates. Red and green alteration surfaces can also be observed. At GPS-point GOT 16 and in sample 497715 disseminated copper- and iron sulphides are found with grain diameters ranging from < 1 mm to a few larger than 5mm.

1.3) Silicified tonalite

The tonalitic rock has been intensely and silicified. The rock consists of fine grained quartz and little plagioclase.

1.4) Hydrothermal formed quartzite

The tonalitic rock is fully altered to quartzite and consists of microcrystalline quartz. The quartzite exhibits both red and green colours which indicate circulation of iron rich fluids. Furthermore the quartzite shows a clear shearing. Strike and dip measurements of this shearing gives an average on 63° and 67° respectively.

1.5) Hematitised tonalite (completely altered)

The rock appears red due to extensive hydrothermal alterations. It is fine-grained and consists mainly of a red mineral, probably hematite. Other accessory minerals are quartz, feldspar and biotite. Furthermore, the rock has a vesicular appearance, because of the holes formed at places where mineral grains were eroded.

2) Tonalite with mafic lenses

This tonalitic rock is medium grained and contains lenses of a dark fine grained mafic rock.

3) Gneiss

In the area studied, gneiss occurs in two varieties. The first one is a dark foliated fine grained rock, composed of quartz, biotite and other dark coloured minerals. This gneiss contains up to 5 cm thick quartz veins. This gneiss is approximately 25 m wide, the foliation strikes parallel with the Ataneq fault which is c. 64°. The second one is high strain gneiss with a medium grain size. It contains up to 20 cm thick quartz veins, which are medium- to coarse grained in size. Furthermore there can be observed lenses of a dark-greenish rock. This gneiss is seen on both sides of a soapstone body in a high shear zone.

4) Mafic dykes

The dyke consists of a medium- to fine grained greenish rock with quartz porphyroclast. The greenish minerals are products of hydrothermal alteration. Other signs of hydrothermal activity are the <2 cm quartz veins cross-cutting the dyke. The dyke is 8–10 m wide.

5) Fine grained amphibolite

The amphibolite is sandwiched by ultramafic rocks and occupies a zone of 10–15 m. At the borders the ultramafics show greenish alteration. There are also 1 to 2 cm large quartz veins penetrating the amphibolite.

6) Ultramafic rocks

Mineralogical, the ultramafic rocks are very similar to the fine grained amphibolite and typically on weathered surfaces have strikingly red appearance resembling granulated rust.

7) Soapstone

The soapstone has a bluish colour. It is very soft and easy to scratch in with a fingernail. It occurs both in forms of 2 to 5 m wide, massive bodies and as pillows of partially altered ultramafics, where the core is unaltered. The main mineral alteration is talc and serpentine, biotite, epidote and chlorite which can be seen as an altered rim around the soapstone.

Ataneq 2

Due to a very tight time schedule, fieldwork in this area had to be focused on two cross sections - one on the west side and one on the east side of the fault (Fig. A9_5). The largest and most detailed was the section on the fault's western side. Both sides contain felsic rocks of three different types. Figure A9_6 shows the geological map of this area.

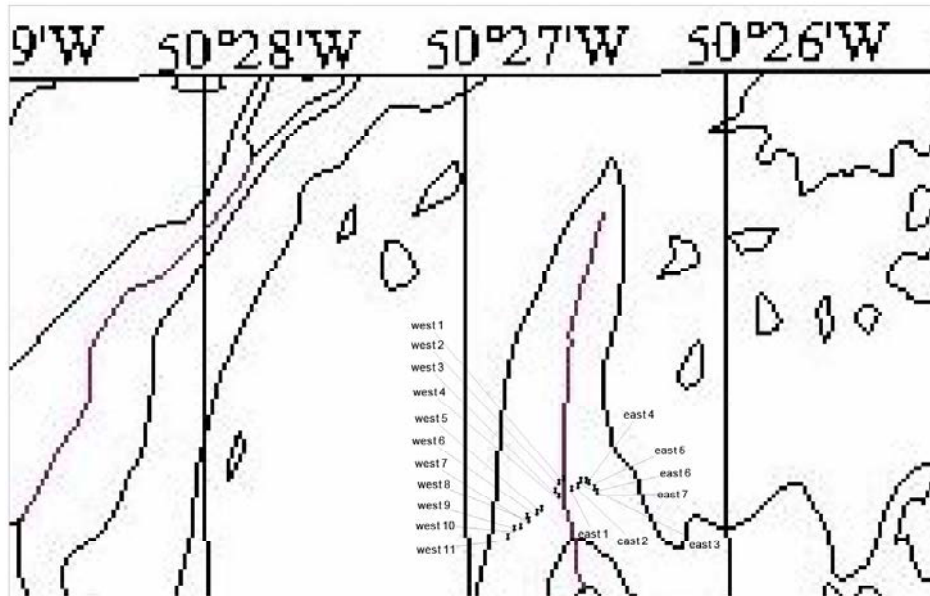


Figure A9_5. GPS-positions of the two cross sections at Ataneq 2.

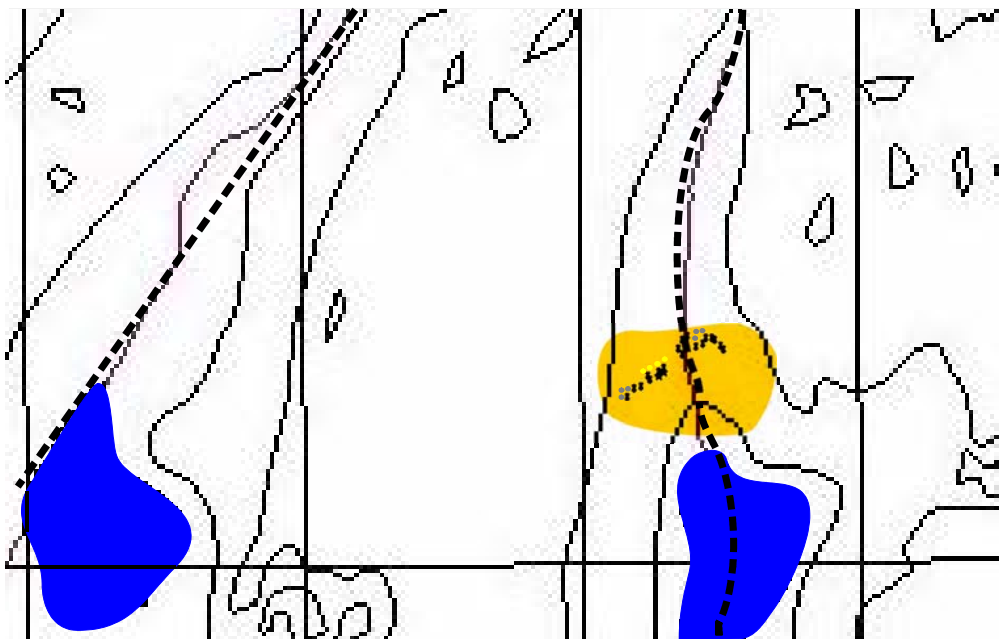


Figure A9_6. Geological map of Ataneq 2.

1) Tonalite

This rock has medium grain sizes, it consists of dark- and light coloured minerals. Furthermore, quartz veins of up to 10 cm across are observed. At point 5 in the cross section quartzite is exposed.

2) Gneiss

This rock shows light and dark coloured minerals in layers in varying thickness. This gneiss is heavily folded due to intense deformation.

3) Quartzite

The quartzite is microcrystalline and shows red and green alteration surfaces. The quartzite contains small fragments < 10 cm in diameter of a dark fine grained minerals. At point 5 in the cross section the quartzite is fine grained instead of microcrystalline; its appearance reminds of the silicified tonalite as describe before (Ataneq 1).

Ataneq 3

Here, eight GPS positions of rock boundaries and other structural features were taken. A single cross section was done (Appendix 8) and five different rock samples were taken, below are there a description of these five samples. The GPS-positions (Fig. A9_7) and the geological map over this area is given in figure A9_8.

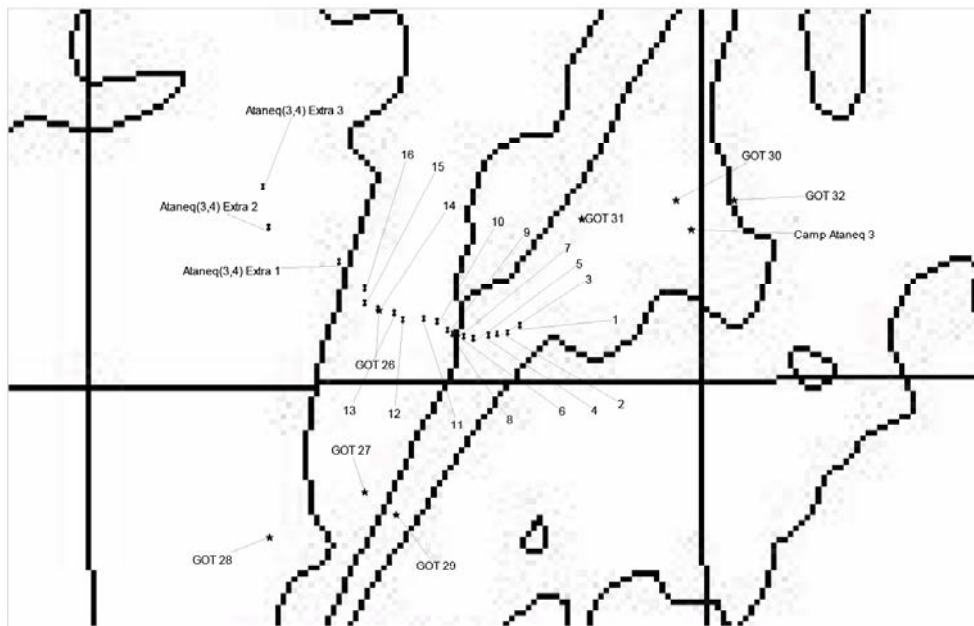


Figure A9_7. GPS-positions of the cross section at Ataneq 3 (the pins) and the GPS-positions of structural features and collected samples (the stars).

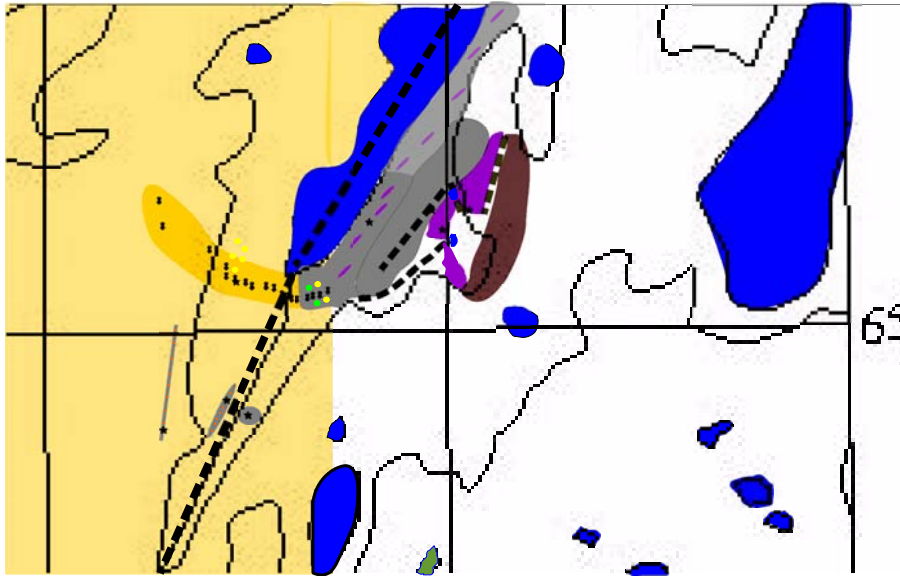


Figure A9_8. Geological map of Ataneq 3.

1) silicified tonalite

This tonalite is medium-grained, consists mostly of light minerals and shows varying degrees of foliation, which ranges from an almost gneissic appearance to the unfoliated structure of a medium grained quartzite.

2) felsic rock (gneiss)

This rock is a rusty weathered fine grained dark coloured rock. Mineralogically the rock consists of biotite, feldspar, small aggregates of quartz, quartz veins, <5 mm aggregates of disseminated sulphides (chalcopyrite), <5 mm large garnet crystals and a greenish mineral probably epidote or chlorite. Because of the quartz veins and the greenish mineral, it is likely that this rock has undergone some kind of hydrothermal alteration. This body is approximately 50 m long, 10 m wide and 10 m high, it was not possible to get an estimate of how deep it is.

2.1) gneiss A

This rock is a continuation of the felsic rock above. This is clearly fine grained foliated weathered (rusty) gneiss. There are <5 mm wide quartz veins and disseminated sulphides. This body is 5 m wide and can be followed for 75 m without finding further signs of disseminated sulphides.

2.2) gneiss B

In comparison to the gneiss in 2.1 this gneiss is very hard, it shows dark and light coloured layers and has a very strong foliations with both micro and macro folds.

3) mica schist

This mica schist consists of two rock types: a greenish dark coloured fine grained schist and a competent dark coloured fine grained rock. The mica part of the schist consists mainly of biotite, the greenish colour come from green alteration minerals, probably epidote

and chlorite. This part of the rock is heavily weathered. The competent part of the rock is dark coloured and consists of fine grained minerals, too small to determine in the field.

Conclusion

During the fieldwork in the summer 2005 32 GPS-positions of rock boundaries and other structural features were taken, at different localities around the Ataneq fault. Combined rock samples (Table A10_1) from this year's campaign and the samples collected last year constitute the foundations of the thesis on a characterisation of the hydrothermal system of the Ataneq fault in southwest Greenland. Of the 24 samples collected this year seven contained disseminated sulphides. A brief description of the collected 2005 is given in Table 10_1.

The most detailed mapping was done around the geophysical cross sections (Appendix 8). Combined with the 32 GPS-positions of rock boundaries and other structural features and of sketches of the areas it was possible to create geological maps of the areas (Fig. A9_4). Ataneq 1 was, with three cross sections and 25 GPS-positions, the largest and the best studied area (Fig. 4). At Ataneq 2 two cross sections were made, one of the west side and one of the east side of the fault. The west cross section was the longest and most detailed here. At Ataneq 3 one cross section was made and 8 GPS-positions of rock boundaries taken and other structural features described. These data combined with two detailed area sketches, constitute the data for mapping this area (Appendix 8).